A STUDY OF MOISTURE DIFFUSION IN POLYMERIC PACKAGING MATERIALS ESPECIALLY AT HIGH TEMPERATURES

SHI YU
(B.Eng(honors), SJTU)

A THESIS SUBMITTED
FOR THE DEGREE OF MASTER OF ENGINEERING
DEPARTMENT OF MECHNICAL ENGINEERING

NATIONAL UNIVERSITY OF SINGAPORE
2002

Acknowledgements

I would like to express my gratitude to all those who gave me the possibility to complete this thesis. I want to thank my supervisor **Prof Andrew Tay A.O.** for his invaluable guidance and advice throughout this research project.

I have furthermore to thank the Senior Group Leader **Mr. Wong Ee Hua**, in IME, for countless help and stimulating suggestions during the execution of the project. I am bound to the **Mr. Ranjan S/O Rajoo** from the Department of Advanced Packaging and Development Support (APDS) for his stimulating support and encouragements during this research. The manager and staff from APDS, supported me in my research work. I want to thank them for all their help, support, interest and valuable hints. Especially I am obliged to **Mr. Xing Zhenxiang** from FAR (Failure and Analysis Research) Department. My schoolmate **Koh Sau Wee** was of great help in difficult times.

I would also like to thank National University of Singapore (NUS) for providing me a scholarship for this research as well as Institute of Microelectronics (IME) for their providing facilities. Especially, I would like to give my special thanks to my family whose patient love enabled me to complete this work.

Table of Contents

Materials

Summary

To state the accurate characterizing of moisture properties of polymeric packaging materials at high temperatures has been a challenge, in this research, the technique of Karl Fischer Titration was explored.

Through comparing with standard and conventional testing technique such as TGA (Thermal Gravimetric Analysis) and with a furthermore confirmation test using GC/MS (Gas Chromatography/Mass Spectrometry), moisture desorption testing with Karl Fischer Titration (KFT) was performed in this research on 3 types of polymeric packaging materials: molding compound, underfill and die attach materials.

Significant differences in the determination of moisture desorption characteristics were observed between the TGA and the KFT techniques. The Outgassing of solvent at high temperatures has been found to affect the result by the TGA technique. The presence of outgassing has been validated using Gas Chromatography/Mass Spectrometry (GC/MS). In comparison, Karl Fischer Titration is not affected by the outgassing and has been demonstrated as a reliable technique for characterizing moisture diffusion at high temperatures.

Both Fickian and non-Fickian behaviors were observed in polymeric packaging materials. Activation energy E_d and D_o of materials were calculated above and below glass transition temperature $T_{g,,}$ respectively. The results showed E_d above T_g is much lower than that below T_g.

Moisture absorption experiments were carried out using different polymeric packaging materials. Results have shown that moisture absorption behaviors are Fickian-like and moisture absorption coefficients D are polymer matrix dependent. The effects of fillers on moisture diffusion in polymeric packaging materials were discussed. Aging in polymeric packaging materials were observed after long-term exposure to 85^{o}C/ 85%RH. The level of aging was found to be polymer matrix dependent. Therefore, to meet the functional needs of packaging, it is important to design polymeric materials with higher T_g to obtain the best performance of materials under severe environments with high temperatures and high relative humidity.

Lists of Tables

List of Figures

List of Abbreviations and Symbols

SMD	Surface mount device
IC	Integrated Circuit
CTE	Coefficient of Thermal Expansion
S	Solubility
D	Diffusivity, diffusion constant
C	Concentration of diffusing substance
C_{sat}	Diffusing Substance Concentration in Saturated Sample
JEDEC	Joint Electron Device Engineering Council the semiconductor engineering standardization body of the Electronic Industries Alliance (EIA), a trade association that represents all areas of the electronics industry
VPR	Vapor phase reflow
EMC	Epoxy molding compound
IPC	In 1999, IPC changed its name from Institute of Interconnecting and Packaging Electronic Circuits to IPC. The name is accompanied by an identity statement, Association Connecting Electronics Industries
IR	Infrared
TGA	Thermo-gravimetric Analysis
GC/MS	Gas Chromatography/Mass Spectrometry
KFT, KF Titration	Karl Fischer Titration
RH	Relative Humidity
Proton NMR	Proton Nuclear Magnetic Resonance
γ	activity coefficient,

P (S= γP)	partial pressure
F	molecular flux
dC/dx	degradation of the concentration
E_d	Diffusion activation energy
R	Ideal gas constant,
T	Absolute temperature
P (P=DS)	Permeability
M_t	the total amount of diffusing substance which enters the sheet during the time t
M_{sat}	the amount of diffusing substance during infinite time
h	the whole thickness of the membrane.
$-\Delta H_s$	Enthalpy of sorption
$(DBE)_D$	Deborah Number
$\theta_D(s)$	The characteristic time of penetrant diffusion
$\lambda_m(s)$	The characteristic time of polymer relaxation processes
M_m	The equilibrium moisture content of a polymeric material
$\varnothing$	Relative Humidity
G_t	Thermal strain energy release rate
G_h	Hygro strain energy erlease rate
G_{tot}	Total strain energy Release Rate
SAM	scanning acoustic microscopy
T_g	Glass transition temperature of polymer
DMA	Dynamic Mechanical Analysis

FTIR-ATR	Atenuated-total-relfectance Fourier transform infrared spectroscopy
V_f	Free volume
V_h	Hole free volume
V_i	interstitial free volume caused by thermal expansion
DSC	Differential Scanning Calorimetry
D_{desorp}	Moisture Desorption coefficient
D_{adsorp}	Moisture Absorption coefficient
I	iodine
W	water content
MC	Molding compound
UF	Underfill
DA	Die attach
δ	Standard deviation

Chapter 1
Introduction

1.2 Background

Moisture diffusion in polymeric materials has become an important issue for IC packaging, since the discovery of failure phenomena of "popcorning" which refers to cracking during the solder reflow process of SMD (Surface Mount Device) packages (Fig1.1).

1.2.1 Popcorn Cracking

SMD type IC packages take a great percentage of the current market because their compact design allows more pin counts in a small area and catches up with the trend of packages that require the thinner package with the larger chip, compared to the though-hole predecessors (Figure 1.2). However, the disadvantage of SMD packages is the exposure of the whole package to a higher temperature (215-260 ^{o}C) (Figure 1.3) during the solder reflow process, in comparison with the through-hole packages which are heated under the board (Figure 1.4). This has caused moisture-absorbed SMD packages to frequently fail in "popcorning". This is due to the great difference in CTE (Coefficient of Thermal Expansion) between the materials composing the packages

and the vapor pressure caused by the moisture absorbed in the polymeric packaging materials. Moisture readily gets access into epoxy molding resin when IC packages are left in an environment of high relative humidity.

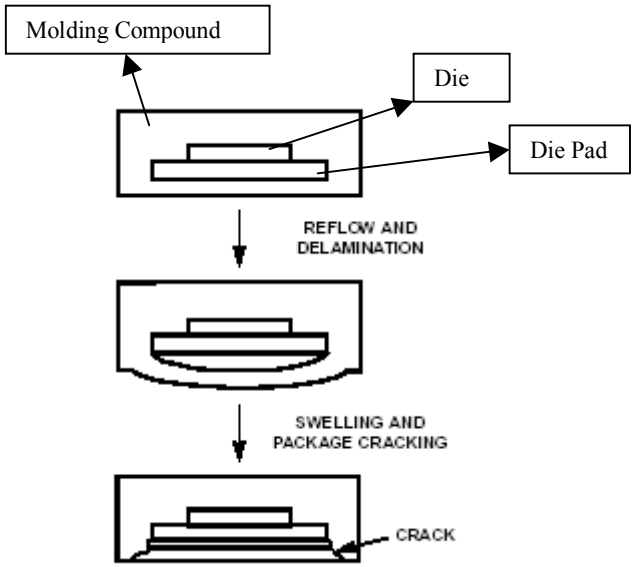

Figure.1.1 Popcorn crack

With the development of new packaging technologies such as lead-free packaging, these effects are getting especially detrimental owing to higher soldering techniques. Hence, an in-depth understanding of the moisture absorption and diffusion characteritics of polymeric packaging materials is essential. Over and beyond this, an accurate characterization of these properties is even more critical.

While there have been standards describing in detail the technique and procedure for characterizing the diffusion characteristic of polymeric materials during moisture absorption such as JEDEC Standard No. 22-A120 and TGA (Thermal Gravimetric Analysis) [Lau and Chang, 1999], these techniques and procedures are not at all

applicable for characterizing diffusion characteristics during desorption at high temperatures, since non-Fickian moisture diffusion and chemical degradation of polymeric materials under a severe environment of high humidity and high temperature have been widely reported [Lowry, et al, 2001, Neve and Shanahan, 1995]. Therefore, a reliable and effective method for moisture diffusion characterization of polymeric materials at high temperatures is in great need.

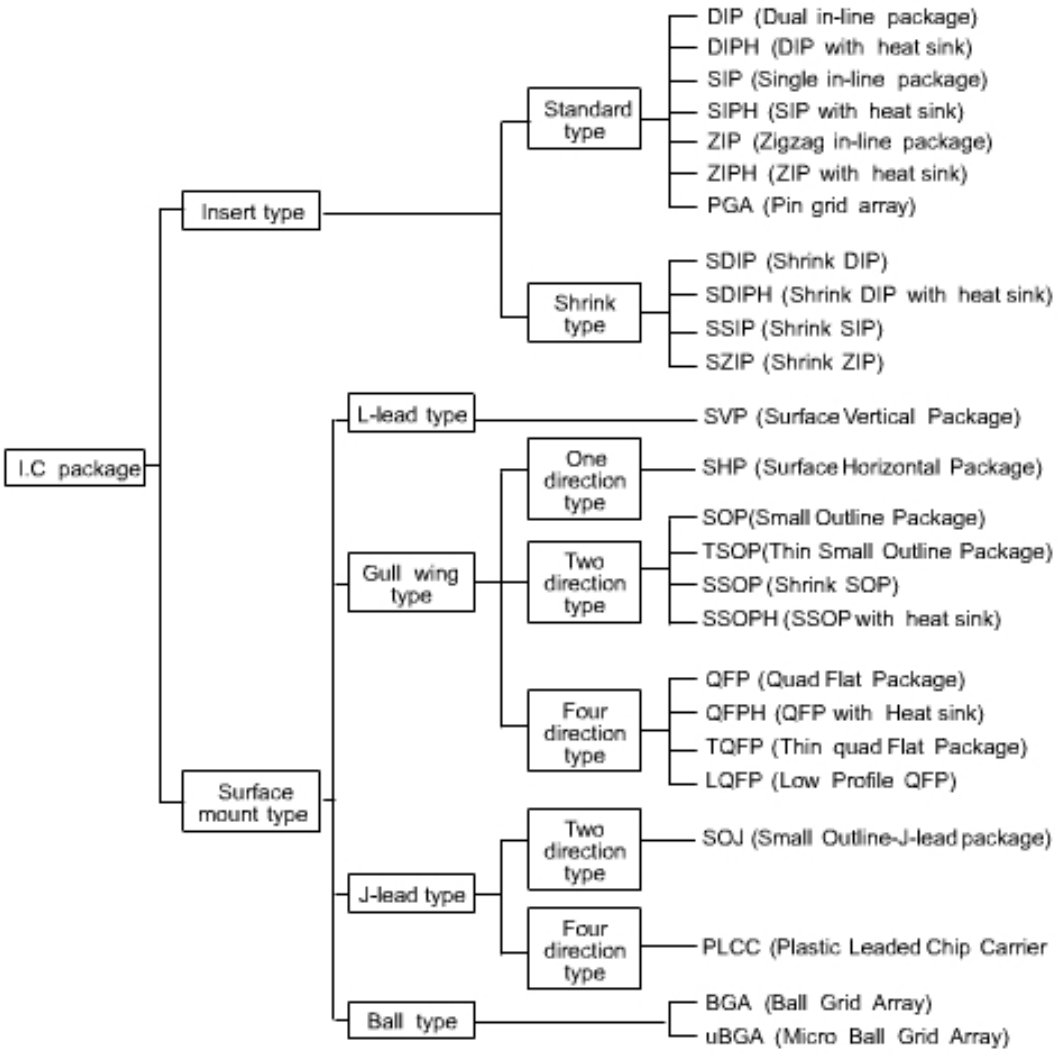

Figure 1.2 Types of IC packages

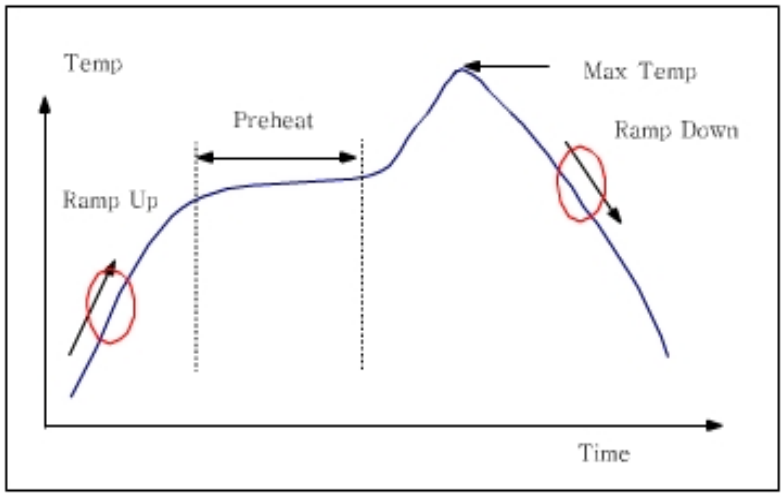

Figure1.3 Temperature Profile of Solder Reflow Process

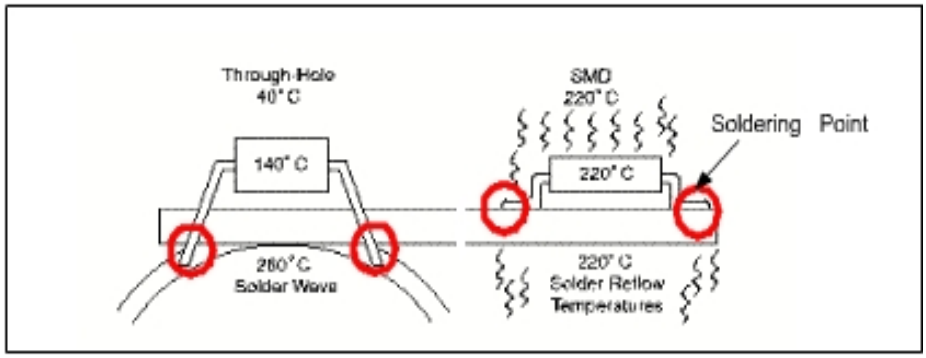

Figure 1.4 Heat Distribution of Surface Mounting Package and Through Hole Package

1.1.2 Influencing Factors on IC Package Cracking During Solder Reflow

It has been known that the dominant cracking mechanism is moisture expansion due to thermal processing acting on concentration of water vapor at the back surface of the die pad [Suhl, 1990]. Hygrothermally induced high compressive and tensile stress

development in the bimaterial interface is responsible for the delamination and popcorn cracking. [Yi, 1995]

The following are considered by Kitano [1988] to be the main factors that influence the fractures of IC packages:

1. Level of moisture saturation and hysteresis of moisture absorption
2. Structure of package
3. Strength of plastic encapsulant

Other factors reported are the dependence on the thermal gradient, built-in molding stress, plastic yield strength and silicon die size [Suhl, 1990]. Generally it is believed that better adhesion between the encapsulant, lead frame, and the silicon chip will result in improved reliability, resistance to package cracking and reduced line movement due to thermal stresses. An enhanced adhesion between the lead frame, chip and the molding compound can reduce or eliminate device delamination and cracking during VPR. [Kim, 1991].

Based on the driving force for crack propagation (the energy release rate) and crack growth resistance (the fracture toughness), the criterion for the growth of the package crack due to the vapor pressure can be made. The package crack propagates when the energy release rate is greater than the fracture toughness of epoxy molding compound (EMC) [Lim, 1998]. Other results found were:

1. The fracture toughness gets smaller when the temperature gets higher.

2. The energy release rate of the package crack is increased with the larger size of the die pad and thinner thickness of EMC.

3. The longer the delamination length, the smaller the effect of thermal loading to the total energy release rate.

1.1.3 Moisture Sensitivity Tests

In order to establish common criteria for the classification of moisture sensitive SMD packages several industry specifications have been drafted. The more widely accepted includes JEDEC STD22B, Test Method A112-A and IPC-SM-786A. These have recently been combined into IPC/JEDEC J-STD-020A [1999]. These specifications outline the test methods for classifying the moisture sensitivity of a given SMD to one of eight different levels (see Table 1.1).

The classification test procedure involves the specific soak durations at the stated floor life conditions for levels 3 through 6. Accelerated conditions are used for level 1 and 2. Following the humidity soak, the packages are subjected to 3 reflow cycles with either vapor phase or IR reflow. The specified maximum reflow temperatures are 219^{o}C/225^{o}C or 235^{o}C/240^{o}C depending on package dimensions [IPC/JEDEC J-STD-020A, 1999]. The product is then subjected to electrical test, visual inspection, cross-sectioning and/or inspection with acoustical microscopy. The package is assigned to the lowest level of moisture sensitivity for which it passes. In this research, all of the samples were preconditioned at level 1 but with a relatively longer time. This was to make sure that the samples were fully saturated.

Level	Floor Life		Soaking requirements	
	Conditions	Time (Note 1)	Conditions	Time
1	30°C / 85% RH	Unlimited (Note 2)	85°C / 85% RH	168
2	30°C / 60% RH	1 Year	85°C / 60% RH	168
2A	30°C / 60% RH	4 Weeks	30°C / 60% RH	672
3	30°C / 60% RH	168 Hours	30°C / 60% RH	192
4	30°C / 60% RH	72 Hours	30°C / 60% RH	96
5	30°C / 60% RH	48 Hours	30°C / 60% RH	72
5A	30°C / 60% RH	24 Hours	30°C / 60% RH	48
6	30°C / 60% RH	6 Hours	30°C / 60% RH	Time on label

Table 1.1 Moisture Sensitivity Levels

NOTES:

1. Time after removing from dry pack in a 30°C / 60% RH ambient.

2. Dry pack not required. Maximum conditions: 30°C / 85% RH.

1.3 Objective of Research

Currently, the standard JEDEC method and a commonly used method for measuring moisture diffusion coefficients of polymeric materials, Thermo-gravimetric Analysis (TGA), are both based on the gravimetric principle. JEDEC standard for high temperature desorption uses a microbalance. The TGA method basically consists of measuring the loss in weight of a sample of material that is heated. It is assumed that this weight loss is entirely due to the moisture loss. While the TGA method is reliable and accurate at relative low temperatures, there is considerable uncertainty over its accuracy in measuring moisture diffusion coefficients of polymeric packaging materials at high temperatures. The reason for this uncertainty is that at high temperatures, volatiles in the polymeric packaging materials may be given off in addition to moisture.

The main purpose of this research is to establish an accurate and reliable method for characterizing moisture diffusion properties of polymeric packaging materials at high temperatures (i.e.: solder reflow temperature). Characterizing moisture diffusion of polymeric packaging materials at high temperatures presents special challenges. These challenges and solutions will be described in detail. Experiments will be carried to measure accurately for the first time, the moisture desorption diffusion coefficients of three widely used polymeric materials-molding compounds, underfills, and die-attach materials- at high temperatures.

1.4 Scope of Research

Conventional and typical polymeric packaging materials of molding compound, underfill and die attach materials were used in this study project. Karl Fischer Titration, Thermal Gravimetric Analysis (TGA) and Gas Chromatography/Mass Spectrometry (GC/MS) tests were performed for these 3 types of polymeric materials. TGA, as one of the conventional methods based on the gravimetric principle, was used to compare with Karl Fischer Titration. GC/MC was used as the confirmation test to explain the deviation between KF titration and TGA.

In addition to desorption tests with Karl Fischer Titration and TGA, Moisture absorption experiments were also conducted for a wide range of polymeric materials.

The scope of this research work is as follows:

Part 1: Critical survey of literature on non-Fickian moisture diffusion behaviors of polymeric materials.

A critical review of previous study of non-Fickian moisture diffusion in polymeric materials will be carried out including the different techniques used in investigating the causes of non-Fickian diffusion.

Part 2: Experiment on Moisture desorption:

1. To find out the possible causes for the decreased D and the larger C_{sat} by TGA tests and to discuss the incapability of TGA and therefore, other gravimetric methods in characterizing moisture diffusion (desorption) at high temperatures.

2. To observe the Non-Fickian behaviors in all of the polymeric materials used in our tests, especially at high temperatures and to seek the causes of Non-Fickian behaviors from the microstructure of polymeric materials and duration of exposure to humidity/temperature environment.

3. To find out the effect of T_g on moisture desorption from the microstructure of polymeric materials.

4. To investigate the efficiency of KF titration for quantifying moisture diffusion at high temperatures (moisture desorption).

5. To plot Arrenhius relationships with the results from TGA and KF Titration and show any change in D_0 and E_d during transition across the glass transition temperature T_g.

6. To establish a reliable and efficient testing method for characterizing moisture desorption properties of desorption of polymeric packaging materials at high temperatures.

Part 3: Experiments on moisture absorption

1. Moisture absorption behaviors of polymeric materials
2. Comparisons of results from absorption and desorption tests
3. Effects of fillers on moisture absorption in polymeric materials
4. Sample thickness effects on moisture absorption in polymeric materials
5. Aging of polymeric materials after long-term exposure at 85^{o}C/ 85%RH

1.5 Organization of Thesis

An extensive literature review is given in Chapter 2. Topics on moisture diffusion in polymeric materials such as diffusivity, solubility, non-Fickian diffusion behaviors and its classification by $(DEB)_D$ number are discussed. Factors influencing moisture diffusion are discussed in both external and internal aspects. Several ways to improve the water resistance of IC packages are discussed as well.

In addition to Chapter 2, in which a brief review has been made on Non-Fickian diffusion of polymeric materials, Chapter 3 gives a detailed literature review on previous studies of non-Fickian moisture diffusion in polymeric materials as well as the different testing techniques used for investigating the causes of non-Fickian diffusion.

Since it has been well acknowledged that the adsorbed moisture in polymeric packaging materials is responsible for 'popcorn' cracking of IC packages during solder reflow, polymeric materials characterization on the properties of moisture diffusion especially at high temperatures becomes very important. Chapter 4 focuses on the design of moisture desorption experiments using KF Titration and conventional TGA method with polymeric packaging materials: molding compound, underfill and die attach materials, in order to fulfill this purpose. The confirmation test GC/MS was used to explain the difference between the results from those 2 methods.

In Chapter 5, the experiment results from desorption tests are discussed. The difference in results from Thermogravimetric Analysis (TGA) and KF Titration was explained as the outgassing at high temperatures by investigating the nature of polymeric materials. Results from Gas Chromatography/Mass Spectrometry (GC/MS) also showed that outgassing of chemicals were severe, especially at high temperatures and confirmed the validity of our prediction. This questioned the use of TGA or any other conventional gravimetric methods for studying moisture desorption properties at high temperatures. Karl Fischer Titration has shown that it is possible to characterize moisture desorption of polymeric materials at high temperatures in a fast and efficient way.

Moisture absorption tests for a wide range of polymeric materials are described and discussed in Chapter 6. These issues include moisture absorption behaviors of polymeric materials, comparisons on results from absorption and desorption tests, filler effects on moisture absorption in polymeric packaging materials and aging of polymeric materials after long-term exposure to 85^{o}C/ 85%RH.

Conclusions of this research are given in Chapter 7.

Chapter 2
Literature Review

2.1 Introduction:

Moisture diffusion in polymeric materials has been discussed extensively in the reported literature. Factors influencing the moisture diffusion were discussed in both external and internal aspects. For the external factors, one can calculate the moisture diffusion coefficient D and the equilibrium moisture content M_m at the particular temperature and RH, respectively. When it comes to the internal factors, there is greater complexity. One can only speculate the effects of interface, coupling agent and voids through water uptake curve and Proton NMR spectra. Some speculations are valuable but much more work needs to be done since there are a lot of uncertain speculations. Also the Proton NMR experiments cannot be carried out with actual IC packages because of the problems arising from conducting materials and radio frequency dissipation and penetration. This method cannot be used to test high-throughput real samples. Non-destructive depth profiling is of value for probing moisture distribution in IC packages. [Sivakesave and Irudayaraj, 2000].

Several methods on modeling and predicting the moisture diffusion have been proposed and give relatively accurate predictions, which are helpful for commercial design and analysis of IC packages [Kitano, 1998; Tay and Lin, 1999].

The adhesion of interfaces within an IC package has a dominant influence on its moisture resistance properties. For example die-attach material plays an important role in joining thin and dissimilar materials and reducing stress concentration. Long-term resistance of this polymeric adhesive to aggressive environments such as moisture at elevated temperatures is essential to the reliability of IC packages. But if the adhesion strength is too high between the leadframe and mold compound, which will result in a poor mechanical performance during Solder Reflow because of the stress relaxation is not effective in the interface [Kim, 1991]. Some semiconductor company such as Philips has found that good performance of a plastic package need a good compromise of adhesion strength properties of the entire package.

2.2 Moisture Solubility and Diffusivity in Polymeric Materials

Moisture molecules dissolve in the surface of a polymer, equilibrating with the atmosphere, establish a chemical potential, and diffuse in the direction of the gradient. Solubility (S) and diffusion constant (D) are two fundamental properties. [(1)] L.L. March and G. S. Springer introduced that the solubility (S) follows Henry's law

$$S = \gamma P \tag{2.1}$$

Where γ is an activity coefficient, P is partial pressure (P).

Diffusion constant (D) which is the ratio of the molecular flux (F) divided by the degradation of the concentration (*dC/dx*) of the diffusion species, i.e., Fick's law,

$$F = -D\, dC/dx. \tag{2.2}$$

Where F is the rate of transfer per unit area of section, C the concentration of diffusing substance, x the space coordinate measured normal to the section, and D is called the diffusion coefficient (D) is independent of the unit if F and C are both expressed in terms of the same unit of quantity, e.g. gram or gram molecules, then it is clear from equation (2.2) that D is independent of this unit and has dimensions $(\text{length})^2(\text{time})^{-1}$, e.g cm^2S^{-1}. The negative sign in equation (2.2) arises because diffusion occurs in the direction opposite to that of increasing concentration.

Therefore, if the diffusion coefficient is constant, the differential equation is

$$\frac{\partial C}{\partial t} = D\left(\frac{\partial^2 C}{\partial x^2} + \frac{\partial^2 C}{\partial y^2} + \frac{\partial^2 C}{\partial z^2}\right) \tag{2.3}$$

If considering an element of volume in the form of a rectangular paralleledpiped whose sides are parallel to the axes of coordinates and are of lengths 2dx, 2dy, 2dz. Let the center of the element be at P(x,y,z), where the concentration of diffusing substance is C. For equation (2.3), if diffusion is one-dimensional, i.e, if there is a gradient of concentration only along the x-axis. The equation simply reduced to

$$\frac{\partial C}{\partial t} = D\frac{\partial^2 C}{\partial x^2} \tag{2.4}$$

Where C is a function of both x and time (t), in this unsteady state (e.g, diffusion through membranes), we have boundary conditions $C(I,t)=C_1$, $C(II,t)=0$, initial condition is $C(X,0)=0$.

Expressions (2.2) and (2.4) are usually referred to as Fick's first and second laws of diffusion.

However, in many systems, for examples, the interdiffusion of metals or the diffusion of organic vapours in high-polymer substances, D depends on the concentration of diffusing substance C. In the case, and also when the medium is not homogeneous, so that D varies from point to point, we have

$$\frac{\partial C}{\partial t} = \frac{\partial}{\partial x}(D\frac{\partial C}{\partial x}) + \frac{\partial}{\partial y}(D\frac{\partial C}{\partial y}) + \frac{\partial}{\partial z}(D\frac{\partial C}{\partial z}) \tag{2.5}$$

where D may be a function of x, y, z and C.

If D depends on the time during which diffusion has been taking place but not on any of the other variables, i.e.

$$D = f(t) \tag{2.6}$$

then on introducing a new time-scale T such that

$$dT = f(t)dt \tag{2.7}$$

the diffusion equation becomes

$$\frac{\partial C}{\partial T} = \frac{\partial^2 C}{\partial x^2} + \frac{\partial^2 C}{\partial y^2} + \frac{\partial^2 C}{\partial z^2} \tag{2.8}$$

which is same as (2.3) for a constant diffusion coefficient equal to unity.

For polymeric materials in IC packages, because glassy polymers are not at equilibrium but they relax slowly toward it, the mass water uptake in the glassy polymer studied was

found to be proportional to time instead of to the expected square foot of time. That means the diffusion behavior is anomalous and doesn't obey Fick's law at higher temperature and higher moisture concentration, the physical mechanism is that of the coupled mass and momentum transport, coupled through swelling, and glassy polymers are inhomogeneous. The diffusion is time-dependent response of the polymer, akin to viscoelastic mechanical response.

Polymers are relatively permeable to gases and liquids. The material transport of gases and liquids through polymers consists of various steps: [Osswald and Menges, 1995]

a. Absorption of the diffusion material at the interface of the polymer, a process also known as adsorption.
b. Diffusion of the attacking medium through the polymer, and
c. Delivery or secretion of the diffused materials through the polymer interface, also known as desoprtion.

A gradient in concentration of the permeating substance inside the materials results in transport of that substance which we call molecular diffusion. The cause of the molecular diffusion is the thermal motion of molecules that permits the foreign molecules to move along the concentration gradient using the intermolecular and intra-molecular spaces.

In the case of sorption and desorption by a membrane, diffusion coefficient D can be solved by [Crank, 1975]

$$\frac{M_t}{M_{sat}} = 1 - \sum_{n=0}^{\infty} \frac{8}{[(2n+1)\pi]^2} \exp\left[\frac{-D(2n+1)^2\pi^2 t}{h^2}\right] \quad (2.9)$$

where M_t donate the total amount of diffusing substance which enters the sheet during the time t, and M_{sat} the corresponding amount during infinite time, h signifies the whole thickness of the membrane.

Sorption and Diffusion are processes activated by heat and as expected to follow an Arrenhius type behavior, Thus, the solubility and diffusivity can be written as

$$S = S_0 \, exp^{-\Delta Hs/RT} \quad (2.10)$$

and

$$D_c = D_0 \, exp^{-Ed/RT} \quad (2.11)$$

where $-\Delta H_s$ is the enthalpy of sorption, E_d is the diffusion activation energy, R is the ideal gas constant, and T is the absolute temperature. The diffusion activation energy E_d depends on the temperature, the size of the gas molecule and the glass transition temperature of polymer. [Osswald and Menges, 1995].

Solubility and diffusion constant (D) are two fundamental properties [March and Lasky, 1981]. The product of the sorption equilibrium parameter (solubility, S) and the diffusion coefficient D, is known as Henry's Law, and is defined as the permeability P of a material

$$P=DS \quad (2.12)$$

Moisture readily gets access into epoxy molding resin when plastic-encapsulated IC packages are left unattended in an environment with high temperature and high relative humidity.

For polymeric materials in IC packages, because glassy polymers are not at equilibrium but they relax slowly toward it, the water uptake in the glassy polymer studied by Marchard Lasky [1981] was found to be proportional to time instead of the expected square root of time. This means the diffusion behavior is anomalous and does not obey Fick's law especially at higher temperatures and higher moisture concentrations. The physical mechanism is that of the coupled mass and momentum transport, coupled through swelling. Glassy polymers are also inhomogeneous [Neogi, 1996]. The diffusion is time-dependent response of the polymer, akin to viscoelastic mechanical response [Cai, and Weitsman, 1994]. The Deborah Number $(DBE)_D$ was introduced to indicate the presence of the non-Fickian effects during absorption experiments [Van Der Wel, and Adan, 1999]:

$$(DEB)_D = \frac{\lambda_m}{\theta_D} \tag{2.13}$$

$\theta_D(s)$ is the characteristic time of penetrant diffusion and $\lambda_m(s)$ can be considerated as the characteristic time of polymer relaxation processes. $(DEB)_D$ may be expressed as a function of C (Moisture Concentration) and T (Temperature). Three zones in a C-T diagram can be defined by lines of $(DEB)_D$ Number. When $(DEB)_D << 1$ (viscous fluid) or $>>1$ (elastic solid), Fickian behavior will occur. Two threshold temperatures T_v (viscous fluid -- above it) and T_e(elastic solid --below it) are defined. Non-Fickian diffusion behaviors have been classified into "two-stage", "sigmoidal" and "Case II" types by the appearance of their kinetic absorption curves [Neogi, 1996; Van Der Wel and Adan, 1999].

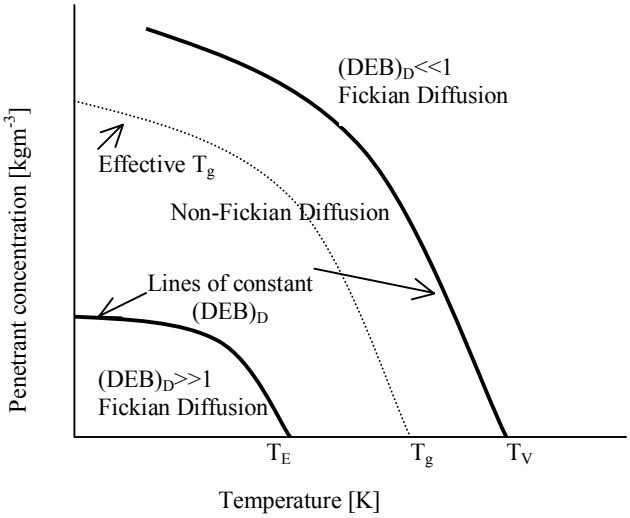

Figure 2.1 Schematic picture of the different zones of diffusion, separated by lines of constant diffusion Deborah number $(DEB)_D$, as related to penetrant concentration and temperature. T_E is the temperature below which pure polymer acts like an elastic solid, T_g the glass transition temperature, and the T_v is the temperature abovewhich pure polymer acts like a viscous fluid.

2.3. Factors Affecting Moisture Absorption in Polymeric Materials

2.3.1 External Factors [Rao, Balasubramanian and Chanda, 1981]

A. Effect of Ambient Temperature (T) – The Arrhenius Relationship

For the polymeric materials under consideration the temperature dependence of the moisture diffusion coefficient can be represented as

$$D = D_0 \exp^{-E_d/RT} \tag{2.14}$$

The fact that the moisture diffusion coefficients increased with temperature readily indicates that equilibrium absorption conditions are reached faster at the higher temperatures.

B. Effect of Relative Humidity ∅

The equilibrium moisture content of olymeric materials is related exponentially to the relative humidity:

$$M_m = a \varnothing^{\,b} \tag{2.15}$$

The constants "a" and "b" have to be evaluated experimentally.

2.3.2 Internal factors: Interface, coupling agent, voids

Diffusion is not enhanced by transport along the epoxy/glass interface [Mcmaster and Soane, 1989]. However significant changes will occur when water reaches the interface. Thicker films delaminate faster due to the larger thermal stresses generated by thermal expansion coefficient mismatch.

To get a better adhesion strength of the Epoxy/Silica system, Silane coupling agents are often applied on the matrix. Silane coupling agents do not function by preventing molecular water from reaching the mineral-polymer interface, but by competing with water molecules for the mineral surface so that water cannot cluster into films or droplets [Plueddemann, 1974].

Using Proton NMR spectra, the existence of the interface has been verified by observed weak spin-diffusion coupling of the spin polarization of the coupling agent and the matrix proton [Plueddemann, 1974]. No definitive evidence was produced when trying to find evidence of water in the coupling agent layer.

Experiments have been performed using Proton NMR to probe the question of the uniformity of water distribution based on possible variations in crosslinking density [Vanderhart, Davis, and Schen, 1999]. They indicate that water molecularly disperse in the epoxy rather than aggregate in a water-like state within voids. There is no evidence for multiple sites for water. It has been speculated that voids in electronics packaging polymeric materials are well distributed and probably have dimensions of 9-100 nm, since there are a lot of inter-particle regions, unwetted by matrix polymer. Using ambient-temperature Bloch-decay proton spectra for samples equilibrated by immersion in water, void volume fraction of 0.0020±0.003 was found, however voids seemed to play a relatively benign role:

1. Voids do not serve as "avoidable additional reservoirs' for water even at high humidity. Thermodynamics dictate that at 29 ^{0}C, voids fill with water only when the RH exceeds 89%.
2. Few of the voids are connected to the surfaces by low-impedance paths.
3. No new pathway created during solder reflow, transport of moisture can probably be accounted for mainly with the context of the high-temperature diffusion of moisture through the matrix.
4. Accelerated aging at 121 ^{0}C and a partial pressure of a water vapour of 2×10^5 Pa, resulted in 20±5% reduction in void water and 45±15% increase in matrix water. It was speculated that accelerated aging and the plasticizing action of water lead to a physical expansion of this high-T_g solid.

2.4 Predicting and Modeling Non-Fickian Moisture Diffusion

To correlate Non-Fickian weight gain data with a time–dependent boundary condition, as motivated by the viscoelastic response of polymers, the methodology to reduce non-Fickian moisture weight gain data in a manner that enables the evaluation of the diffusion coefficient and moisture profiles across the thickness of composite laminates was proposed by Cai and Weitsman, [1994]. The results demonstrated that in some circumstances the non-Fickian moisture profiles result in residual hygro-thermal stresses, which differ by about 25% from predictions based upon classical diffusion.

Wetness fraction has been introduced to cater for the concentration discontinuity in the application of Fick's diffusion equation to multi-materials systems of IC packages [Wong, Teo and Lim, 1998]. Commercial thermal diffusion software was adapted to model the transient moisture diffusion in IC packages. The wetness fraction also makes it possible and simple to compute the vapour pressure in a delaminated region within IC packages at high solder reflow temperature (about 220-260^{o}C).

Moisture diffusion in IC packaging materials depends on the concentration gradient (Fick's law) as well as the moisture concentration itself [Wong, et al., 1999]. An integrated non-linear finite element diffusion modeling and optimization procedure was proposed to characterize moisture diffusivity as a continuous function of moisture concentration from a single moisture sorption experiment. The moisture distribution

within an IC package can be accurately predicted and the result can be used for package design and analysis.

Moisture weight gain and loss in a PBGA as a function of time including package geometry and materials selection was used in Finite Element Analysis and critical moisture concentration which led to package cracking was found for this package [Galloway and Miles, 1997]. Transient variations of fracture toughness G_t (Thermal strain energy release rate), G_h (Hygro strain energy erlease rate) and G_{tot} (Total strain energy Release Rate) during solder reflow were calculated using a virtual crack closure technique. G_h has been found to have a significant impact on package delamination [Tay and.Lin, 1999]

2.5 Improving Water Resistance and Crack Resistance of IC packages

2.5.1 Improving Water Resistance of IC Packages

The reliability of IC packages is sensitive to moisture; therefore it is important to improve water resistance of the IC packages. In recent years, approaches by enhancing the packaging material properties or improving the design of the package structure or applying some hydrophobic coating for die have been proposed in military application. [RTC Group,2000].

Mold compounds have been found to have the strongest correlation with package moisture performance [Teo, Wong and Lim, 1998]. By matching the material combination, the best combination has been achieved close to Level 1 performance. Package moisture performance is dominated by the moisture properties, M_{sat} (Water Mass at saturation) and diffusivity of mold compound, and also affected by CTE (Coefficient of Thermal Expansion) of package materials. For die-attach material, high adhesion shear strength is to be recommended. It has been found that die attach material has a significantly weaker effect on package moisture performance.

It is generally believed that better adhesion between the encapsulant, leadframe, and the silicon chip will result in improved reliability [Kim, 1991]. Samuel Kim investigated the adhesion with various test methods including conventional destructive and nondestructive scanning acoustic microscopy (SAM) analysis. He concluded that adhesion between the leadframe, chip and molding compound can reduce or eliminate delamination and cracking during VPR (Vapor Phase Reflow). Adhesion influences the integrity of IC packages and is directly influenced by the viscosity of the molding compound. Leadframes are required to have strong oxide layers for good adhesion. For copper leadframes, surface finishing and alloy plating are effective to improve the adhesion properties [RTC Group, 2000]. Sn-Ni alloy plated leadframe has been found to have a low moisture penetration due to its CTE close to the epoxy resin and good adhesive properties. A minimized area of silver-plating (Ring plating) for leadframe has been achieved to reduce the Al corrosion. [Kim, 1991]

Other methods, such as dimpled lead frame; UV-ozone cleaning for slot lead frame packages increases the interfacial strength [Tae-je, et al. 1996]; Moisture blocking planes---large metal power and ground planes [Shook, 2001] were also proposed in recent years.

2.5.2 Improving the Resistance to Cracking of IC packages

It is very important to improve the resistance to cracking of IC packages since cracking would cause financial loss and bad package reliability. The methods have been proposed in recent years to improve moisture resistance [Kitano, 1988; Suhl, 1990]:

1. Prevent the package from absorbing moisture. It was found that wrapping packages with a moisture protective film, could enable the packages to be stored 10 times as long as unwrapped ones.
2. Bake and hermetically seal the backed components in dry nitrogen ambient bags prior to SMT exposure. This adds a step to the assembly process thereby adding time, cost and process control.
3. Design structure of package to decrease maximum stress of plastic due to vapor pressure, such as increasing thickness for samples with moderate sized die, annealing to reduce the residual molding strain.
4. Use a Tab to make the rigid surface more flexible.
5. Use sockets, which are solder mounted to the board.
6. Apply a chemical adhesion promoter (HMDS, which is hydrophobic) to the leadframe and die just prior to the molding operation. Tests have been done with several adhesion promoters, without mold release agents, with a range of thermal

expansion and glass transition values, and with built-in moisture collectors. None had any significant effect on cracking rates but several had severe effects on the mold.

7. Develop plastic with high strength at high temperature.

Although the proposed methods are not difficult to apply, the appropriate method to use will obviously depend on the particular circumstance and the strengths and weaknesses of the manufacturer.

Chapter 3
Non-Fickian Moisture Diffusion in Polymeric Materials

3.1 Introduction

In chapter 2, a brief review has been made on non-Fickian diffusion of polymeric materials. In this chapter, a detailed literature review on past studies of non-Fickian moisture diffusion in polymeric materials is described. Results from different testing techniques are collected and compared as well.

3.2 The Classification of Non-Fickian Moisture Diffusion

In the presence of higher temperature and higher moisture concentration, moisture diffusion in polymeric materials no longer follows Fick's Law, non-Fickian diffusion occurs and it is classified by kinetic absorption curves into (1) Two-stage (2) Sigmoid and (3) Case II.

3.2.1 Fickian Sorption

We have discussed Fick's Law in Chapter 2, we will compare different diffusion behaviors by analyzing the Figure 3.1 (a) is a typical plot of Fickian sorption kinetic and its characteristic features are [Van der wel and Adan, 1999]

1. An initially linear plot of M (Mass of obtained moisture) as a function of $t^{1/2}$ (Time for sample reach mass equilibrium).
2. With increasing t, the absorption curve smoothly levels off to a saturation level M_∞ (Mass of obtained moisture at equilibrium).
3. When M_t/ M_∞ is plotted as a function of $t^{1/2}/L$ (where L is the film thickness of the sample) a "reduced" plot is obtained, which is identical for different values of film thickness.

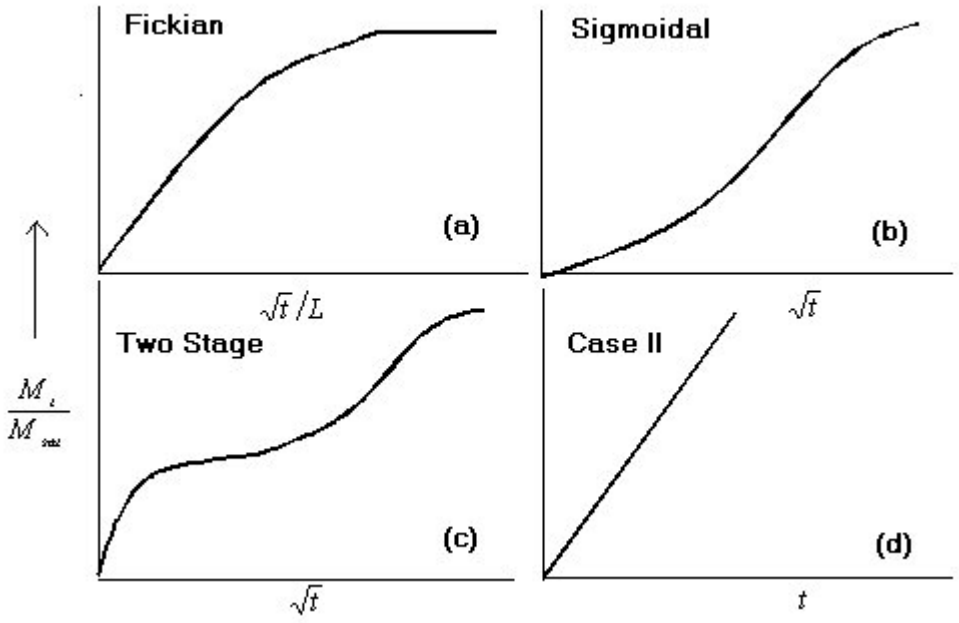

Figure 3.1 Classical Fickian sorption and the diffusion classes of non-Fickian sorption

Fickian desorption curves show the same features. "Reduced"absorption and desorption curves coincide over the entire range of $t^{1/2}$ when D is constant, " Reduced " absorption curves lie above the corresponding desorption curves coincide over the

entire range of $t^{1/2}$; when D is an increasing function of concentration, "Reduced" absorption" curves lie above the corresponding desorption curves. The features that are described here only apply when two conditions are met: (1) First, local equilibrium at the material surface must be maintained. (2) Secondly, the external penetrant activity must be kept constant over the entire experiment. Actually, in most of cases, the assumption that D is constant may not be valid. So the solution as equation 2.1 may only be considered as an averaged value $\overline{D}$ of D(t).

3.2.2 Sigmoidal Sorption

Figure 3.1(b) shows an S-shaped curve with a point of reflection. A "variable surface concentration" (VCS) model was proposed to explain the behavior. Based on the assumption that the transport process in the film is Fickian, but due to slow establishment of equilibrium at the surface of the film, the kinetics appears anomalous.

3.2.3 Two-stage Sorption

Two-stage sorption is a frequently encountered anomalous type of absorption. Figure 3.1(c) shows that the curve appears to be composed from two different parts: (1) fast Fickian absorption (2) slow non-Fickian absorption. The curve is Fickian from the start and then it starts to level off. The curve is extended through a non-Fickian part instead of reaching the typical Fickian saturation level of absorption. A diffusion-relaxation model has been used to describe these features satisfactorily. The total weight gain at time t may be expressed as the linear superposition of two phenomenologically independent contributions:

$$M(t) = M_f(t) + M_R(t) \quad (3.1)$$

where M(t) is the total weight gain at time t, $M_f(t)$ is the diffusion part governed by Fick's Laws, and $M_R(t)$ is the structural part resulting from polymer relaxations.

3.2.4 Case II Sorption

It was noted that some systems of polymer sheets and liquid penetrant showed linear kinetics as shown in Figure 3.1(d), i.e. mass uptake proportional to time, accompanying by a considerable amount of swelling. As case II sorption principally requires a sharp diffusion front and a constant progress of that front in time, overall linear kinetics will not occur in case of a geometry other than a uni-dimensional sheet (e.g. a sphere).

3.3 History-dependent Non-Fickian Diffusion & Physical and Chemical Effects of Moisture on Polymeric Materials

March and Lasky[1981] observed that the diffusion process in epoxy and epoxy-glass composite can be clearly described by a model embracing type II diffusion involving a mobile component and a component trapped at unspecified sites but whose number is fixed. The reaction is endothermic. Additionally the absorption is exposure- history dependent, requiring further study on the base laminate chemistry to get a better understanding of the solution process. The distribution of occupied bond sites set initially at the lamination is a significant factor in the absorption process and stabilizing treatments above T_g are important in desorbing the water.

Distinctive Non-Fickian diffusion behavior with thick, free and thin, glass supported epoxy films have been observed [Mcmaster and Soane, 1989]. Water-up is equilibrated via a two-stage process. Plasticization of polymer by the penetrated water is indicated by higher sorption diffusion coefficient than the desorption one and increased stress relaxation rate in supported films exposed to moisture.

The sorption of water in epoxy-based materials can significantly alter their properties. De Neve and Shanahan [1995] has found that long term exposure of epoxy adhesive to water led not only to physical (reversible) weakening due to water ingress caused by plasticisation but also chemical (irreversible) degradation brought by hydrolysis. Gravimetric experiments have been conducted which measured the equilibrium weight changes with absorption/desorption cycles. The initial weight increase being due to chemically combined water to the subsequent weight loss resulting from leaching of severed chain segments.

In 1985, Wong and Broutman proposed that film thickness scaling as an important technique for diagnosing non-Fickian sorption of water in epoxy resins. The molecular relaxation of the epoxy network in the diffusion processes was used to explain the thickness anomaly and history (hygro-thermal) dependent diffusion. They concluded that a cycle of sorption and desorption increases the preexisting free volume in the polymer network and subsequently changes the sorption behaviour. Non-Fickian sorption may occur for (1) an insufficiently cured resin which undergoes further crosslinking upon absorption of water; (2) oxidation of the resin during sorption experiments which gives a higher sorptive affinity of resin towards water. It was shown that the lack of conformity between successive sorption cycles was not a result

of permanent damage but a reflection of network alterations which could be relaxed by annealing. Later they proposed a model for the diffusion mechanism of water in glassy epoxy resin by dividing the glassy epoxy network into 2 regions in which water molecules possess different mobilities: free volume and occupied volume. This mechanism was used to describe the concentration-dependent D in sorption and resorption and explain concentration-independency of D at T close to T_g of epoxy-water binary mixture.

Diamant, Marom and Broutman [1981] pointed out that water molecules could exist in a polymeric medium in two states-unbound as well as bound to the polymer molecules. The unbound molecules are contained in the free volume and relatively free to travel through the holes. The bound water molecules are immobilized and cause swelling. More free volume within the polymer will results in more unbound water molecules while a higher resin polarity accounts for more water molecules in the bound state. They also concluded that the coefficient of moisture diffusion depended on four main factors:

(1) the polymer network structure

(2) the polymer polarity, determining polymer-moisture affinity

(3) the physical morphology of the polymer (e.g a two-phase structure);

(4) the development of microdamage under severe humidity conditions.

It is difficult to predict which of these factors or a combination thereof dominates the moisture diffusion process into a given epoxy resin.

By using compounds with different, from moderate to high, concentration of silica and alumina nitride fillers, Schitsky and Suhir [2001] did a weight-gained analysis. The

analysis indicated that the moisture diffusion was of non-Fickian type and depended mainly on the specimen's relative humidity and the filler direction. The hygro-thermal stresses, caused by moisture diffusion, although relatively low, led to an appreciable decrease in the material's elasticity, resulting in a substantial increase in the material's plasticity.

Bonniau and Bunsell [1981] proposed 2 diffusion models to interpret the absorption of water by 3 different glass epoxy composites with different hardeners under both vapour and liquid conditions (1) Single phase absorption: water weakly bonded to the polymer by hydrogen bonding (2) Two phase absorption: classical diffusion and the other phase water more firmly fixed to the sites in the polymer. It was also found that the behaviors of diffusion were different for water vapor and liquid water because of the different mechanisms. Additionally, accelerated aging test in boiling water was shown to be invalid as different mechanisms such as cracking and chemical attack were involved.

Bao, Yee and Lee [2001] investigated moisure diffusion in Bismaleimide Resin (similar thermosetting resin) by submerging thin specimens in water. They found that initially moisture uptake obeyed Fick's Law while in later stages the rated moisture diffusion kept increasing. Thus they proposed a 2-stage diffusion model that considered the structure relaxation induced by absorbed moisture (a good plasticizer of the resin). Desorption and re-absorption demonstrated that the structural relaxation was irreversible upon desorption of water molecules, since the absorption process was a self-accelerating process while desorption was a self-retarding process. The politicizing and rejuvenating effect of water, which would lead to a more open

network structure, faster relaxation, and cause faster diffusion and higher uptake level in the 2nd absorption, was demonstrated by dynamic mechanical analysis.

Li, Miranda and Sue [2001] also studied hygrothermal diffusion behavior in Bismaleimide resin. They employed the Langmuir model to describe the non-Fickian diffusion behavior observed at two different hygrothermal conditioning temperatures. Dynamic Mechanical Analysis (DMA), Atenuated-total-relfectance Fourier transform infrared spectroscopy (FTIR-ATR) and swelling experiments were conducted and the results revealed that both hydrogen bonding and the nature of the network architecture strongly affect the hygrothermal diffusion behavior of the bismaleimide resin. Moisture diffuses and majority of absorbed moisture occupies free volume as unbound water, while less water can form hydrogen bonds with the polymer to become bound, at the initial stage of absorption. At later stages, majority water becomes bound but unbound water can still diffuse into unoccupied free volume.

El-Sa'ad, Darry and Yates [1990] attempted to explain the reverse thermal effect of epoxy resins with thermodynamics. Reverse thermal effects, which means the sudden increase in moisture absorption when epoxy resins experience a temperature drop near saturation. The results from the swelling experiments showed that changes of free volume of the polymer could not explain the observed reverse thermal effects. The assumption that water absorption in the polymer is an exothermic process was made, and therefore more water must be absorbed accompanying a temperature drop in order to liberate heat and prevent the drop in temperature. These suggest that it was the more tightly bound water, which was mainly responsible for swelling of the polymer (which is responsible for the reverse thermal effect) but not the weakly bound water.

With 3 different resins, Fremont et.al, [2001] found that the amount of absorbed water strongly depended on the resin type though they showed similar moisture absorption behavior. In a first approach, the penetration could be considered as a diffusion process following the Fick's Law, the diffusion coefficient D and the saturation coefficient S could be deduced from the measurements as a function of the relative humidity. The presence of leadframe did not sensibly change the absorption curve, so the above results of D and S could be used for Finite Element Analysis and the simulation model could be simplified. It was found that a first "saturation" occurred after a few hours of aging, and a new diffusion process occurs not leading to a real saturation if samples were left longer in the oven and hence the non-Fickian diffusion.

Masatsugu Ogata, Noriyuki Kinjo and Tatsuo Kawata [1993] clarified the relationship between crosslinking density and physical properties of epoxy resin and factors governing their physical properties, by considering two free volumes, hole free volume V_h and interstitial free volume V_i:

$$V_f = V_h + V_i \tag{3.2}$$

where V_f is free volume, V_h is hole free volume and V_i is interstitial free volume caused by thermal expansion. As the crosslinking density increased, T_g rose and the relaxation behavior shifted to longer times. And the coefficient of linear thermal expansion became smaller in the rubbery region, because as the linking density increased, V_h decreased. Since crosslinking density increase on cured resins, the coefficient of linear thermal expansion, water absorption, diffusion coefficient, and permeability become larger, and the elastic modulus becomes smaller in the glassy

region because, as the crosslinking density increases, vi increases and, accordingly, molecular chain packing became looser; i.e., the specific volume increased.

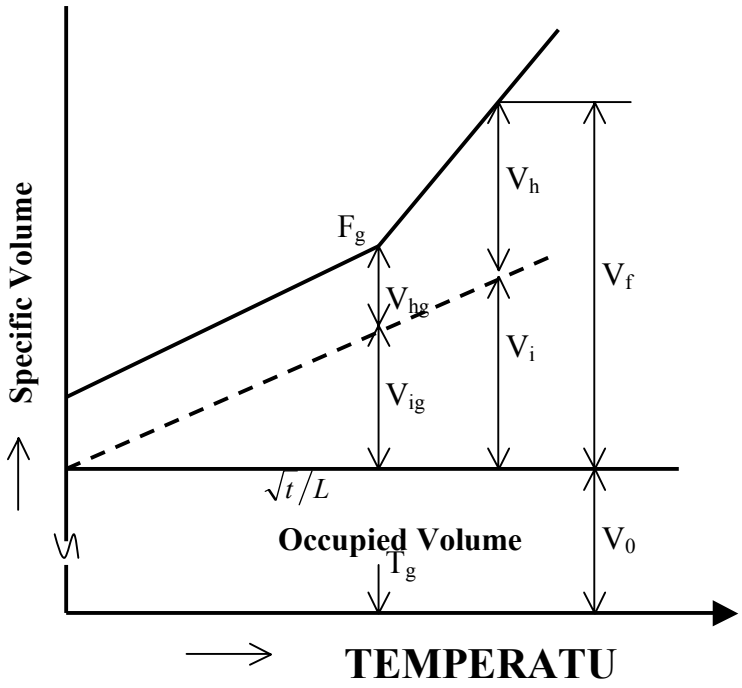

3.2 Schematic representation of composition of free volume

Moisture diffusion in epoxy systems was studied as a function of epoxy-amine stoichiometry and the resulting microstructure [Vanlandingham, Eduljee and Gillespie, 1998]. Differences in diffusion behavior were related to the relative importance of diffusion through the low density and high-density phases for the different stoichiometries. Increasing the humidity level only caused a corresponding increase in saturation level. However, increasing the temperature caused more pronounced non-Fickian behavior. Postcuring caused a decrease in the diffusion coefficient for stoichiometric samples because the holes in the networks through which moisture diffuse would be smaller and the activation energy would increase. Moisture-induced swelling strains increased with increasing moisture content, the reduction in T_g range

from 5 to 20 ^{o}C and were generally larger for amine-rich samples than for epoxy-rich and stoichiometric samples.

Water absorption experiments of exposure to 97% relative humidity over 23 to 75 ^{0}C were conducted on three DCEBA type epoxy resins, by Woo and Piggott [1987]. The results showed that the activation energy for diffusion was independent of relative humidity but the diffusion constant was directly proportional to it. The solubility was not determined by Henry's Law but determined by relative humidity to the 1.4th power instead. Water does not appear to be bound to polar groups or hydrogen bonding sites in the resin since the polarizability is much reduced, although dielectric tests indicate that it does not behave as free water. Clustering of the water molecules in the polymer, rather than complete separation of the molecules since the reduction in effective dielectric constant of the water was only about 55 to 77%.

They concluded that composites obeyed Fick's Law and the volume of water absorbed at equilibrium by the composites usually determined by the polymer matrix volume. They investigated carbon and glass reinforced epoxies over humilities with a range of 33-97%, temperatures from 23 to 100^{0}C. Diffusivities decreased linearly with the square root of fiber volume fraction for both carbon and glass fibers. Fibers appeared as barriers to diffusion and there was strong evidence to show that composites had regions with enhanced diffusivity. Fick's Laws were no longer applicable if the aging is continued after the "first saturation".

In 1988, Woo and Piggott found that 60%-75% water concentrated in disk-shaped regions. The remainder of the water was probably molecularly dispersed. The

proportion of this phase depended on the polar groups in the polymer. By immersing glass fiber reinforced epoxy pultrusions with a range of fiber volume fractions, they found that water provided conducting paths were probably caused by the inter-connection of regions of water concentration at the fiber-matrix interface. In the absence of significant conducting paths, the permittivity obeys simple mixture rules.

Woo and Piggott [1987] also concluded that at least for carbon-epoxy and glass – epoxy, the most important conducting path for water transport in fiber reinforced plastics was provided by voids, since the interphase diffusion model did not agree so well with the experimental data.

3. 4 Testing Methods for Water Sorption

Different testing methods are listed below together with their capabilities and limitations.

JEDEC Standard No 22-A120 [2001], which uses high-resolution balance to measure weight gain/loss, is the standard industrial test for moisture absorption (below 100^{o}C) and moisture desorption (above 100^{o}C). The results can also be used for calculation of Activation Energy E_d for moisture.

Differential Scanning Calorimetry (DSC) [Lin, Teng and Yuen, 1998] was also used to test epoxy resin using the principle that water is a kind of elasticizer and the endothermic peak is related to the relaxation of uncured epoxy resin. An endothermic peak at about 40-50^{o}C was found which proved that DSC was highly sensitive to

moisture absorption. The area under the peak indicates moisture absorption level: the longer the time, the smaller the area.

Proton NMR [VanderHart, Davis and Schen, 1999; Marjanski, Srivasarao, and Mirau, 1998] spectra was obtained by filling the sample voids with water. Spectral line width and chemical shift differences distinguish water in 2 regions: voids and polymer matrix [Chapter 2, pp19].

Solid state nuclear magnetic resonance (NMR) techniques (both ^{1}H NMR and ^{2}H NMR) were used to study the binding states of water within two epoxy formulations along with the possible plasticizing effects of moisture affecting the mobility of polymer chains. [Luo and Wong, 2001].

Schen and Wu et.al, [NIST, 1997] **Combined X-Ray and Neutron Reflectivity Techniques** to determine moisture density profiles and/or atomic composition in the interfacial region of extremely thin polymer films.

Deiasi and Schulte [1988] used **Nuclear Reaction Analysis to m**easure the localized moisture content through the thickness of composite material (graphite epoxy composites with a size: e.g 2.5cm×1.8cm×0.2 cm) based on conditioning samples with D_2O instead of H_2O. Moisture profiles with resolution of 12μm in the direction of the gradient were measured in unidirectional graphite/epoxy composites and found to be consistent with classical diffusion theory. And the results also indicates that D_2O and H_2O are both hydrogen bonded to the electronegative functional groups on the epoxy

resin and contribute equally to a disruption of secondary crosslinking and subsequent reduction in T_g after moisture absorption.

FTIR-ATR (Attenuated Total Reflection) [Buchhold, et al, 1998] was used to study moisture diffusion in the polyimide thin film with a thickness of 2.5μm. The principle used was that pores filled with moisture would result in characteristic OH band and hydrogen bonding at characteristic polar groups of the polymer layer would cause a shift of IR absorption bands. This is not suitable for epoxy based polymeric materials since epoxy itself contains OH band.

X-Ray Diffraction was employed to study the changes in residual strains in crystalline filler particles due to the moisture sorption. It was used to investigate the moisture history of graphite epoxy laminates, which was filled with Aluminum (crystalline filler) particles. [Predecki and Barrett, 1988]

A Screening Dielectric Loss Technique, [March, Van Hart and Kotkiewicz, 1985] was used to investigate moisture absorption in epoxy-glass composites. The principle used is that exposure to various partial pressures of moisture at certain temperature (e.g. 90^{o}C) permitted a kinetics analysis from which an estimate was made of the diffusivity of water in the composites. Values of dielectric loss at saturation level were used to establish a moisture/dielectric loss calibration at 90^{o}C, which can be used to estimate the macroscopic internal moisture content of samples.

Chapter 4
Measurement of Desorption Diffusion Coefficients of Polymeric Packaging Materials

4.1 Introduction

It has been well acknowledged that the absorbed moisture in polymeric packaging materials is responsible for 'popcorn' cracking of IC packages during solder reflow. Many methods such as using microbalance [JEDEC No. 22-A120, 2001; Designation: D5229/F5229M-92, 1992] and TGA [Lau and Chang, 1999] have been proposed to determine the moisture desorption properties of these polymeric packaging materials including molding compound, underfill and die attach materials.

Lead-free solder is becoming widely used in the industry in the recent years, and consequently higher solder reflow temperatures up to 260^{o}C are becoming common. There is thus a growing need to characterize moisture diffusion at high temperatures. However, characterization of moisture desorption properties of polymeric packaging materials at high temperatures remains a problem.

Polymeric packaging materials display a complicated diffusion behavior with the temperature. For example, one type of molding compound which will be later used in this research, preconditioned at 85°C/85% RH for more than 1 year, was tested with Thermo-Gravimetric Analysis (TGA) with a ramp-up temperature profile from 30°C to 600°C at the rate of 10°C/min. Figure 4.1 (a) shows the sample weight decreased dramatically at the temperature around 350°C, which is the decomposition temperature. It is noticed that

there is also a change of slope at around 140°C, which was around the glass transition temperature T_g (144°C) of this molding compound. Diffusion obviously increases in a higher rate in the temperature above T_g than that below T_g. Although the decomposition behaves very obviously around 350°C, it is hard to tell at what temperature it starts to take place since polymeric materials are complicated. Polymers have a flexible rubbery microstructure above T_g while below T_g they are in a rigid glassy state. It is reasonable to suspect a certain amount of chemical volatiles in addition to the moisture coming out at high temperatures between 144 °C and decomposition temperature 350°C.

In order to solve the problem mentioned above, Karl Fischer Titration is proposed here as an effective method for characterizing moisture desorption of polymeric packaging materials.

Due to the advantage of eliminating interfering factors during high temperature desorption testing, Karl Fischer (KF) Titration has been widely used in pharmacy and chemistry [Wu and McGinity, 2000; Buchhold, et al, 1998; Isengard, 1995] for the determination of moisture content in different substances. Its advantages are: excellent reproducibility and selectivity, no need for the system calibration and be capable of ramp-

up heating, and the ability to distinguish between physically bonded surface water, chemically bonded water and water produced by decomposition.

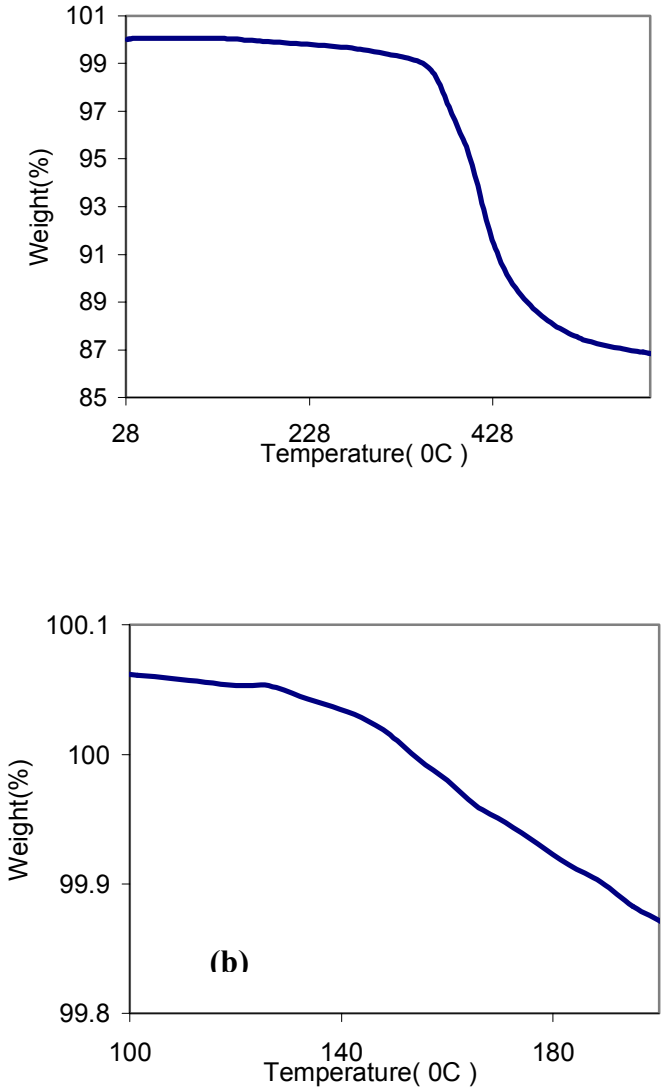

Figure 4.1 Weight loss of molding compound by TGA with a temperature ramping up from 30°C to 600°C at 10°C/min
(a) Whole process (b) Zoom-in curve

4.2 Experiments

4.2.1 Objectives

The objectives of the experiments described in this chapter are:

a) To seek an effective and reliable methodology for characterizing moisture properties of polymeric materials
b) To find the effects of glass transition temperature T_g on moisture desorption coefficient D_{desorp}c) To compare D_{desorp} to D_{adsorp}d) To determine the cause of non-Fickian diffusion behavior

Samples of molding compound, underfill and die attach materials were preconditioned at 85^0C/ %85RH till saturation and then desorbed by Karl Fischer Titration at 5 different temperatures. Thermo-gravimetric Analysis (TGA) was also done for comparison with Karl Fisher Titration. The differences between the results obtained using these two techniques could be attributed to outgassing at high temperatures by investigating the nature of polymeric materials.

4.2.2 Materials

The materials used in this study are: Molding Compound , Underfill and Ablebond Die Attach [Confidential info]. Molding Compound is an epoxy-based system filled with fumed silica, with a T_g of 144^oC, while Underfill is silica fillers/cyanate ester matrix with

a T_g around 138°C (TMA) and 152°C (DSC). Die Attach is epoxy-based filled with silver particles and its T_g is 100^0C.

Square-chip samples with dimension of $10\times10\times1mm^3$ (Molding Compound/MC), $15\times15\times0.6mm^3$ (Underfill/UF), $15\times15\times 0.5mm^3$(Die Attach/DA), were made for the Karl Fischer Titration tests. For TGA tests, materials were made into column and then machined into 3 dimensional shapes: MC {cubic: $4\times4\times3$ mm^3), UF (disk: diameter 4mm, height 4 mm), DA, (disk: diameter 4mm, height 4.5 mm) due to the size limitation of the sampler of the TGA used.

4.2.3 Karl Fischer Titration

Karl Fischer titrator MKC-510 with Evaporator ADP-511 (KEM company) was used in this experiment. Karl Fischer Titration is a titration method for determining the water content of samples using a pair of platinum electrodes and a reagent containing iodine, sulfur dioxide, pyridine, and methanol. A polarizing current is applied to the electrodes and the resultant potential is measured. Most pH/mv meters are equipped on the rear panel with a pair of connectors which provide a 10-microampere current continuously during the titration. A relative drift stop of 0.01μg/s was set in our tests.

The principle of Karl Fischer Titration is based on an electrochemical reaction:

$$I_2+SO_2+3Base+ROH+H_2O \longrightarrow 2Base\text{-}HI+Base\text{-}HSO_4R$$

The reaction takes place in the presence of a base and a solvent. Examples of the base include: imidazole or primary amines and a typical solvent might be methanol or ethyleneglycolmonomethylether or diethyleneglycolmonomethylether.

A chemical reaction takes place between water (W) and iodine (I). There is a strict ratio of 1:1 between W and I:

1I + 1W------->Reaction

Once the concentration of iodine in the Karl Fischer reagent is determined, the unknown concentration of water in the sample can be determined. As one I reacts with one W, the amount of I used during the titration must be equal to the amount of water present in the sample.

There are 2 types of Karl Fischer Titration: Volumetric and Coulometric. In this study, coulometric titration is used because it is more precise. With a coulometric Karl Fischer titration, the amount of water present is determined by measuring the AMOUNT OF CURRENT (Coulombs) generated during the titration. Coulombs are a measurement of current (ampere) multiplied by (titration) time (seconds). There is a relationship between the iodine (I) used for titration, the sample's water content (W) and the current:

Current (A) x time (sec) = Coulombs (C)---->I + W---->KF Reaction

According to Faraday's Law: 2 x 96,485 Coulombs are needed to generate 1 mole of iodine. Once the current generates the iodine, it reacts 1:1 with water in the KF reaction.

The coulometric Karl Fischer titrator performs the following three (3) functions:

1) Instead of dispensing KF reagent as in a volumetric titration, this instrument actually makes the reagent inside the cell. A current flows through the solution and iodine is generated by this current.
2) It detects the endpoint (end of titration).

3) It calculates the end result.

The main components of a coulometric titrator are as follows :

1) & 2) The anode and cathode are each comprised of a platinum electrode which conducts current through the cell. At the anode, iodine is generated. Thus, the standard KF reagent is formed in the cell and goes on to react with water.

3) The platinum measuring (indicating) electrode determines if iodine needs to be generated to react with any water that might be present. The circuitry in the electrode voltametrically senses when water is present. As long as the electrode detects the presence of water, it will electronically "tell" the instrument to continue generating current through the anode and cathode to produce iodine to react with the water. When the electrode determines that all the water is gone, it "tells" the instrument to stop generating current and the endpoint is reached.

4) The microcomputer records the total amount of current (coulombs) consumed and the titration time in seconds. Based on the relationship between coulombs and iodine, the exact amount of iodine generated can be determined. Since water reacts 1:1 with iodine, the amount of water present can then be calculated.

Figure 4.2 Karl Fischer Titrator

Figure 4.3 Evaporator

Three different samples were preconditioned at 85°C/85%RH over 1500 hours to obtain moisture saturation and a relatively static moisture concentration across the thickness. The samples were then and immediately placed into the Evaporator for testing. Karl Fischer Titrator had an initial stable drift of 0.02ug/s and the temperature of the evaporator was preset at the certain value and stabilized before testing. A nitrogen flow around 250ml/min was used to purge the heating tube of evaporator where the samples were heated to release the moisture, to assure the detected moisture was completely from

the tested samples. Software "Labview" was used to acquire the data that was given by titration at every minute.

4.2.4 TGA (Thermo gravimetric Analysis)

TGA is a thermal analysis technique used to determine changes in sample weight as a function of temperature. It can also be used to study changes in sample weight as a function of time at a constant temperature (isothermal TGA). The analysis can be performed under nitrogen, in the presence of air, or other reactive atmospheres.

Figure 4.4 Thermo-Gravimetric Analysis (TGA)

TGA has a lot of applications:

A) Determination of thermal and thermo-oxidative stability of various inorganic, organic and polymeric substances at desirable time and temperature conditions in a desirable environment

B) Determination of moisture and volatile content

C) Determination of reinforcement fractional weight in composites

D) Study of kinetics of reactions involving weight loss (dehydration, decarboxylations, etc) or weight gain (oxidation).

TGA operates on a null-balance principle. A pair of photodiodes is used to register the displacement of the balance beam. A low thermal resistance furnace performs the heating of the sample. The temperature of the sample is monitored by a thermocouple located close to the sample boat, and is recorded as the X-axis. A plot of mass or mass percent versus time or temperature is called a thermogram or thermal decomposition curve. The sample is usually degraded or evaporated and cannot be recovered in its original state.

Samples of same materials (MC, UF, DA) with 3 dimensional shapes were tested with TGA (PERKIN ELMER Thermogravmetric Analyzer TGA7). Samples that were preconditioned at the same condition of 85^{o}C/85%RH were placed into TGA sampler and heated up at a rate of 100^{o}C/min to testing temperatures (220^{o}C, 170^{o}C, 140^{o}C, 120^{o}C, 85^{o}C, respectively). Nitrogen purging was applied to the heating tube of the TGA to eliminate the effect of atmospheric moisture. TGA testing durations were 6, 16, 16, 30, 50 hours for the tests at 220^{o}C, 170^{o}C, 140^{o}C, 120^{o}C and 85^{o}C, respectively. Weight loss data of samples were collected every minute and used to calculate moisture desorption coefficient D.

Another TGA test with a ramp-up temperature profile of ramping from 30^{0}C to 600^{0}C at the rate of 10^{0}C/min and holding at 600^{0}C for 20 minutes was done with MC samples. The purpose of this test was to identify the weight loss trend with the temperature changes.

4.2.5.GC/MS (Gas Chromatography/Mass Spectrometry)

GC analysis is a common confirmation test. Among its uses are drug testing and environmental contaminant identification. GC analysis separates all of the components in a sample and provides a representative spectral output. Sample is injected into the injection port of the GC device. The GC instrument vaporizes the sample and then separates and analyzes the various components. Each component ideally produces a specific spectral peak that may be recorded on a paper chart or electronically. The time elapsed between injection and elution is called the "retention time." The retention time can help to differentiate between some compounds. The size of the peaks is proportional to the quantity of the corresponding substances in the specimen analyzed. The peak is measured from the baseline to the tip of the peak.

GC/MS separates chemical mixtures (The GC Component) and a very sensitive detector (The MS component) with a data collector (the computer component). Identification of a compound is based on the fact that every component has a unique fragmentation pattern. A library of known mass spectra which may be several thousand compounds in size is stored on the computer and may be searched using computer algorithms to assist the analyst in identifying the unknown compound.

Preconditioned samples of MC and UF were tested with GS/MS. The purpose of using GC/MS in this work was to identify the released substances at different temperatures ($220^{o}C$, $170^{o}C$, $140^{o}C$, $120^{o}C$, $85^{o}C$). A ramp-up temperature profile was used to differentiate the spectra collected at certain temperatures. An amount of particle sample which is less than 10mg was heated up to $85^{o}C$ after being injected and held for 10

minutes to obtain the GC/MS spectra at this temperature. Other samples were similarly tested and the spectra at 120°C, 140°C, 170°C and 220°C were obtained.

4.3 Data Analysis of KF Titration and TGA tests: Calculation of Desorption Diffusion Efficient D and Activation Energy E_d

By using Microsoft Excel Solver embedded with a visual basic program to solve the acquired data [Koh, 2001, Appendix 1], moisture diffusion coefficients (D) at different temperatures (220°C, 170°C, 140°C, 120°C, 85°C) of different materials (MC, UF, DA) were obtained, respectively.

Based on the 2 assumptions, (1) constant diffusion coefficient (2) concentration diffusion coefficient, this program fits the experimental curve with the analytical one by utilizing the least square regression method.

4.3.1 Assumption for Excel Solver to Extract the Value of Diffusivity

The application is based on the assumption that immediately the sheet is placed in the vapor the concentration at each surface attains a value corresponding to the equilibrium uptake for the vapor pressure existing, and remains constant afterwards. The sheet is considered to be initially free of vapor. For diffusions with constant diffusion coefficient, D are obtained from equation (4.1) and (4.2). For concentration-dependent diffusion coefficients, application of equation (4.1) and (4.2) to experimental curves at each temperature yields some mean value $\overline{D}$ of the variable diffusion coefficient averaged over the range of concentration appropriate to each curve. This method devised by Crank and

Park depends on the fact that, for any experiment, $\overline{D}$ provides a reasonable approximation to $(1/C_0)\int_0^{C_0} Ddc$, where 0 to C_0 is the concentration range existing in the sheet during that experiment. In this case, the approximation of $\overline{D}$ is sufficiently accurate. [Crank, 1975]

Therefore, the desorbed moisture weight M_{sat}, which was considered as the moisture weight in sample at the saturation, of the sample approximately equaled the detected moisture weights in KF Titration tests, and for TGA tests, the lost weight.

4.3.2 1-dimensional and 3-dimensional Diffusion

According to Crank 1975, that "edge effect" means that the usual assumption of one - dimension diffusion is not strictly correct, with thin membranes (l/a≤0.2) edge effects may safely be neglected". The KF Titration samples have the l/a value of 0.6mm/15mm=0.04 ≤0.2, therefore, 1 dimension diffusion equation is applied. With a given thickness of the sample, moisture desorption coefficient D was solved according to the equation solution, for a Fickian specimen subjected to the 1-Dimensional diffusion which is represented by the following equation [Crank, 1975]

$$\frac{M_t}{M_{sat}} = 1 - \sum_{n=0}^{\infty} \frac{8}{[(2n+1)\pi]^2} \exp\left[\frac{-D(2n+1)^2\pi^2 t}{h^2}\right] \qquad (4.1)$$

where M_t is the moisture uptake (in this study, the desorbed moisture) at time t, M_{sat} is the equilibrium moisture uptake (in this study, total of desorbed moisture). D is the diffusivity and h is the thickness of the thin specimen.

For TGA tests, the following 3-Dimensional equation was used considering the TGA sample shape. [Blikstad, Sjoblom and Johannesson, 1984]

$$\frac{M_t}{M_{sat}} = 1 - \frac{512}{\pi^6} \sum_{n=0}^{\infty} \exp\left\{ \frac{-Dt}{(2l+1)^2(2m+1)^2(2n+1)^2} \left[\frac{(2l+1)^2\pi^2}{\chi^2} + \frac{(2m+1)^2\pi^2}{y^2} + \frac{(2n+1)^2\pi^2}{z^2} \right] \right\} \qquad (4.2)$$

The diffusivity and the saturated concentration were extracted from the experimental moisture (moisture desorption data by Karl Fischer Titration or weight-loss by TGA in this study) using the least squares regression method as shown in Fig 4.5. To obtain an accurate D, the experimental data plot that shows certain level of equilibrium is required. The lack of the points shows equilibrium will affect the accuracy of the calculation and causes false D and C_{sat}.

4.3.3 Excel Solver Program to Extract the Value of Diffusivity

Microsoft excel can help you find an optimal value for a formula in one cell -- the target cell on a worksheet. By working with a group of cells that are related either directly or indirectly to the formula in the target cell, solver adjusts the values in the adjustable cells defined earlier, and produces the results based on the target cell formula. Constraints can be applied to restrict the values solver can use in the model and the constraints can refer to other cells that affect the target cell formula.

Constraints are the limitations placed on a Solver problem. Constraints can be applied to adjustable (changing) cells, the target cell, or other cells that are directly or indirectly related to the target cell. In the case of linear problems, there is no limit on the number of constraints. In the case of nonlinear problems, each adjustable cell can have the following constraints: a binary constraint; an integer constraint plus upper, lower, or both limits. And you can specify an upper or lower limit for up to 100 other cells.

Formula 4.1 and Figure 4.2 are used to extract the value of diffusivity from the experimental data by employing the least square regression method. The least square regression method [Appendix 2], as discussed in the previous section, is as follows:

The theoretical equation should be fitted through a set of points in which the square of the vertical distance of these points from the straight line is a minimum. [Kreyszig, 1999]

This can be accomplished by using of Excel inherent solver program. The function mt1d (n_0, h, d, t, m_{sat}) has been written, using formula (4.1), to generate the value of mass loss, M_t, at each time step t with a certain value of D. Hence, with this value, the error between the theoretical and experiment value for each time step for that value of D can be found. Setting the total sum of the square of error as the target cell in the Excel solver to minimize using the Generalized Reduced Gradient (GRG2) nonlinear optimization code [The Microsoft Excel Solver tool uses the Generalized Reduced Gradient (GRG2) nonlinear optimization code developed by Leon Lasdon, University of Texas at Austin, and Allan Waren, Cleveland State University. Linear and integer problems use the simplex method with bounds on the variables, and the branch-and-bound method, implemented by John Watson and Dan Fylstra, Frontline Systems, Inc. http://www.frontsys.com], the value of D can then be extracted from the experimental results. Furthermore, an "artificial" mathematics constraint of D greater than 0.0005 is applied so that the values of D obtained comply with the physic of diffusivity always having a positive value. An example of curve fitting is shown as Figure 4.5. The uncertainty of the experiment is discussed in the section 4.4.

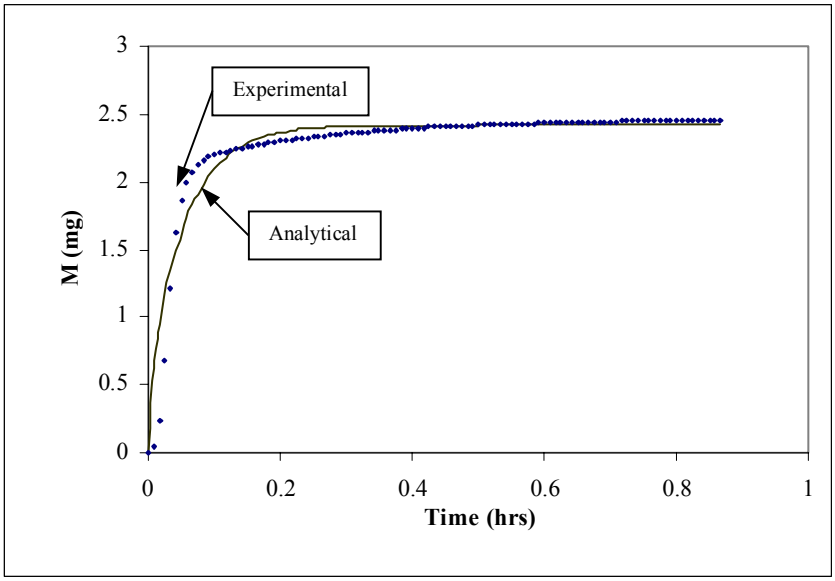

Figure 4.5 Extracting material properties (Moisture diffusion coefficient D) using curve fitting (Sample data)

Furthermore, in order to get a better fitted, the assumption of that the saturated mass has been reached can be relaxed by including the saturated mass as an optimization parameter. However, this will be done at the expense of the computation time required to optimize the value of *D*. Hence, the chart of the mass loss against time is plotted from the experimental data to determine the needs for relaxation of this assumption.

4.3.4 Arrenhius Relationship

Since D often exhibits a dependence on temperature that follows an Arrenhius relationship given by [Rao, Balasubramania and Chanda, 1981]

$$D(T) = D_o \exp(-E_d/RT) \tag{4.3}$$

Then,

$$\text{Ln}(D) = \text{Ln}(D_o) - (E_d/RT) \tag{4.4}$$

where D(T) is moisture diffusion coefficient, D_o is the pre-exponential factor for fitted line, E_d is the activation energy, R is the universal gas constant (R = 8.314 J/mole.K) and T is in degrees Kelvin.

A plot of the diffusion coefficient and 1/T will then be helpful in evaluating the pre-exponential factor D_o and the activation energy for diffusion E_d. The Arrenhius relationship plots were also discussed based on the experimental results of KF titration and TGA.

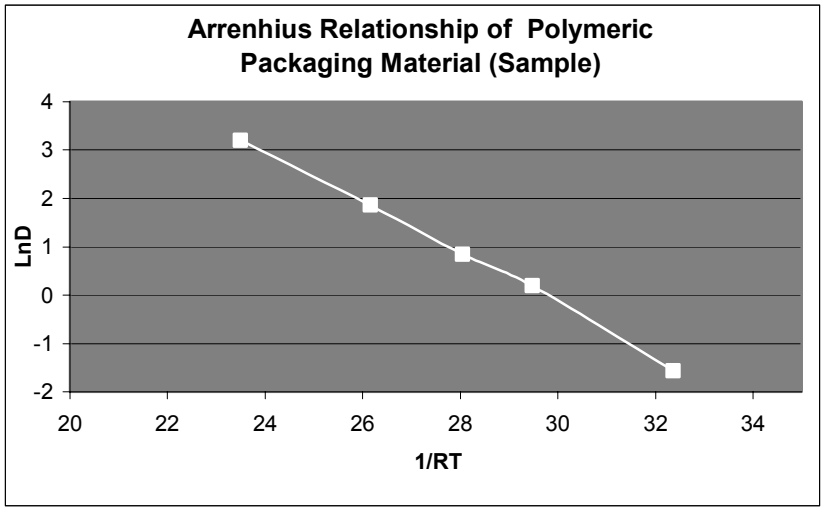

D_0=Diffusion Coefficient
E_d=Activation Energy
T =Temp(K)
R =8.63X10^{5}ev/K

Figure 4.6 Arrenhius Relationship

4.4 Accuracy and Repeatability of the Results

The accuracy of the measurement of a quantity such as desorbed moisture mass in this experiment depends not only on how the measurement was made, but also on how the

measuring device was calibrated. Furthermore, it will also depend on the accuracy of the measuring equipment, which is the smallest numerical value that can be estimated with the measuring device. Besides these systematic errors, there is also unavoidable uncertainty in the measurements due to the random errors which can only be minimized but not eliminated

Since the diffusivity D computed is a function of time, temperature and weight, the systematic error will be the sum of all of the errors in percentages form. If we ignore the errors from time and temperature based on the assumption that these two factors are handled properly during the tests, we will focus on the error of the weight. It is also the error for other corresponding parameters calculated in this paper.

Since random errors, as the name suggests, affect a measurement in a random manner, taking a large number of measurements will produce values that are distributed on either side of the true value and hence, the mean error will cancel each other out and hence, reducing the random error. However, it will never be sure that the value toward which the mean is converging really represents the true value or whether it represents the true value modified by some small determinate error. In practice, assuming the mean equals the true value will work most of the time.

The center of the normal distribution of the experimental data will be the mean value of the mass computed and the width of the normal distribution is given by the standard deviation.

Standard deviation can then be used to compare computed values with the experimental data. If the experimental data and computed data fall within two standard deviations, there will be 95.5% confidence that the next set of measurements will agree with the computed diffusivity.

The standard deviation will be computed as follows:

1. Curve-fit the experimental data with the theoretical equations 4.1 and 4.2.
2. Compute the sum of square of errors between the experimental and computed mass loss.

Standard deviation δ will be computed as follows:

$$\delta = \sqrt{\frac{\sum (m_{\exp} - m_{cal})^2}{n-1}} \tag{4.3}$$

In equation 4.3, $m_{\exp}$ is the experimental data, m_{cal} is the computed mass loss and n is number of samples.

Therefore, for our experiments, the relative error of the measurements maybe estimated by

$$\text{Relative Error} = \frac{\delta}{M_{sat}} \times 100\% \tag{4.4}$$

Due to the long duration of experiments, the large number of measurements and the complicated sample preparation procedure, it was not practical to repeat every measurement. However, some preliminary trial experiments were done before the whole series of experiments were started, in order to test the repeatability of KFT experiments due to its sensitivity which will influence automatic ending of an experiment. No

repeatability tests have been conducted for the TGA experiments as the TGA test is very much more established than the KFT test.

The results of the repeatability trials for the KFT test are shown in Table 4.1 below. The raw data for these trial tests are given in Appendix 3. As can be seen the repeatability for the KFT test is acceptable.

Table 4.1 Repeatability Trials for the KFT Test

Temperature	85°C		120 °C		140°C		
Results	Set 1	Set 2	Set 1	Set 2	Set 1	Set 2	Set 3
Diffusivity D(mm^2/hour)	0.310	0.404	0.569	0.203	0.291	0.188	0.245
C_{sat} (mg/cc)	2.073	2.015	4.612	5.509	5.501	6.308	5.648
M_{sat}(mg)	0.203	0.197	0.452	0.540	0.539	0.618	0.554
Standard Deviation δ (mg)	0.037	0.040	0.028	0.092	0.011	0.008	0.010
Relative Error = δ /M_{sat} ×100%	3.516	3.864	1.185	3.267	2.038	1.236	1.743
Mean $\overline{D}$ (mg)	0.357		0.386		0.241		
$\frac{D-\overline{D}}{\overline{D}}\times 100\%$	-13.143	13.142	47.428	-47.428	20.763	-22.198	1.435

Temperature	170 °C			220 °C		
Results	Set 1	Set 2	Set 3	Set 1	Set 2	Set 3
Diffusivity D(mm^2/hour)	0.679	0.723	0.710	1.052	1.456	1.202
C_{sat} (mg/cc)	6.629	6.743	6.841	7.547	7.391	7.867
M_{sat}(mg)	0.650	0.661	0.671	0.740	0.724	0.771
Standard Deviation δ (mg)	4.070	3.467	4.193	6.316	3.569	7.178
Relative Error = δ /M_{sat} ×100%	0.041	0.035	0.042	0.063	0.036	0.072
Mean $\overline{D}$ (mg)		0.704			1.237	
$\frac{D-\overline{D}}{\overline{D}}\times 100\%$	-3.544	2.683	0.862	-14.920	17.732	-2.812

Chapter 5
Moisture Desorption Experimental Results and Discussions

5.1 Introduction

Samples made of Molding Compound, Underfill and Die Attach were preconditioned at 85^{o}C/ %85RH till saturation and then desorped by Karl Fischer Titration (KFT) at 5 different temperatures. For each temperature, 3 identical samples were used to obtain 3 groups of the data with repeatability and one group data was used for finally analysis since the data displayed a good repeatability for Karl Fischer Titration (KFT) and Thermo-gravimetric Analysis (TGA). Thermo-gravimetric Analysis (TGA), which was also done for comparison with Karl Fisher Titration. The differences in the results obtained using these two techniques are attributed to the outgassing at high temperatures by investigating the nature of polymeric materials.

Results from Gas Chromatography/Mass Spectrometry (GC/MS) showed that outgassing of chemicals were severe, especially at high temperatures and confirmed the validity of our expectation. This questioned the use of TGA or any other conventional gravimetric methods for studying moisture desorption properties at high temperatures. Karl Fischer

Titration has shown that it is possible to characterize moisture desorption of polymeric materials at high temperatures in a fast and efficient way.

5.2 Results and Discussions

5.2.1 Moisture Desorption by KF Titration

The results of the 3 different materials used in the KF titration tests were showed in Figures 5.1, 5.2 and 5.3 respectively. KF titration detected the desorbed moisture from the sample and the mass of accumulated desorbed moisture from samples was recorded. Therefore, the mass of accumulated desorbed moisture from samples instead of the mass of sample was plotted, and the plot displayed the increasing trend. That is, the "Moisture Content" in the above figures stands for the mass of accumulated desorbed moisture from the sample. As shown in Figure 5.1, desorption rate of molding compound increases with the temperature increases, especially at the initial stages. For each temperature, the desorbed moisture weight tended to reach certain equilibrium different from those of other temperatures. At 220^{o}C, the desorbed moisture weight was particularly higher. There is a sudden stop for tests at the low temperature of 85^{o}C. Compared to the Molding Compound, Underfill and Die Attach materials showed an obviously different desorption behavior. Moisture was desorbed very fast at the initial stages at different temperatures, except at 85^{o}C, where moisture was desorbed at a relatively lower rate. For Underfill, the desorbed moisture weight reached some certain equilibrium at temperatures except 85^{o}C. However, with Die Attach materials, similar equilibriums were obtained at all temperatures.

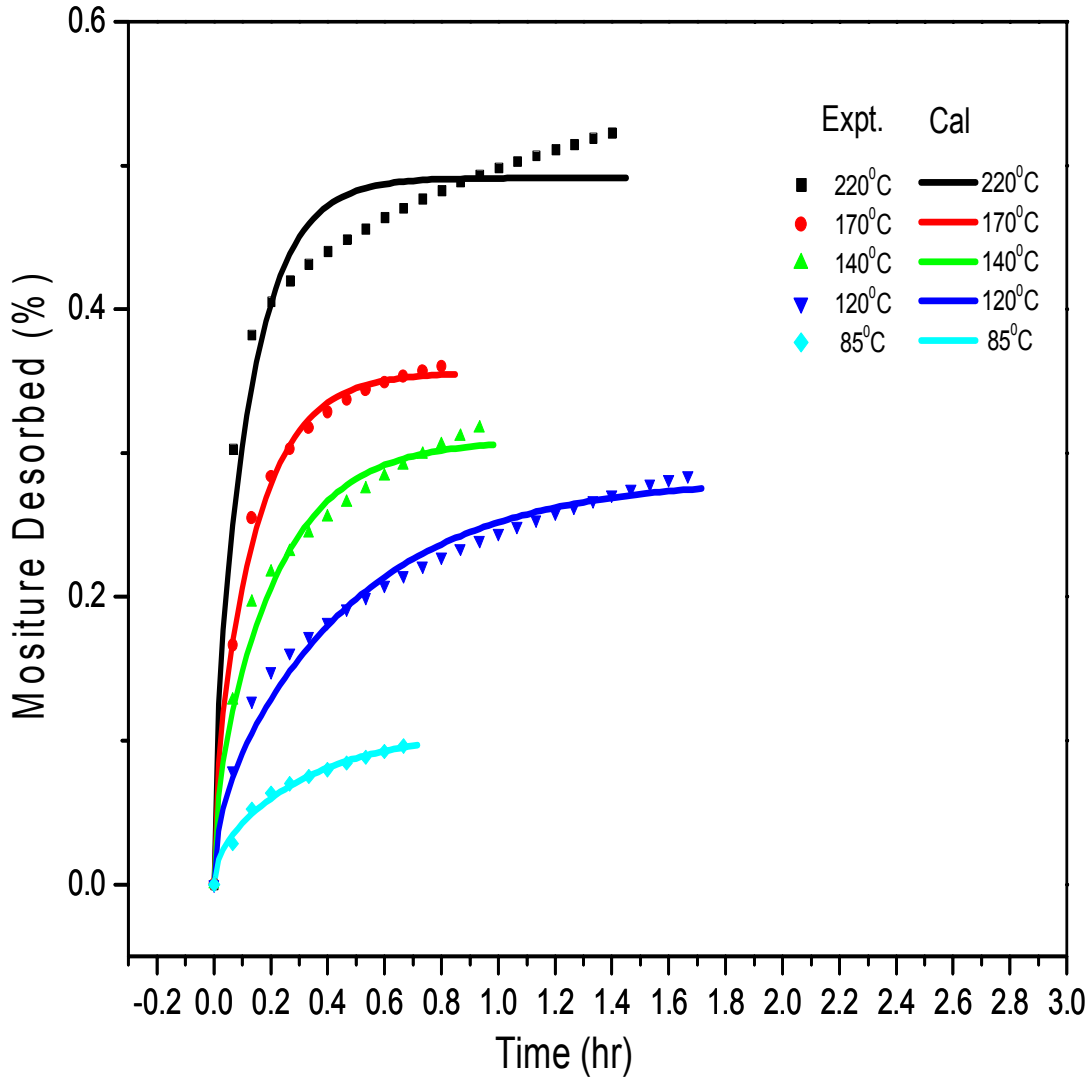

Figure 5.1 Moisture desorption of Molding Compound at temperatures of 220°C, 170°C, 140°C, 120°C and 85°C, respectively. By Karl Fischer Titration
Note: Samples were preconditioned at 85°C/85% RH for more than 1 year

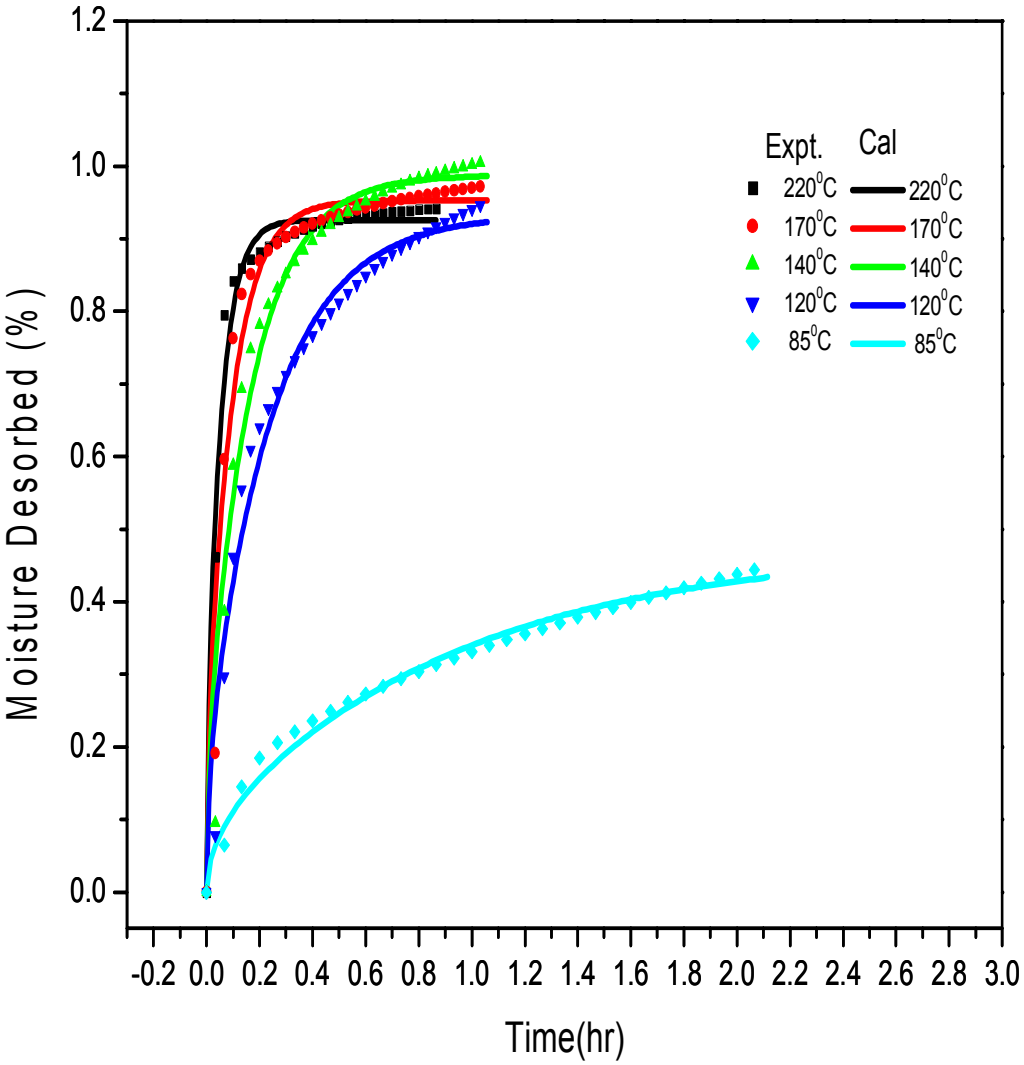

Figure 5.2 Moisture desorption of Underfill at temperatures of 220°C, 170°C, 140°C, 120°C and 85°C, respectively. By Karl Fischer Titration

Note: Samples were preconditioned at 85°C/ 85% RH for 2 months

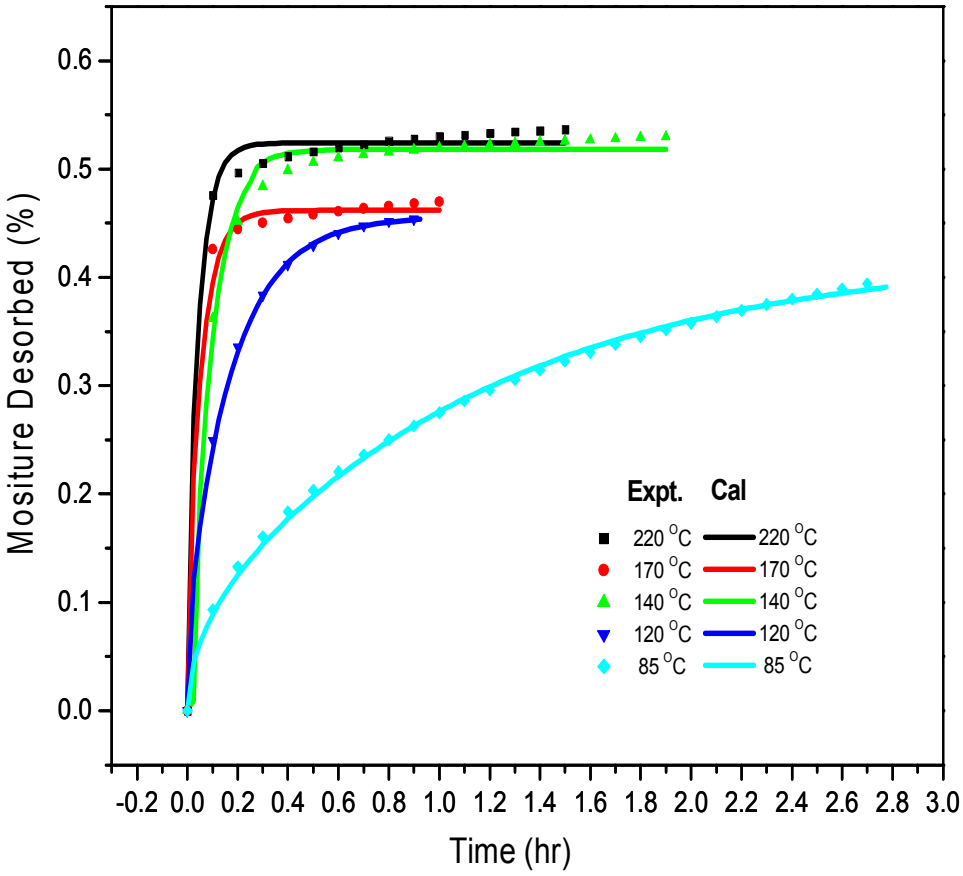

Figure 5.3 Moisture desorption of Die Attach at temperatures of 220°C, 170°C, 140°C, 120°C and 85°C, respectively. By Karl Fischer Titration

Note: Samples for 220°C, 170°C tests were precondioned at 85°C/85% RH, for 2 months, for the others, 3 months

5.2.2 Sample Weight Loss by TGA

Results using TGA with the same materials are shown in the Figures 5.4, 5.5 and 5.6.

For all of these materials, the rate of weight loss increases when the temperature increases. At different temperatures, weight losses are different too, for all the materials. Based on the trends of these curves, we assume that they are asymptotically to equilibrium value. However, an obvious phenomenon is, at 220^0C, weight loss of each material increases dramatically and keeps increasing even after a long period of testing.

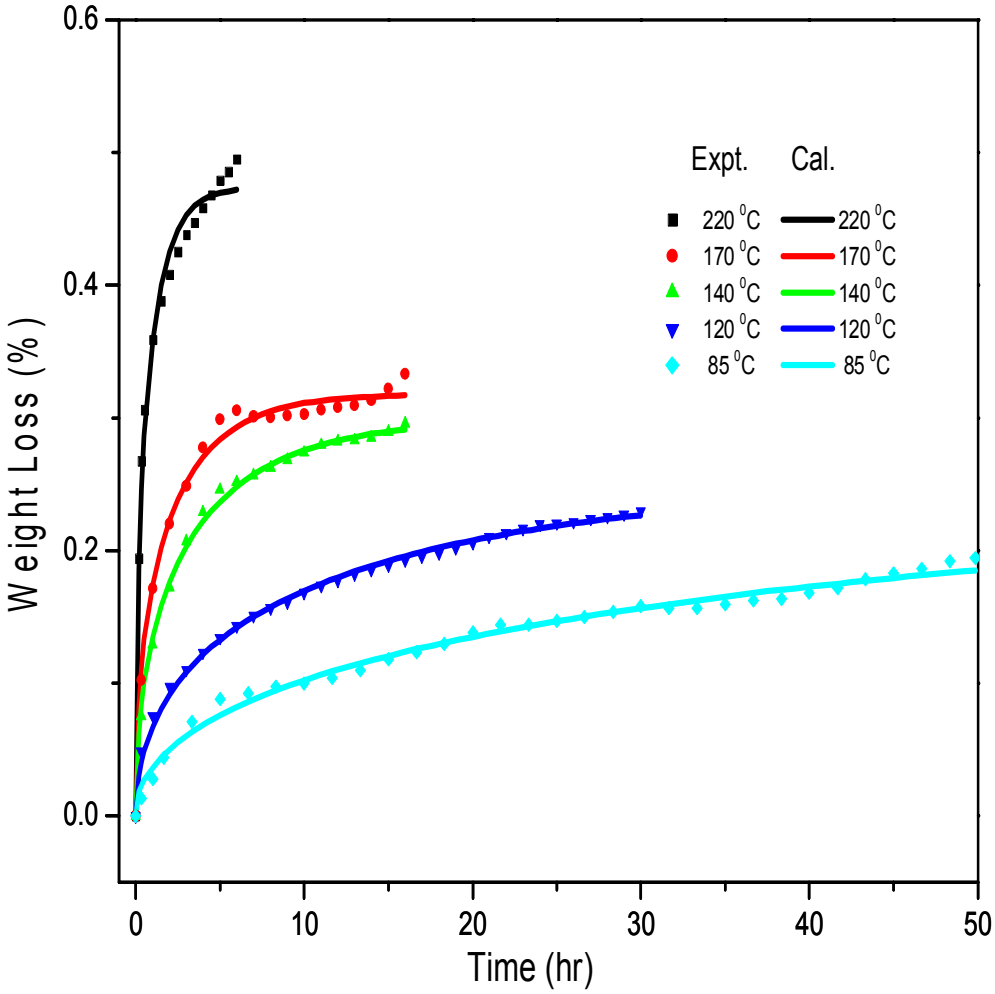

Figure 5.4 Weight loss of Molding Compound at temperatures of 220°C, 170°C, 140°C, 120°C and 85°C, respectively. By TGA
Note: Samples preconditioned for 1 year at 85°C/85%RH

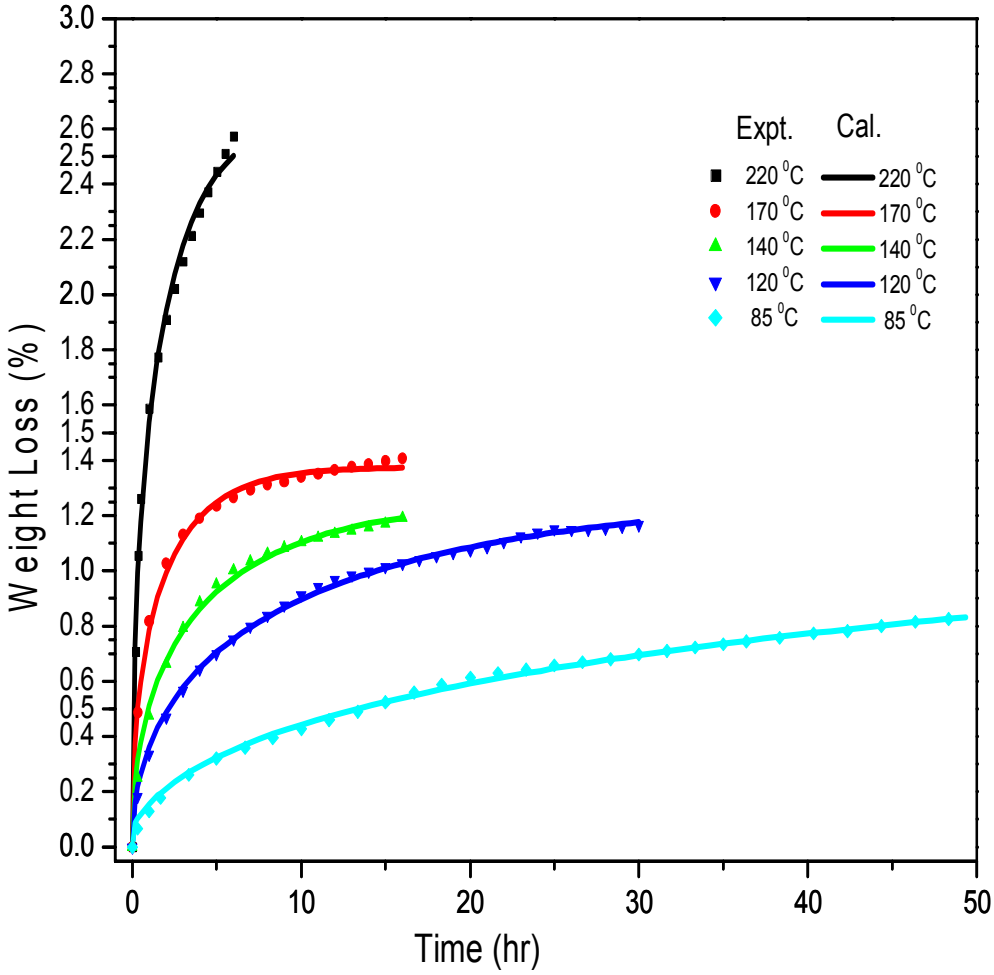

Figure 5.5 Weight loss of Underfill at temperatures of 220°C, 170°C, 140°C, 120°C and 85°C, respectively. By TGA
Note: Samples preconditioned for 2 months at 85°C/85%RH

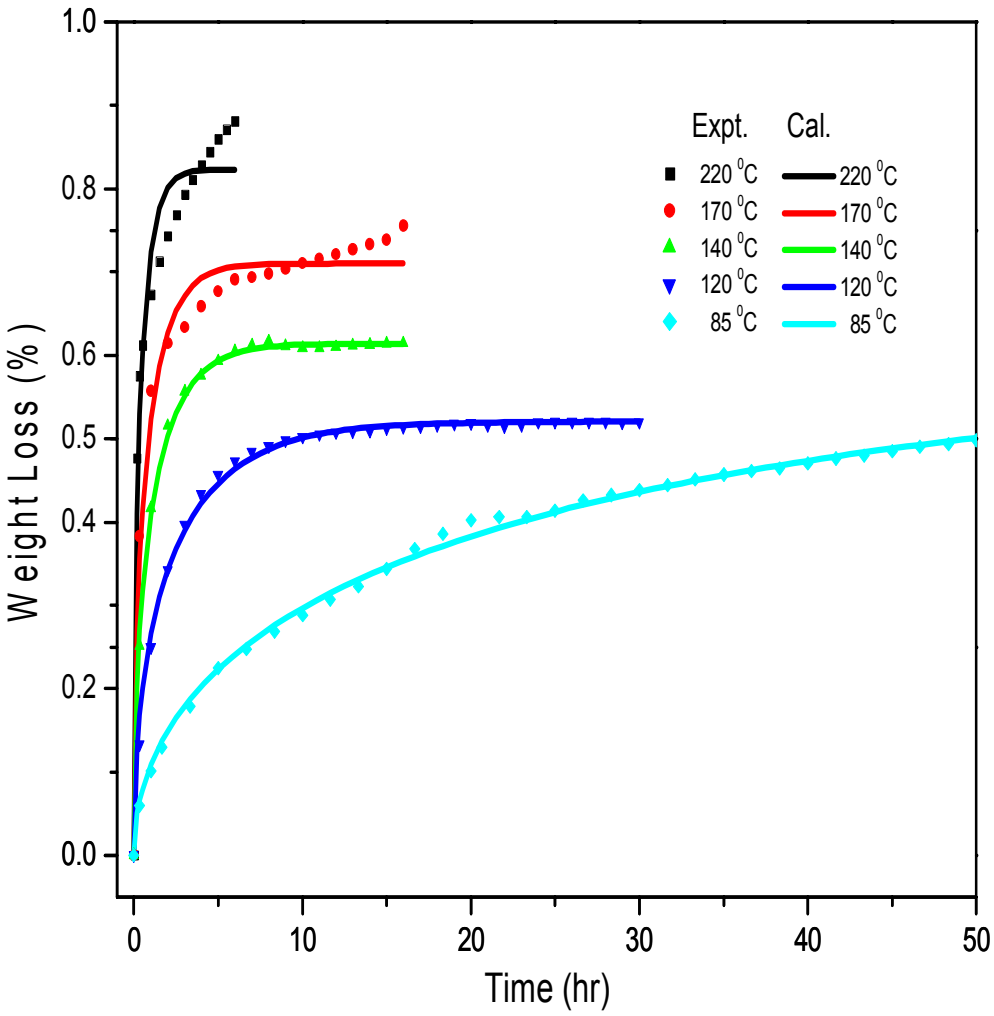

Figure 5.6 Weight loss of Die Attach at different temperatures of 220°C, 170°C, 140°C, 120°C, 85°C, respectively, by TGA.
Note: Samples preconditioned for2 months at 85°C/85%RH

5.2.3 Comparison of the Results from KF Titration and TGA Tests

Moisture diffusion coefficients D and moisture concentration at saturation (C_{sat}) of these materials are solved by a visual basic program [Koh, 2001] used with Excel Solver as mentioned in chapter 4.3. The results are shown in Table 5.1. Obviously, molding compound has a steady increase in D and C_{sat} as the temperature increased. However, C_{sat} of Underfill are similar at all temperatures except 85^{o}C. Die Attach, especially shows a similarity in C_{sat} at all temperatures. D in all of these materials at high temperature of 220^{o}C, are all at around 2×10^{-6} cm^2/s.

C_{sat} by TGA are obviously larger than those by KF Titration. On the contrary, moisture desorption coefficients D by TGA are smaller than those by KF Titration. A dramatic increase in C_{sat} happens from 140^{o}C to 170^{o}C for underfill. For Molding Compound and Die Attach, this happens from 120^{o}C to 140^{o}C and from 85^{o}C to 120^{o}C, respectively. These ranges of temperature are around the T_g of these materials, respectively.

In Table 5.1, moisture diffusion coefficients D_{TGA} obtained according to the Fickian fits were not true at 220 ^{0}C due to the very poor curve fitting since there are no experimental points displaying certain level of saturation, which could be seen in Figures 5.4, 5.5 and 5.6. Particularly, for Underfill and Die Attach materials, TGA tests at high temperatures show a higher weight loss compared to KF Titration tests. For example, TGA test at 220^{0}C for Underfill has a weight loss of 2.5% while KFT only has 1%. For Die Attach, TGA test at 220 ^{0}C, has 0.9% while KF Titration has

0.5%. However, KF Titration test at 220 ^{0}C shows the tendency of equilibrium at a time when the TGA test at 220 ^{0}C is still initiating mass diffsuion. Therefore it is expected that the evolution of volatiles at high temperature cause the big difference between D by KF titration and that by TGA. This also causes the abnormality in the Arrenhius plots for TGA results. As shown in Figure 5.8, except for the 220^{0}C point of Underfill, all of the plots are almost linear for $T < T_g$ and for $T > T_g$, respectively, and the plots go through T_g smoothly.

Mat'ls	T	Titration		TGA		$(D_{KF}-D_{TGA})/D_{KF}$	$(C_{KF}-C_{TGA})/C_{TGA}$
		D_{KF}	C_{sat}	D_{TGA}	C_{sat}		
	(°C)	$10^{-9}cm^2/s$	mg/cc	$10^{-9}cm^2$	mg/cc	%	%
UF T_g=138 °C (TMA test result) T_g=152 °C (DSC test result)	85	105.45	8.1	14.32	22.38	86.420	-63.807
	120	344.44	16.47	95.62	21.86	72.239	-24.657
	140	597.22	17.98	229.83	21.44	61.517	-16.138
	170	1130.56	16.19	519.81	24.41	54.022	-33.675
	220	2155.56	15.17	546.58	45.3	74.643	-66.512
MC T_g=144 °C	85	861.4	2.07	18.86	4.88	97.811	-57.582
	120	563.19	5.51	74.79	4.77	86.720	15.514
	140	1249.14	6.02	251.65	5.61	79.854	7.308
	170	1838.43	6.94	417.08	6.11	77.313	13.584
	220	2544.37	9.57	1070.62	8.96	57.922	6.808
DA T_g=100 °C	85	71.86	12.75	29.44	20.54	59.031	-37.926
	120	477.85	13.96	287.4	20.11	39.856	-30.582
	140	958.14	15.66	601.64	23.55	37.208	-33.503
	170	1213.33	13.38	824.38	26.3	32.056	-49.125
	220	1913	13.21	1658.21	31.25	13.319	-57.728

Table 5.1 Moisture diffusion coefficients (D) at desorption and moisture concentration at saturation (C_{sat}) by KF Titration and TGA

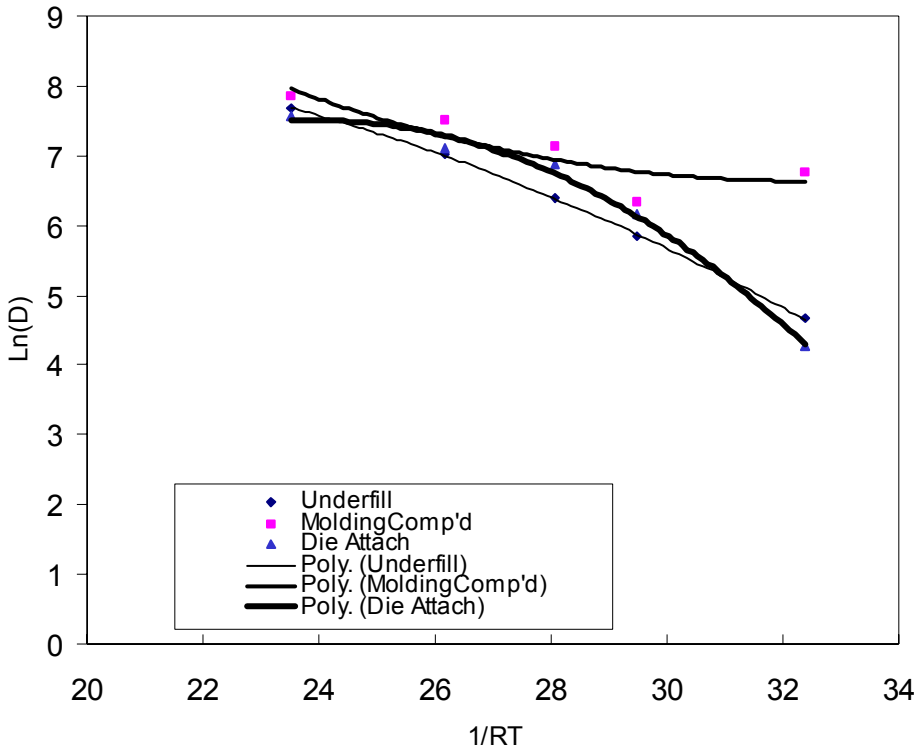

Temp	1/RT	Underfill		Molding Compound		Die Attach	
		D	LnD	D	LnD	D	LnD
(°C)		(10^{-9}cm^2/s)		(10^{-9}cm^2/s)		(10^{-9}cm^2/s)	
85	32.37	105.45	4.66	861.40	6.76	71.86	4.27
120	29.48	344.44	5.84	563.19	6.33	477.85	6.17
140	28.06	597.22	6.39	1249.14	7.13	958.14	6.86
170	26.16	1130.56	7.03	1838.43	7.52	1213.33	7.10
220	23.50	2155.56	7.68	2544.37	7.84	1913.00	7.56

Figure 5.7 Arrenhius relationship of Molding Compound, Underfill and Die Attach materials by Karl Fischer Titration

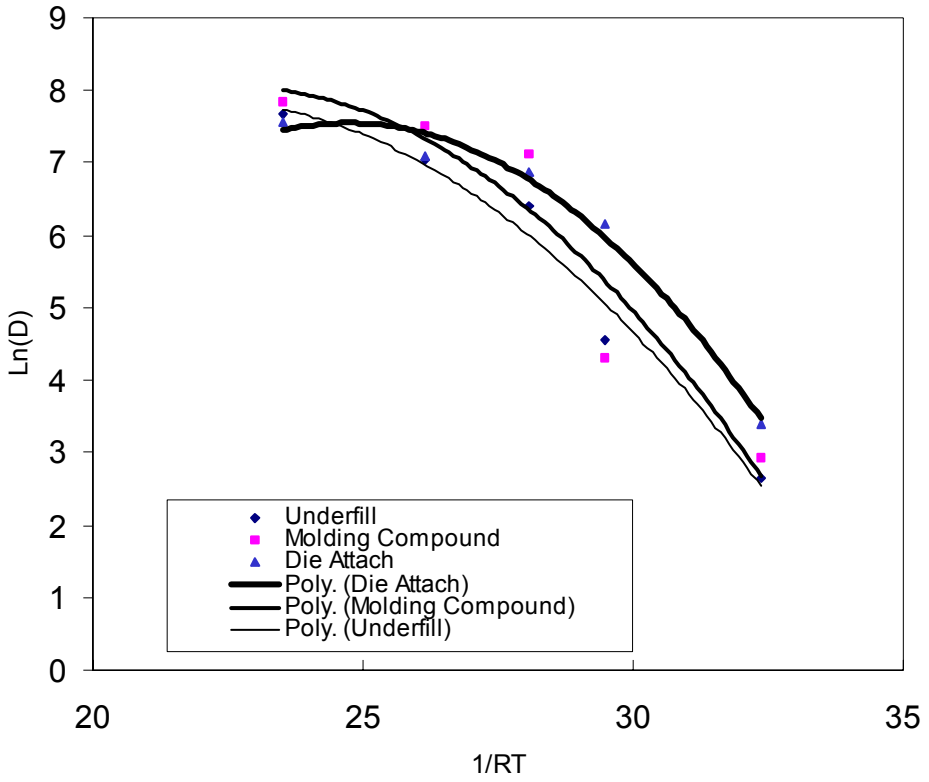

Temp	1/RT	Underfill		Molding Compound		Die Attach	
		D	LnD	D	LnD	D	LnD
(°C)		(10^{-9}cm^2/s)		(10^{-9}cm^2/s)		(10^{-9}cm^2/s)	
85	32.37	14.32	2.66	18.86	2.94	29.44	4.27
120	29.48	95.62	4.56	74.79	4.31	287.40	6.17
140	28.06	229.83	5.44	251.65	5.53	601.64	6.86
170	26.16	519.81	6.25	417.08	6.03	824.38	7.10
220	23.50	546.58	6.30	1070.62	6.98	1658.21	7.56

Figure 5.8 Arrenhius relationship of Molding Compound, Underfill and Die Attach materials by TGA

.

Why did TGA tests result in a bigger C_{sat} and smaller moisture desorption coefficients D when compared to KF titration tests? Take equation 4.1 as an example, in which D is decided by M_{sat} because M_t is given experimentally. In this study, total moisture content from KF Titration tests and total weight loss from TGA tests were used as M_{sat} to solve desorption diffusion coefficients D. We assume that

M_t is a constant at a certain time t_0, then D will decrease as M_{sat} increases. That is, in the case of TGA tests, if the weight loss M_{sat}' obtained includes other volatiles released from the samples due to the unreacted monomers and curing agents or chemical degradation besides water,

$$M_{sat}' = M_{water} + M_{volatiles} \tag{5.3}$$

it will be larger than the real M_{sat} since only the M_{water} is supposed to be obtained as M_{sat} for deducing moisture desorption coefficient D.

In addition to the above, TGA tests encountered another problem during the initial experiment stage due to its heating system. Volatiles due to chemical degradation may not explain the big difference in D between TGA and Titration at low temperatures like 85^{o}C. The chemical degradation only takes a small percentage of the weight loss at the initial stage. The difference in heating mechanisms between KF Titration and TGA has a big impact in causing the decrease in D by TGA.

In order to avoid weight loss during the stabilization period, which would not be collected, a temperature profile with a heating rate of 100^{0}C /min was used (Figure 5.9). It lessened the weight loss during stabilization compared with that directly releasing the sample into the sample holder at a fixed preset temperature.

However, a weight loss M_{loss} occurred during the stabilization with this temperature profile. Therefore, $\frac{M_t}{M_{sat}}$ changed into $\frac{M_t - M_{loss}}{M_{sat} - M_{loss}}$, and the value became smaller. Therefore, M_{loss} caused another decrease in D besides the decrease caused by the chemical volatiles. When the stabilization was reached, the weight loss data began to

be collected; the testing temperature was still in the ramping up process, which was below the actual testing temperature. Therefore, the collected weight loss was less than what was supposed to be and caused another weight loss M_{loss}'. Therefore a further decrease in D occurred. The above 2 phenomena were especially severe at 220°C since it takes a longer time to reach. However, for Titration, samples were released into the evaporator with the set temperature and moisture desorption data was collected immediately.

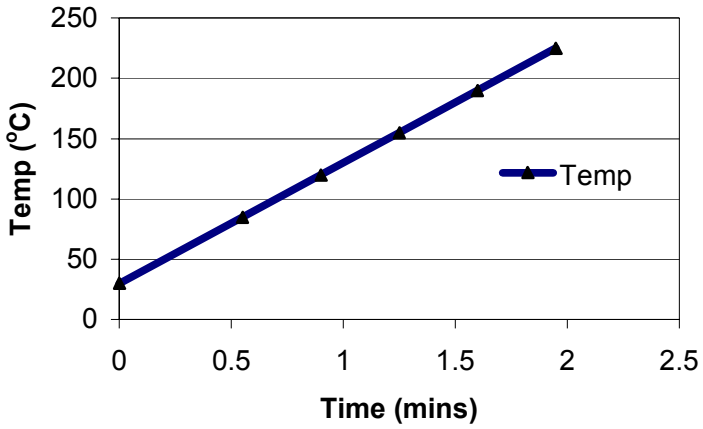

Figure 5.9 Temperature Ramping-up profile for TGA tests
Ramping up rate: 100 °C /min

C_{sat}, the moisture concentration at Saturation, is deduced from

$$C_{sat} = M_{sat} / V \tag{5.4}$$

where M_{sat} is total moisture obtained in desorption, and V is the volume of the sample. Therefore, TGA tests resulted in bigger C_{sat} as M_{sat} increases due to the chemical volatiles. This also indicated that M_{loss} and M_{loss}' caused by the heating mechanism are far less than the $M_{volatiles}$.

We conclude that the possible causes for the decreased D and the larger C_{sat} by TGA are: (1) Chemical volatiles are released out samples at high temperatures especially around solder reflow temperatures. There volatiles probably include the unreacted monomers and curing agents, which gain more flexibility at high temperature due to polymer microstructure become more flexible at high termperature, and the products of chemicals degradation; (2) Weight loss caused by the heating mechanism of TGA, includes the weight loss M_{loss} during stablization process and the weight loss M_{loss}' due to the ramping-up process in experiment.

Is the Titration time long enough for estimating D? Why is there a sudden stop on KF Titration experimental curves at 85^{o}C? What's the disadvantage of KF Titration? Samples used for KF titration tests are that counted as 1dimensional square chips.

In the case of flow through a membrane, if one face x=0 of a membrane is kept at a constant concentration C_1 and the other x=l at C_2, and the membrane is invitially at a uniform concentration C_0. Q_t is the total amount of diffusing substance through the membrane in time t. For the case $C_0=C_2=0$, plotting a graph of $Q_t / l\, C_1$ as a function of Dt/l^2, within the accuracy of plotting the steady state--equilibrium is achieved when

$$Dt/l^2=0.45 \qquad (5.5)$$

approximately. Where l is the thickness of the sample and D is the diffusion coefficient at the particular temperature [Crank, 1975]

Therefore, we use equation 5.5 to calculate the time for reaching equilibrium state. The results are shown in Table 5.2. Due to the poor Fickian fit at temperatures below

T_g at which the experimental curves don not exhibit any level of equilibrium, moisture desorption coefficients D obtained for these temperatures are doubted. While at higher temperatures, Fickian fits agree well with the experimental curves. In Table 5.2, it could be seen that time for reaching equilibriums are short and correspond to the experimental curves around the points at which it starts approaching equilibrium. This is particularly true for tests at 220°C. Obviously, for samples with a thickness less than 1mm, KF titration is capable of moisture desorption at high temperatures above T_g.

A drawback due to sensitivity limitation probably accounts for the sudden ending at 85°C of KF Titration experimental curves. The restrained mobility of absorbed moisture below T_g perhaps cause a very slow rate of moisture desorption which cannot be detected at a sensitivity of 0.01μg/s.

Materials	Tempture (°C)	D (E-9 cm2/s)	t (hrs)
Underfill	85	105.45	4.26743
	120	344.44	1.30647
	140	597.22	0.75349
	170	1130.56	0.39803
	220	2155.56	0.20876
Molding Compound	85	861.4	1.17541
	120	563.19	1.79779
	140	1249.14	0.81056
	170	1838.43	0.55074
	220	2544.37	0.39794
Die Attach	85	71.86	6.26218
	120	477.85	0.94172
	140	958.14	0.46966
	170	1213.33	0.37088
	220	1913	0.23523

Table 5.2 Saturation durations (90% equilibrium) for different polymeric packaging materials, by KF Titration

KF titration has shown its advantages in selectivity, easy sample preparations and fast testing duration. To obtain the best experimental data, the following issues should be noted: (1) Titration sample should be prepared with an even thickness and carefully to avoid voids; (2) Tests should be carried out in a stable environment with low humidity, without venting near Titrator and a room temperature of around 20^{o}C; (3) Sample handling should be careful and fast; (4) To avoid temperature overshoot, we used a metal mesh sampler instead of the glass sampler which will cause a temperature overshoot during the initial stages of testing.

5.2.4 GC/MS Tests for Confirmation of Volatiles

Furthermore, with a confirmation test of GC/MS, large amount of organics was detected during a short period.

Figure 5.10 shows the results of Molding Compound by GC/MS. Spectra collected at different temperatures of 220^{o}C, 170^{o}C, 140^{o}C, 120^{o}C and 85^{o}C, respectively. Spectra differ at different temperatures with different peaks. The interpretations for these peaks are shown in Table 5.4. The 'Area%' indicated the quantities of the substances that were corresponding to the specific peaks. As shown in Table 5.3, at lower temperature below T_g of 144^{o}C, moisture takes a weight percentage of over 93%. While at higher temperature, even at 170^{o}C, which is about 26^{o}C higher than T_g, moisture content only took 50% in the weight loss. At 220^{o}C, all of the weight loss is chemical volatiles.

A similar phenomenon is also seen in Figure 5.11 and Table 5.4 for Underfill material. Underfill released more volatiles than molding compound even at lower temperatures below T_g, although these volatiles took a small amount of weight loss. This was due to Underfill having different polymer matrix and curing agent from molding compound. In different stages, at 140^{o}C that is around T_g or above, volatiles took the 20% of the lost weight. In this case, at 140^{o}C Underfill is already in the rubbery state, more volatiles (unreacted monomers and curing agent) managed to escape from the polymer matrix structure that is rigid in glassy state at the temperatures below T_g. Furthermore, Underfill showed a weight percentage of 73.60% and 100% volatiles at 170^{o}C and 220^{o}C respectively.

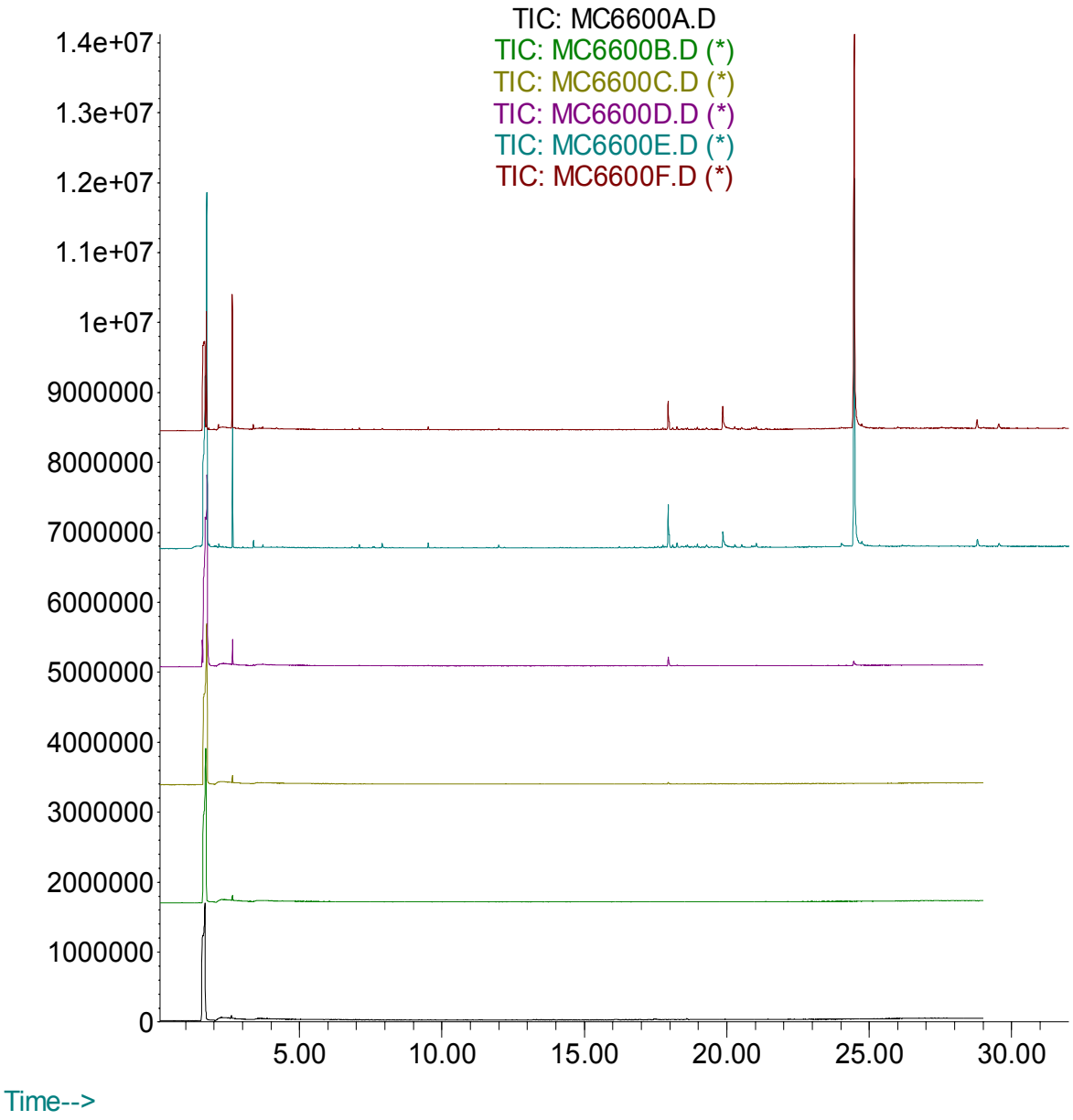

Figure 5.10 GC/MS spectra of Molding Compound with a ramp-up temperature profile as in Figure 5.12: heating up from room temperature to 85^{0}C(MC6600A) at a rate of 100^{0}C/min and then holding for 10 minutes, followed a same procedure with the temperatures of 120^{o}C(MC6600B), 140^{o}C(MC6600C), 170^{o}C(MC6600D), 220^{o}C(MC6600E), 230^{o}C(MC6600F)

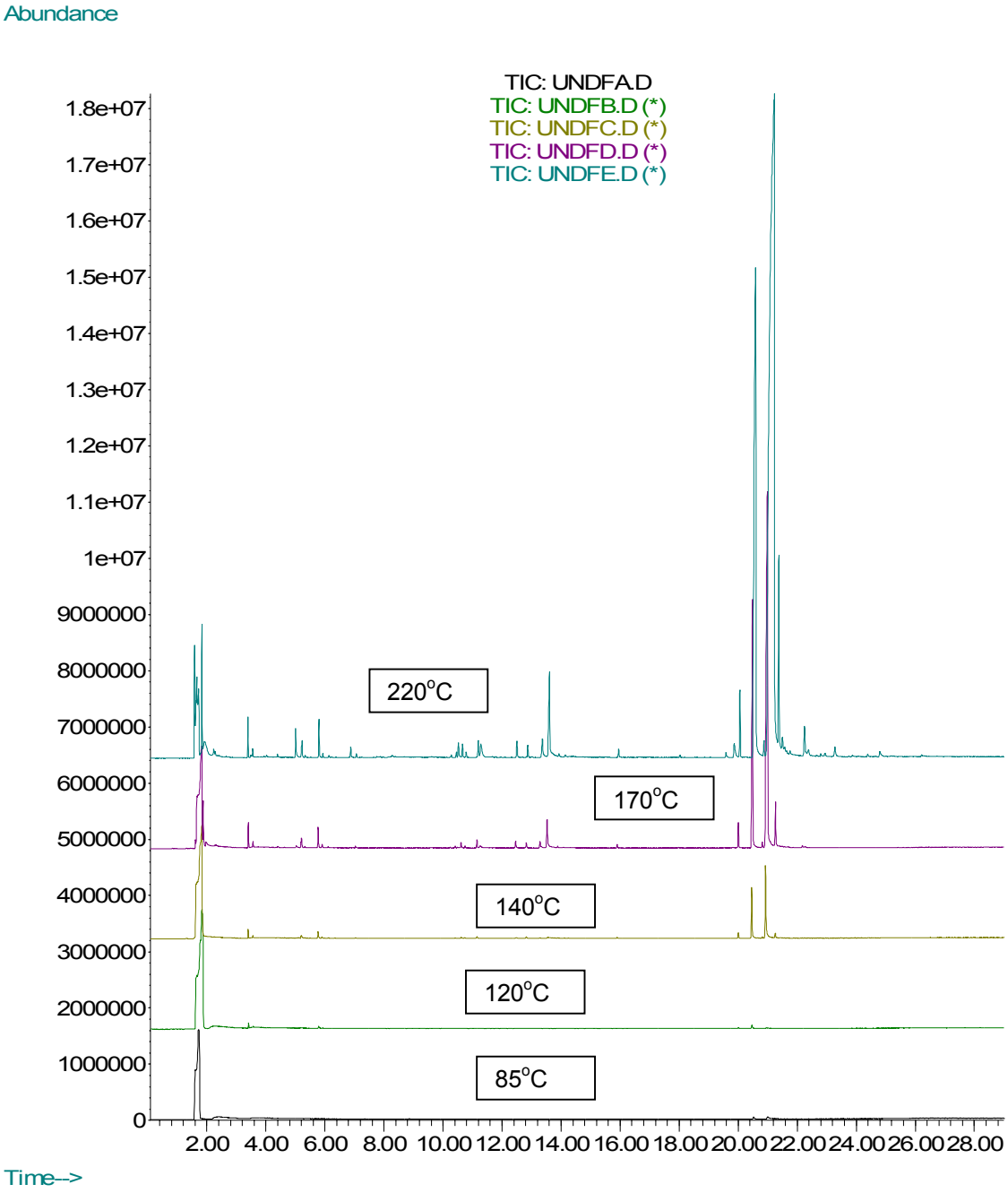

Figure 5.11 GC/MS spectra of Underfill with a ramp-up temperature profile as in Figure 5.12: heating up from room temperature to 85^{0}C (UNDFA) at a rate of 100^{o}C/min and then holding for 10 minutes, followed a same procedure with the temperatures of 120^{o}C(UNDFB), 140^{o}C(UNDFC), 170^{o}C(UNDFD), 220^{o}C(UNDFE)

A ramping-up temperature profile as Figure 5.12 was used for Molding Compound and Underfill samples. The results showed for a certain sample, the majority substances obtained from the test were water at low temperature such 85°C, 120 °C, 140°C. However with a further increase in temperature, chemical volatiles took a larger percentage of the total substances, till 220°C, no water was showed in the obtained spectra. The phenomena was so severe even during the test of 10 minutes at 85°C, organics with a percentage of 1% - 5% in total substances were obtained for both Molding compound and Underfill samples.

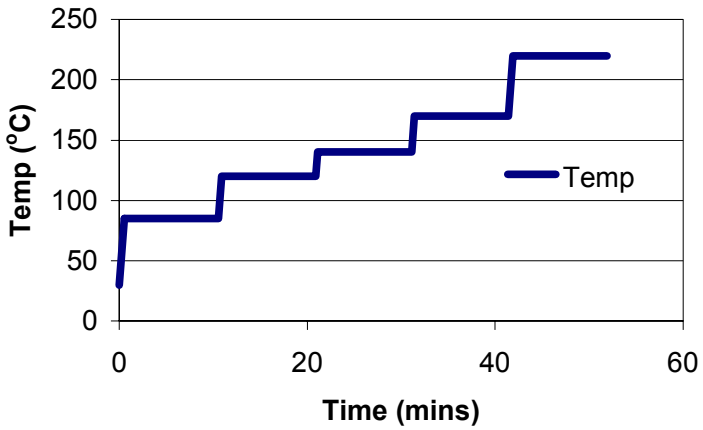

Figure 5.12 Temperature profile for GC/MS tests

Heating up from Room Temperature to 85°C at a rate of 100°C/min and then holding for 10 minutes, followed a same procedure with the temperatures of 120°C, 140°C, 170°C, 220°C

Actually, chemical degradation of polymeric packaging materials under high temperatures or high humidities was reported in a lot of literatures. Lowry and Hanley [2001] observed the clear chemical and physical degradation occur when polymeric materials were exposed to high temperatures for long times. They also speculated that the onset for decrease in weight lies in the temperature between 200°C and 230°C. It

was also concluded that long-term exposure of epoxy adhesive to water leads to reversible (physical) and irreversible (chemical) degradation of the materials [De Neve and Shanahan, 1995]. Resin oxidation will happen when we expose them to elevated temperature [Resin Oxidation]. Unreacted crosslinking agent, low molecular weight uncrosslinked epoxy monomer and solvents used in sample preparation (In our experiments, samples for TGA tests were machined into the required shape with certain solvents, while Titration samples omitted this procedure), caused the irreversibility between the first and subsequent sorption runs [Mcmaster and Soane, 1989].

Therefore, the abnormality of weight loss at high temperatures especially at 220 ^{o}C by TGA tests can be explained. On the contrary, KF titration curves reached a certain equilibrium after a short desorption period at 220^{o}C which is more reasonable, because the detection selectivity of KF titration is very high and moisture diffuses faster from the samples at high temperatures. Additionally, results in table 5.3 and table 5.4 showed that in short period, moisture can be totally desorbed out from the samples and reach equilibrium at high temperature near solder reflow (e.g 220 ^{o}C) instead of non-stop diffusion after long testing duration (e.g TGA tests at 220 ^{o}C). This also confirmed that the weight loss at high temperatures obtained from TGA includes a large number of other substances besides water.

T (^{0}C)	PEAK #	RT	Area %	Libarary / ID
85	1	1.68	98.81	Ammonia, Water, Carbamiv acid, monoammonium salt
	2	2.61	1.19	Benzene
120	1	1.71	93.85	Ammonia, Water, Carbamiv acid, monoammonium salt
	2	2.65	6.15	Benzene
140	1	1.74	94.44	Ammonia, Water, Carbamiv acid, monoammonium salt
	2	2.65	5.56	Benzene, 1.3-hexadien-5-yne
170	1	1.59	1.71	Carbon dioxide, Carbon dioxide, Nitrous Oxide
	2	1.70	50.99	Ammonia, Water, Carbamiv acid, monoammonium salt
	3	1.76	43.91	Ethanol, Ethanol, Ethanol
	4	2.65	2.01	Benzene, Benzene, Benzene
	5	17.95	1.39	2H-Furo[2,3-h]-1-benzopyran-2-one, ,6-Dioxaspiro[4.4]nona-2,8-diene, 2-Amino-3-methy1-imidazo(4,5-f)qui
220	1	1.74	54.35	Ethanol, Ethanol, Ethanol
	2	2.65	6.87	Benzene, Benzene, Benzene
	3	3.38	0.31	Methyl Isobuty1 Ketone; Methyl Isobuty1 Ketone; Methyl Isobuty1 Ketone
	4	17.95	3.34	2H-Furo[2,3-h]-1-benzopyran-2-one, Naphtho[1,2-b]furan-4,5-dione, 3,6 Adamantane, 2,2-ethylenedithio-
	5	19.87	1.82	Phosphine oxide, methyldipheny- ;Phosphine oxide, methyldipheny; 1'-Acetonaphthone, 2'-hydroxy-4'-m
	6	24.49	33.31	Thriphenyphosphoine oxide; Thriphenyphosphoine oxide; Formylmethylenetriphenylphosphoran

Table 5.3 Interpretation of GC/MS results of Molding Compound

T (^{0}C)	Peak #	RT	Area %	Libarary / ID
85	1	1.60	25.47	Ammonia, Water, Carbamiv acid, monoammonium salt
	2	1.73	69	Ammonia, Water, Carbamiv acid, monoammonium salt
	3-5	2.33 /20.52 /21.00	2.63/0.92/1.98	Other chemical volatiles
120	1	1.67	20.79	Ammonia, Water, Carbamiv acid, monoammonium salt
	2	1.83	77.06	Ammonia, Water, Carbamiv acid, monoammonium salt
	3-5	2.15/3.41/20.46	0.75/0.65/0.75	Other chemical volatiles
140	1	1.83	78.99	Ammonia, Water, Carbamiv acid, monoammonium salt
	2-7		21.01	Other chemical volatiles
170	2	1.83	26.40	Ammonia, Water, Carbamiv acid, monoammonium salt
	1,3,4-14		73.60	Other chemical volatiles
220	1-16		100	Other chemical volatiles

Table 5.4 Interpretation of GC/MS results of Underfill

5.2.5 Calculation of D_o and Activation Energy E_d

According to JEDEC Standard No. 22-A120 it is suggested that experimental data at the temperatures (which are 20-30^{o}C above or below T_g) should be obtained and activation energy E_d and D_o should be calculated for both temperature ranges, respectively. Based on the discussions above, that the results from TGA were relatively reliable at the temperatures below T_g while those from KFT were more relatively reliable at the temperatures above T_g, Arrenhius curves of these 3 materials were plotted as below. Arrenhius curves were plotted at temperatures below or above Tg, respectively as Figure 5.13 shown, since it was seen that in the whole temperature

range, Ln(D) values didn't follow a straight line. The discussions about why the Arrenhius curves plotted as Figure 5.13 were carried out as below and E_d and D_0 were given from the Arrenhius Curves as well.

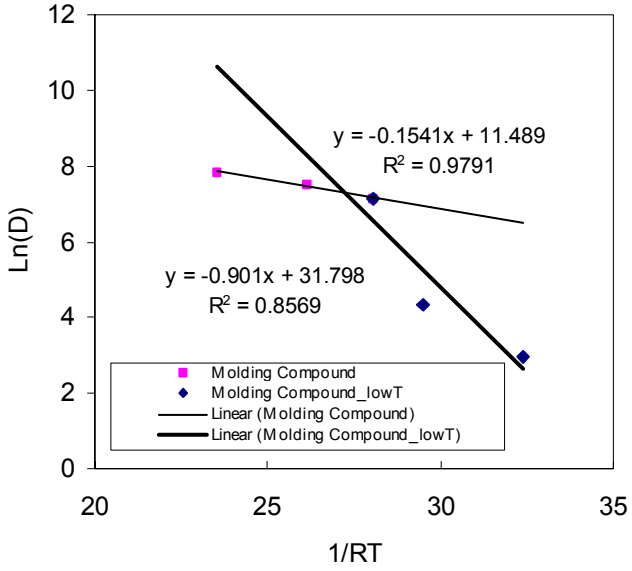

(a)

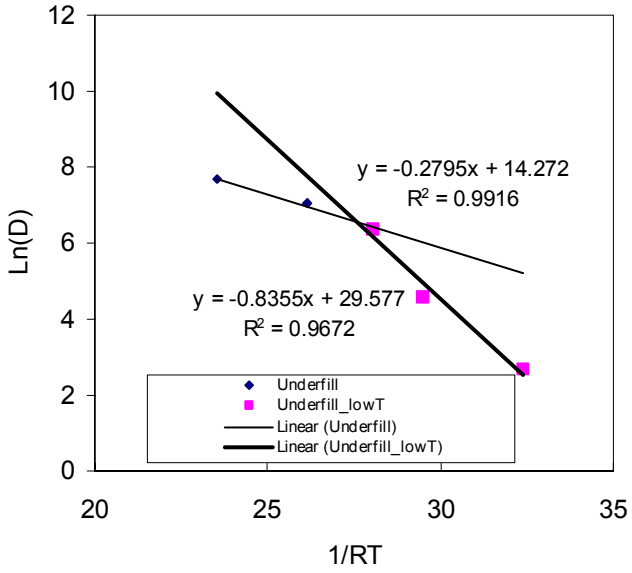

(b)

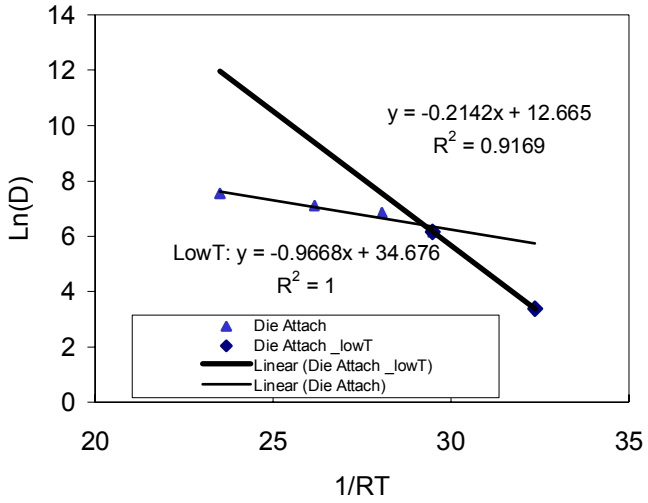

(c)

Figure 5.13 Arrenhius curves of polymeric packaging materials (Molding Compound (a), Underfill (b), Die Attach (c)) using Karl Fischer Titration (KFT) and Thermo-gravimetric Analysis (TGA): the points below marked with lowT taken from TGA tests and the points above T_g without the marking of lowT are taken from KFT tests.

Note: for Molding Compound, T_g=144°C;
for Underfill, T_g=138°C (TMA test result) T_g=152°C (DSC test result) ;
For Die Attach, T_g=100°C

Therefore, it is necessary to discuss how Glass Transition Temperatures T_g of polymeric packaging materials affect moisture desorption in them and the implication of the Arrenhius relationships.

Apparently, experimental curves by KF Titration reveals different desorption behaviors with raising temperatures. This is the case especially when it is hard to see any equilibrium at 85°C even after a long titration time for all of the 3 materials. This is due to the fact that 85°C is far below the glass transition temperatures, which are 138-152°C, 144°C and 100°C for underfill, molding compound and die attach, respectively.

Elevated-temperature exposure to moisture of epoxy rich samples can result in much stronger interactions between the unreacted epoxy molecules and the absorbed water molecules. Absorbed moisture may not be desorbed out completely below T_g [Vanlandingham, Eduljee, and Gillespie, 1998]. It is clear that temperatures in excess of the glass transition temperature are required to remove the residual moisture [March and Lasky, 1981]. It is can also be seen in (b) in Figure 5.13, that the diffusion rate was relatively low at temperatures below T_g. On the contrary, water in an epoxy in its rubbery state above the glass transition has a much higher mobility, which is similar to that of pure water, than in a polymer in its glassy state [Luo and Wong, 2001]. The experimental curves by KF titration at high temperatures tend to reach equilibrium in our tests, which further confirms this.

It has been shown that the glass transition temperature of polymeric materials do no exist as single numbers, but as a range of values that are very dependent on measurement techniques and processing methodology [Kongarshi]. That is, different measurement techniques will have wide deviations and will affect the data for T_g. T_g also depends on the rate of heating or cooling of the system. It is characteristic for the total system including possible penetrant [Van Der Wel and Adan, 1999]. It has been widely reported that absorbed moisture reduces the glass transition temperature (T_g) and it may cause a decrease of 5-20^oC [Vanlandingham, Eduljee and Gillespie, 1998; Luo and Wong, 2001]. However, upon desorption, T_g will rise up again close to the original value, although the isothermal diffusion coefficients appears to be clearly dependent on temperature. It was discovered that no discontinuities were found upon traversing the T_g. Instead, D increased smoothly with increasing temperature [Van Der Wel and Adan, 1999]. This is corresponding to the Arrenhius relationships for

our Titration tests except for the point for molding compound at 85°C. This could also be used to explain the different equilibriums at different temperatures around or above T_g, since T_g is traversing in a range due to the chemical structure change and moisture desorption. We could conclude that this phenomenon depends on the polymer matrix since different deviations for different samples were observed in our tests.

As shown in figure 5.7 and 5.8, there is a slight convex towards the X-axis in the Arrenhius curves, which indicates that a D_0 and activation energy E_d are different at temperatures above T_g from those below T_g [JEDEC Standard No. 22-A120, 2001]. Above T_g, water mobility is much higher and does not apprear to be affected by hydrogen bonds [March and Lasky, 1981]. Thus, lower activation energy E_d would be expected above T_g. However it's unexplainable from the curve in both figures, since it will lead to the opposite: higher Ed. This problem is solved when we combine the results from TGA and from KF Titration tests, since TGA is reliable at lower temperature and KF Titration at high temperature. Therefore, Arrenhius curves were plotted as Figure 5.13 with the experimental results from TGA at low temperatures and KFT and then the corresponding E_d and D_0 were obtained at. Temperatures below and above Tg..

T_g effects on moisture desorption are polymer matrix dependent. KF titration is good at desorbing moisture at high temperatures far above T_g. However, it is not suitable for moisture desorption at temperatures below T_g as some absorbed moisture are immobilized, which may not be desorbed below T_g. Arrenhius relationships show a smooth change in D_o and E_d as the temperatures vary across T_g. E_d decreases with temperature.

Results in table 5.5 shows that E_d and D_o above T_g for all the polymeric packaging materials are much smaller than that below T_g. This is expected because at temperatures above T_g, Activation Energy of a reaction, E_a, is the minimum amount of energy reactant molecules must possess in order to form products. less activation energy is needed for moisture molecule to break the hydrogen bond due to the flexible rubbery microstructure of polymer matrix of polymeric packaging materials. However, at temperatures below T_g, the rigid glassy structure of polymer matrix restraint the movement of molecules and more activation energy is needed for moisture molecules to escape from the sample. R^2, which is a measure of goodness of linear regression. The value of R^2 is a fraction between 0.0 and 1.0 and has no units. An value of 0.0 means that knowing X does not help you predict Y. There is no linear relationship going through the mean of all Y values. When R^2 equals 1.0, all points lie exactly on a straight line with no scatter. In our experiments, we could see that the values of R^2 were almost close to 1, which kept a good linear regression to obtain accurate E_d and D_0.

	R^2 Value	E_d (eV)	D_o	Arrenhius Curves: $LnD=LnD_0-Ed/RT$ (Y=aX+b; Y=LnD, $D_0=\exp(b)$, $E_d=-a$)	
Underfill	0.9916	0.2795	1.58E+06	Above T_g	y = -0.2795x + 14.272
	0.9672	0.8355	7.00E+12	Below T_g	y = -0.8355x + 29.577
Molding Compound	0.9791	0.1541	9.76E+04	Above T_g	y = -0.1541x + 11.489
	0.8569	0.901	6.45E+13	Below T_g	y = -0.901x + 31.798
Die Attach	0.9169	0.2142	3.16E+05	Above T_g	y = -0.2142x + 12.665
	1	0.9668	1.15E+15	Below T_g	y = -0.9668x + 34.676

Table 5.5 E_d and D_o of polymeric packaging materials at temperatures below and above T_g

5.2.6 Classification of Moisture Desorption Behaviors for Polymeric Packaging Materials Tested

Both Fickian and Non-fickian behaviors in moisture desorption are observed for all of the three materials. As we discussed in section 5.2.3, we use TGA experimental curves for low temperatures moisture diffusion and KF Titration experimental curves for high temperature moisture diffusion. Moisture content versus $t^{1/2}$ graphs are plotted (Figure 5.14) in order to compare the experimental curves to Figure 3.1. Obviously, moisture diffusion at low temperatures are Fickian-like although it does not show any level of saturation at 85^{o}C for all the three materials studied.

This is because the moisture diffusion is very slow at lower temperatures and the testing duration was not enough for saturation to be reached at 85^{o}C. However, we could tell clearly that, by using TGA, the moisture diffusion are Fickian type for molding compound at 140 ^{o}C, Underfill at 120 ^{o}C, 140 ^{o}C, Die Attach at 120 ^{o}C. Moreover, using KF Titration, moisture diffusion shows Fickian-like at temperatures above T_g for Undefill and Die Attach, compared to figure 3.1. By comparing figure 5.13 to figure 3.1, for the curves of Underfill and Die Attach using KFT at higher temperatures, there are similarity to Fickian curve in figure 3.1. The behavior of Molding Compound, appeared to be different. The reasons for this will be discussed next.

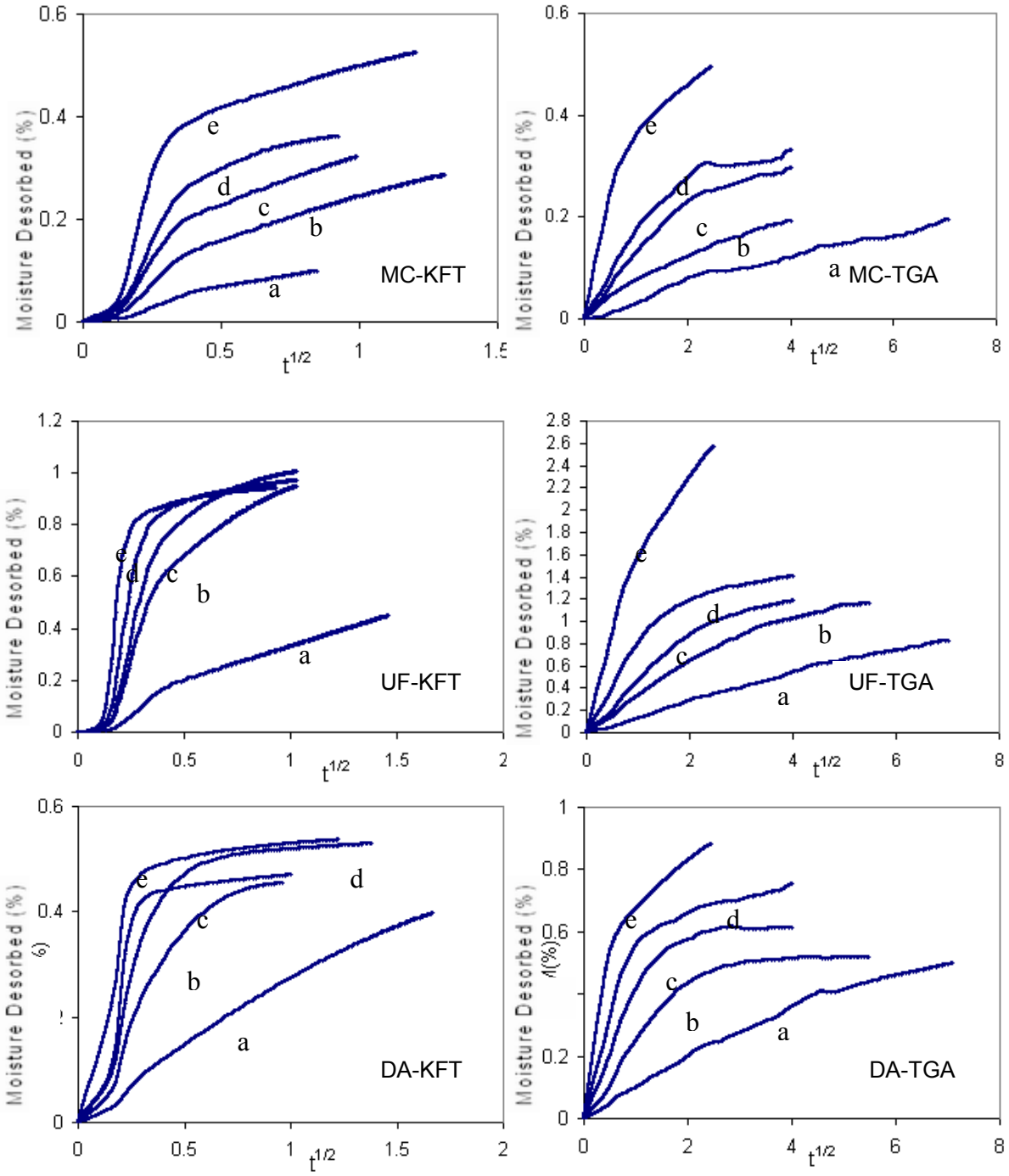

Figure 5.14 Moisture desorption behaviors of polymeric packaging materials: (Molding Compound – MC, Underfill-UF, Die Attach-DA) using Karl Fischer Titration (KFT) and Thermo-gravimetric Analysis (TGA). Mass loss in percentage (%) versus square roots of time (hour) at (a)85 °C (b)120 °C (c)140°C (d)170 °C (e)220 °C

Molding Compound (Figure 5.14, MC-KFT) shows a two-stage non-Fickian diffusion for each temperature above T_g. Meanwhile, it shows that at different temperature, moisture diffusion reaches different level of "first saturation". In order to investigate the nature of moisture resident in the molding compound samples, the following tests were carried out. The samples that were tested at 170°C, 140°C, 120°C and 85°C went through an immediate test at 220°C, therefore, the moisture weights at these 2 stages were collected separately and the total moisture weight was calculated. Table 5.6 shows the results of moisture contents in molding compound samples at desorption of different temperatures. It can be seen that the moisture weight obtained at the first testing stage increases with the testing temperature. The remaining water in the samples can be desorbed out at 220°C and the total moisture contents are similar for the tests at all temperatures. There is not much difference in the results for 220°C and 250°C, which implies that above 220°C, all of the water molecules can easily diffuse out of the sample.

This is so because difference in diffusion behavior is related to the availability of molecular-sized holes in the polymer structure and the polymer-water affinity. For polymeric materials, moisture diffusion is dominated by bulk resin matrix [Smith, Androff and Kamla, 1997; Miettinen, Narva, and Vallittu, 1999; Fremont, Deletage, and Danto, 2001; Vanlandingham, Eduljee, and Gillespie, 1998] (This could also be used to explain the different desorption behaviors for the 3 different materials used in our tests).

Temp (^{o}C)	Exp. M_{sat} (mg)	Water Content (%)	220^{o}C- after Test M_{add} (mg)	M_{total}	Total Water Content (%)
85	0.187	0.097	0.862	1.060	0.538
120	0.547	0.286	0.375	0.915	0.483
140	0.615	0.320	0.319	0.909	0.486
170	0.692	0.365	0.227	0.917	0.503
220	1.003	0.525		0.938	0.525
250	0.920	0.488		0.920	0.488

Table 5.6 Moisture desorption of Molding Compound at temperatures of 250^{o}C, 220^{o}C, 170^{o}C, 140^{o}C, 120^{o}C and 85^{o}C. By KF Titration
A further desorption test at 220^{o}C followed for the same sample of tests at 170^{o}C, 140^{o}C, 120^{o}C and 85^{o}C

The preconditioning durations for samples also influenced the moisture desorption behaviors. Samples of Molding Compound used for tests were left in humidity chamber at 85oC/85%RH for more than 1 year, while for samples of Die Attach and Underfill samples, around 2 months. Moisture absorption in molding compounds was a very long process. The first saturation occurred after a few hours of aging, but if it was left longer, a new diffusion process would occur, not leading to a real saturation [Fremont, Deletage and Danto, 2001; Li, Miranda and Sue, 2001]. This is so because water can exist in a polymeric medium in two states: unbound as well as well as bound to the polymer molecules [Mcmaster and Soane,1989; Diamant, Marom and Broutman,1981; Bonniau and Bunsell]. Bounded moisture causes swelling of the polymer and also could introduce time-dependent relaxation processes [Shirrell; Bao, Yee and Lee, 2001]. It takes a long time for equilibrium to be established between bound and unbound water. The majority of absorbed water becomes bound during the later stage of absorption while the unbound water still diffuses into unoccupied free volume [Li, Miranda and Sue, 2001]. Structure relaxation and bounded water caused the non-Fickian diffusion behavior. Meanwhile, the network structure change during

water absorption is irreversible due to the fact that absorption process is a self-accelerating process, while desorption process is a self-retarding process [Bao, Yee and Lee, 2001]. On the other hand, this could be caused by the oxidation during sorption experiments which gives rise to non-Fickian processes. An oxidized resin has a higher sorptive affinity towards water [Wong and Broutman, 1985]. Thus, an obvious Non-Fickian behaviors appeared for long-term preconditioned molding compound during desorption, especially at high temperatures, at which moisture has a higher probability of becoming unbound at higher temperature [Li, Miranda and Sue, 2001] It was reported that the mechanism or mechanisms responsible for the non-Fickian behaviors might depend on temperature, since that deviations from Fickian behavior are certainly more pronounced in the elevated-temperature environment [Vanlandingham, Eduljee, and Gillespie,1998].

Therefore, besides the nature of the polymer matrix of molding compound, long-term exposure to 85^{o}C/85%RH, which complicated the microstructure of the sample and the moisture states in the sample, was also another reason contributing to the non-Fickian behavior of molding compound.

5.3 Accuracy of the Experiments

Standard deviation δ for the measurements of the desorbed moisture were calculated according to section 4.4, corresponding to different tests of different materials at different temperatures, using KFT and TGA respectively. The values are given below.

		KFT			TGA		
	T (^{0}C)	**Standard Deviation δ (mg)**	**M_{sat} (mg)**	**Relative Error = δ /M_{sat} ×100%)**	**Standard Deviation δ (mg)**	**M_{sat} (mg)**	**Relative Error = δ /M_{sat} ×100%)**
	85	0.007	0.203	3.516	0.006	0.260	2.170
	120	0.018	0.540	3.267	0.003	0.253	1.260
MC	140	0.024	0.590	4.028	0.005	0.298	1.659
	170	0.026	0.680	3.753	0.009	0.327	2.657
	220	0.049	0.938	5.256	0.014	0.475	3.017
	85	0.017	1.621	1.025	0.009	0.745	1.198
	120	0.043	1.763	2.411	0.012	0.660	1.771
DA	140	0.052	1.944	2.692	0.011	0.783	1.467
	170	0.070	1.542	4.511	0.025	0.865	2.839
	220	0.046	1.749	2.616	0.056	1.061	5.319
	85	0.030	1.125	2.672	0.012	1.154	1.021
	120	0.091	2.104	4.310	0.011	1.085	1.032
UF	140	0.121	2.485	4.882	0.023	1.099	2.055
	170	0.120	2.330	5.165	0.019	1.202	1.577
	220	0.123	2.416	5.100	0.041	2.294	1.778

Table 5.7 Standard Deviation for desorption weight loss by KFT and TGA

As can be seen the Standard Deviation of relative error are less than 5%. The errors at lower temperatures are lower. The errors are within normal experimental errors.

Chapter 6
Moisture Absorption Experiments

6.1 Introduction

To further understand the moisture diffusion in polymeric packaging materials, moisture absorption tests were done at 85^{o}C / 85%RH with different materials including Underfill, Die Attach and resins with different amount of different fillers. The purposes of absorption tests are

1. To determine the effects of filler contents on moisture absorption in polymeric materials;
2. To study the absorption behavior of different materials: Underfill, Die Attach, Conductive Adhesives (resins with silver filler), Non-conductive Adhesives (resins with silica filler);
3. To compare D_{absorp} and D_{desorp}

6.2 Experiments

Disk-shaped samples of various materials were made with a diameter of 50mm and a thickness ranging from 0.32 to 2.6mm. After curing with the corresponding recommended temperature profiles, samples were collected and baked for 24 hours to get rid of the moisture in the samples. Samples were then weighed before being released into the humidity chamber of 85^{o}C/ 85%RH. During the experiments, samples were continuously weighed, in the first half day, the interval was 1 hour, 6 hours from the second day, and then twice a day. From the second week, samples were weighed daily and as time went by, every 3 days.

Weight gain of samples versus time is plotted. Moisture absorption coefficients D and moisture concentration at saturation C_{sat} are solved with the same 1-dimensional program for moisture desorption.

6.3 Results and Discussions

6.3.1 Moisture Absorption of Resins

Figure 6.1 shows the moisture absorption behaviors of different polymeric packaging materials. Obviously, different polymeric materials behaved totally differently during the moisture absorption. For some materials, such as resins (Resin/Hardener, Resin/Highsilica, Resin/Lowsilica, Resin/Highsilver and Resin/Lowsilver), Die attach and UnderfillC, almost reach equilibrium within 20 hours; while for other materials such as UnderfillA, even after 500 hours, the saturation could not be reached. This indicates that

moisture absorption behaviors are dependent on the polymer matrix of polymeric material.

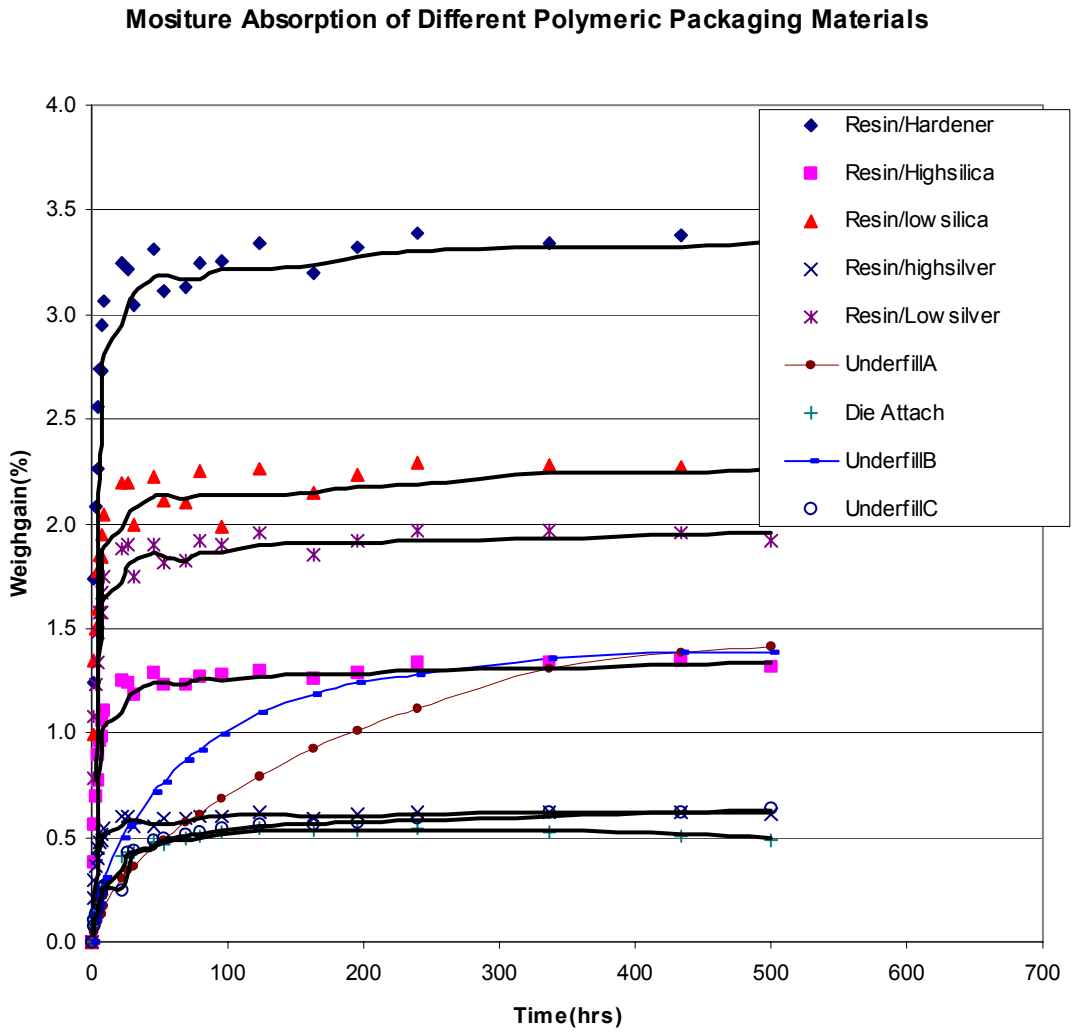

Figure 6.1 Moisture absorption behaviors of resins with different amounts (high cont ent and low content) of different fillers (silica and silver), Underfill and Die Attach materials

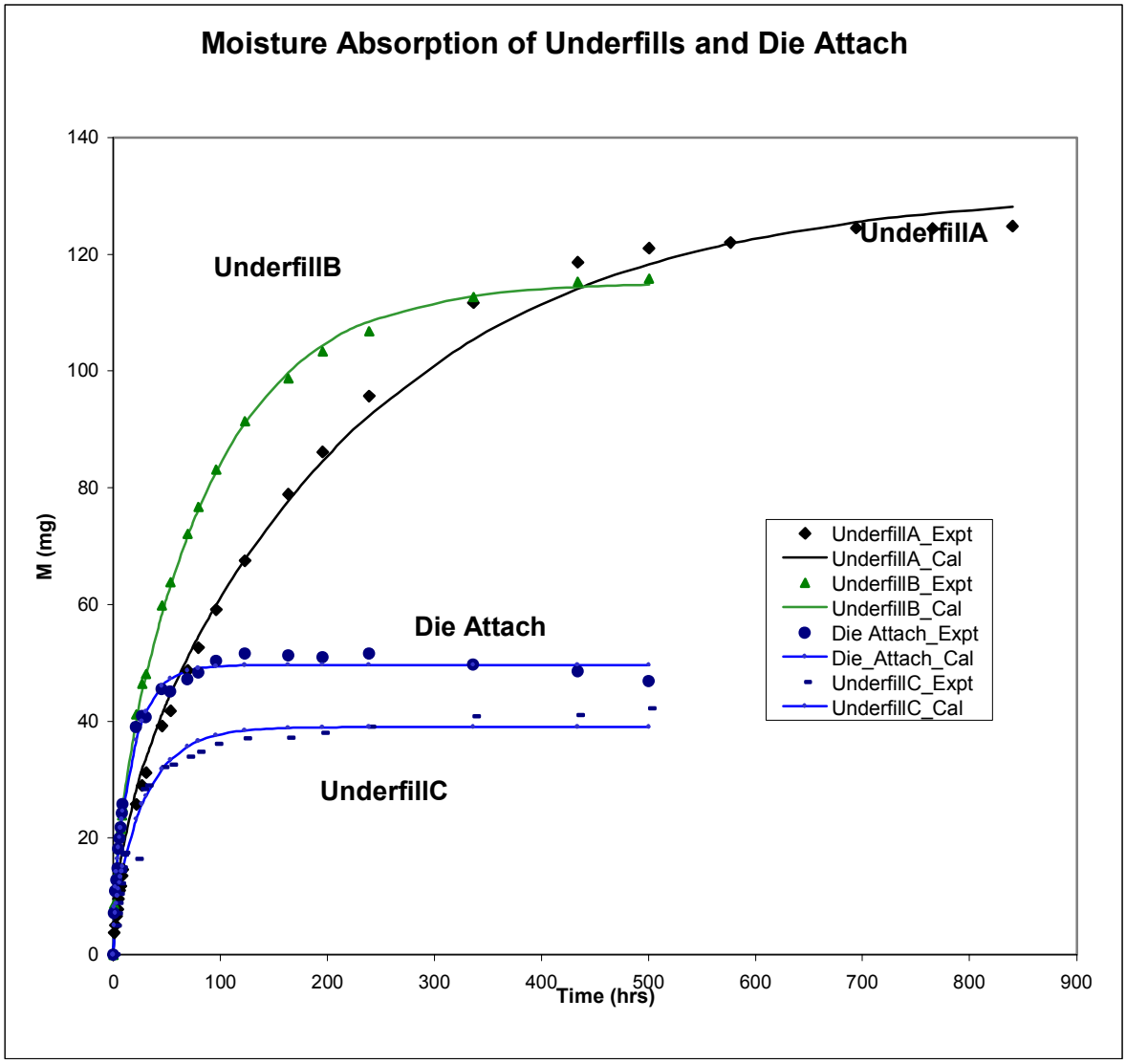

Figure 6.2 Experimental plots and Fickian fits for moisture absorption in Underfills and Die Attach materials

Samples for Underfills, Die Attach, resins with different fillers, with a thickness range from 1.82mm to 3.05mm displayed a moisture absorption behavior similarly to fitting curves by Fick's Law, as shown in Figures 6.2, 6.3 and Tables 6.1, 6.3.

Material	D (10^{-9}cm/s)	Msat (mg)	C_{sat} (mg/cc)	Thickness (mm)	t_{sat} =0.45l^2/D (hrs)	t_{sat} =0.45l^2/D for 1mm thickness (hrs)	Standard deviation (mg)	Relative Error= = δ /M_{sat} ×100%
UndefillA	5.830	148.000	29.550	2.560	1405.146	214.408	2.857	1.930
UndefillB	48.180	38.990	8.630	2.300	137.240	25.943	2.139	5.486
UndefillC	28.790	115.170	19.230	3.050	403.940	43.423	1.027	0.892
Die Attach	74.600	49.650	11.290	2.240	84.080	16.757	1.383	2.785

Table 6.1 Comparison of moisture absorption and desorption coefficients D and moisture concentration at saturation C_{sat} at 85 ^{o}C, for Underfills (A, B andC) and Die Attach

6.3.2 Comparisons on Results from Absorption and Desorption Tests

Moisture absorption coefficients D and moisture concentration at saturation C_{sat} are obtained according to equation 4.1. In order to compare the desorption and absorption behaviors of polymeric materials, Table 6.2 shows a list of information on Underfill and Die Attach which are also used in desorption experiment in Chapter 5. In Table 6.2, D of absorption and desorption at 85^{o}C are compared. For Underfill, D at desorption with TGA is more reasonable since it is close to D at absorption. However, D at desorption with KF titration is unreasonable for Underfill. For Die Attach material, it shows the opposite case. Probably this was due to the different microstructures and the different glass transition temperatures T_g of Underfill and Die Attach. The Underfill used in this research has a relatively high T_g around 138-152 ^{o}C while Die Attach has a T_g just around 100^{o}C. Additionally, a slight drop range from 5-20 ^{o}C in T_g might have occurred in the

presence of absorbed moisture. Since polymer matrix will experience a dramatic change around T_g and the molecular chain will gain a lot of flexibility compared to its rigid glassy structure below T_g, Die Attach will tend to release more moisture at 85°C since it is close to its T_g, which includes the bonded water molecules which cannot be desorbed below T_g. On the contrary, Underfill cannot release out the bounded water molecules since the temperature is far below its T_g. KF titration is more reliable at high temperatures (above T_g) while TGA is more reliable at low temperatures below T_g.

Material	Experiments	D ($10^{-9}cm^2/s$)	C_{sat} (mg/cc)	M_{sat} (mg)	Standard deviation (mg)	Relative Error= $= \delta / M_{sat} \times 100\%$
Underfill	**Absorp**	5.833	29.553	148.000	2.857	1.930
T_g138°C (TMA) and 152°C(DSC)	**Desorp (KFT)**	105.556	8.098	1.125	0.030	2.672
	Desorp (TGA)	14.444	22.378	1.154	0.012	1.021
Die Attach	**Absorp**	74.722	11.288	497.000	1.383	2.785
T_g138°C	**Desorp (KFT)**	71.944	12.754	1.621	0.017	1.025
	Desorp (TGA)	29.444	20.543	0.745	0.009	1.198

Table 6.2 Comparison of moisture absorption and desorption coefficients D and moisture concentration at saturation C_{sat} at 85 °C

6.3.3 Filler Effects on Moisture Absorption in Polymeric Materials

Filler effects were studied by using the samples with the same resin matrix. Different fillers such as silver and silica were mixed into resin with different amounts (high/low). The results from these samples with fillers were then plotted (Figure 6.3, 6.4, 6.5) and compared with the pure resin sample (Table 6.3).

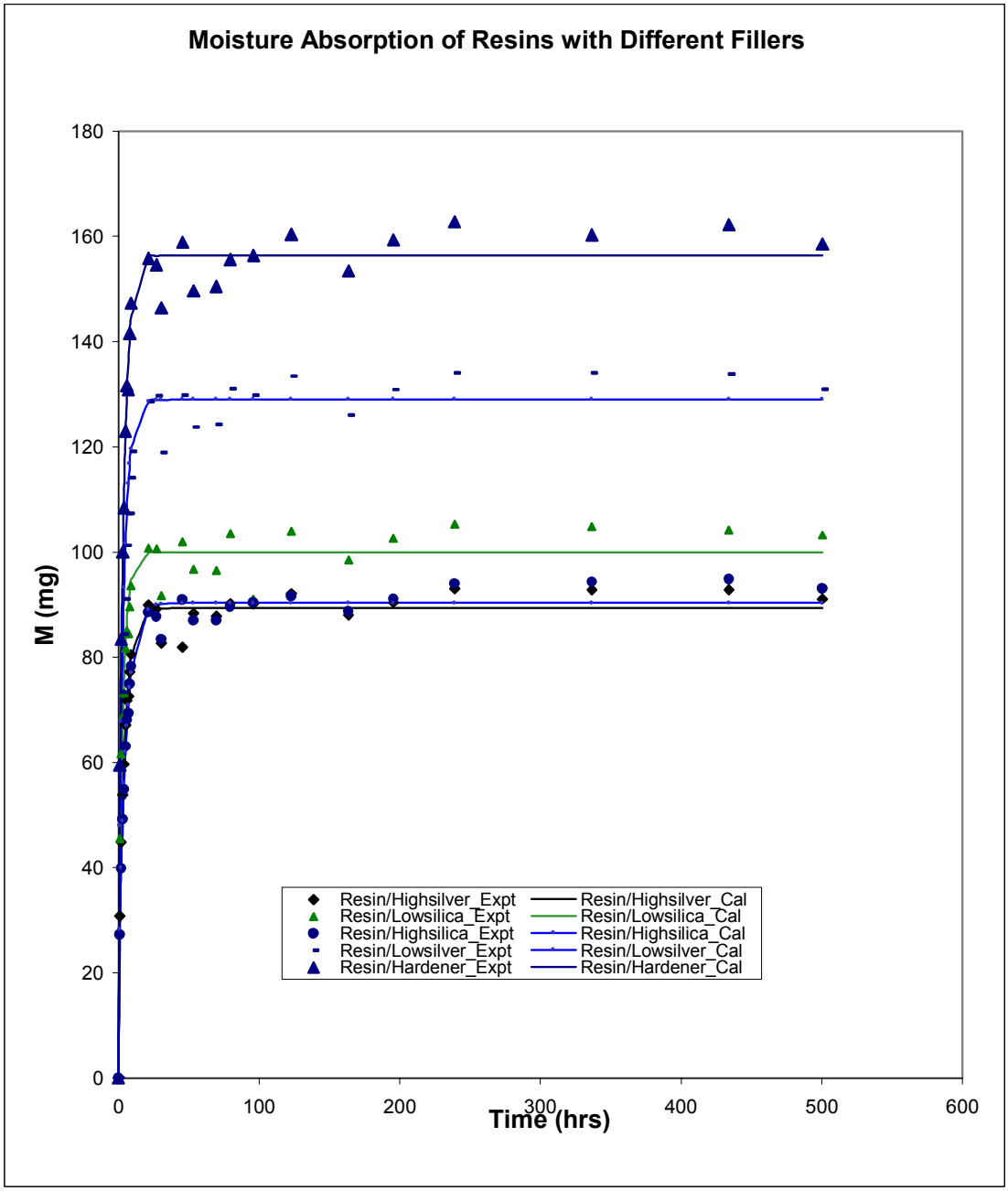

Figure 6.3 Experimental plots and Fickian fits for moisture absorption of resins with different amounts (high content and low content) of different fillers (silica and silver)

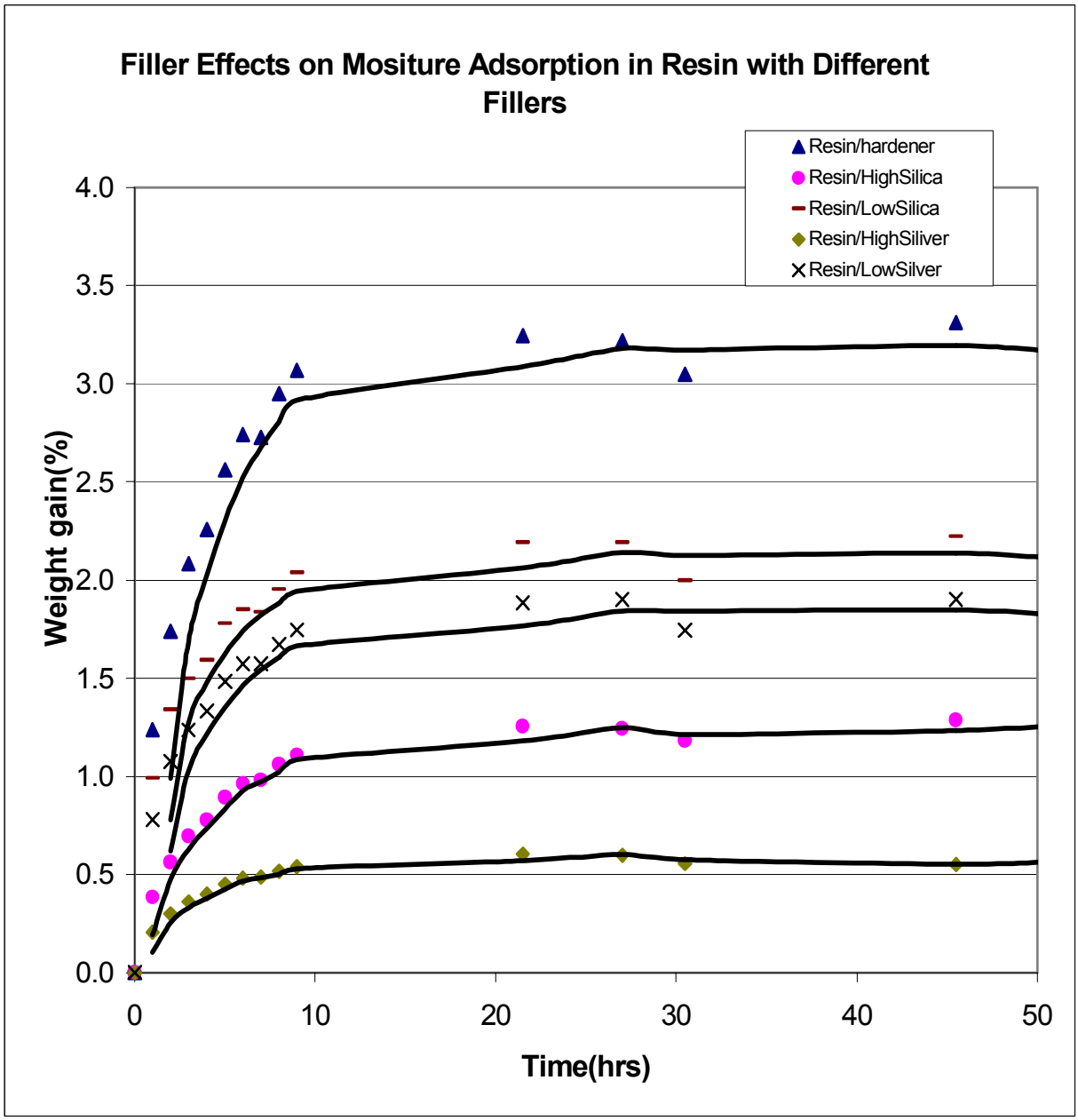

Figure 6.4 Moisture absorption behaviors of resins with different amounts (high content and low content) of different fillers (silica and silver) (50hours)

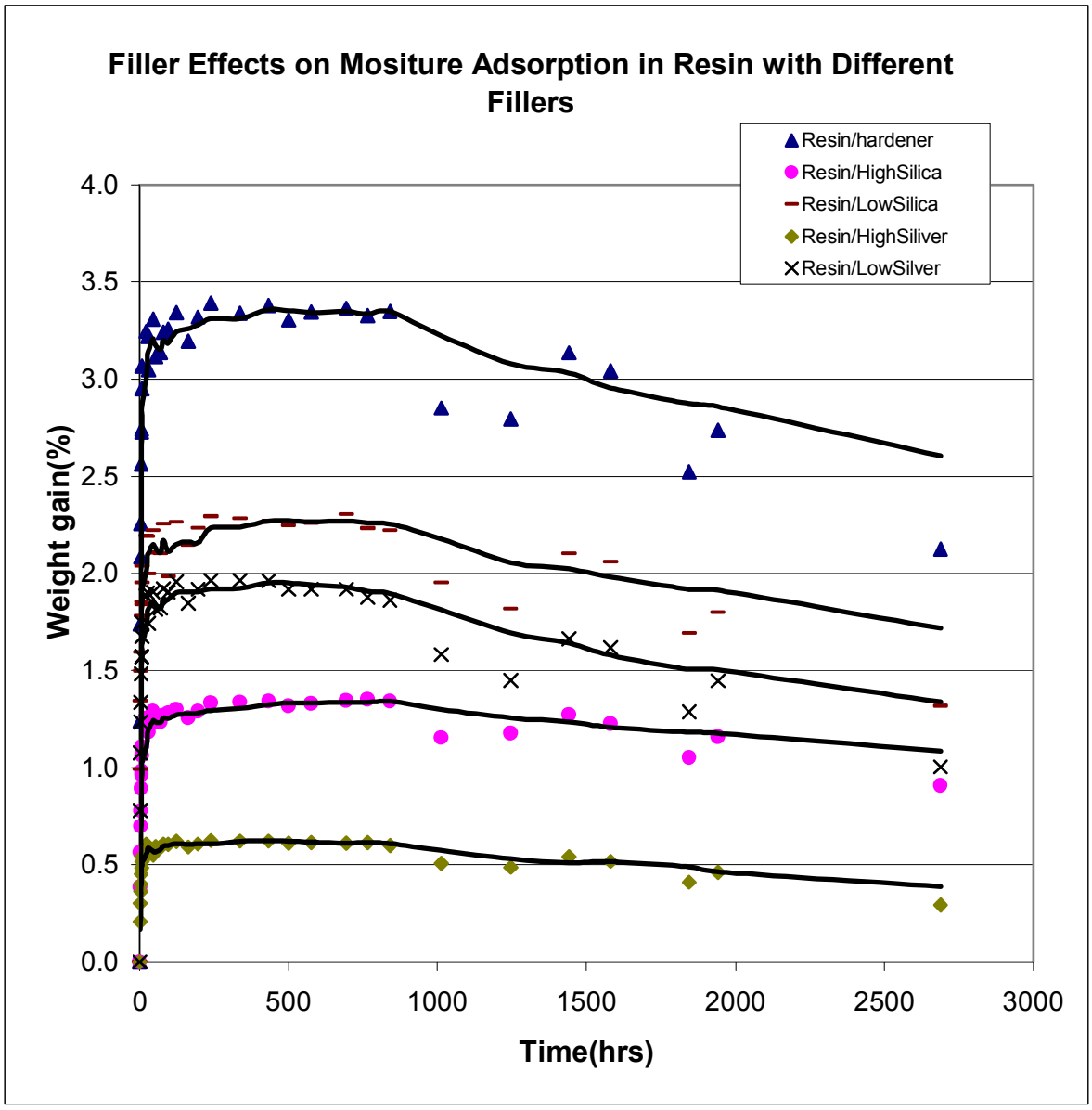

Figure 6.5 Moisture absorption behaviors of resins with different amounts (high content and low content) of different fillers (silica and silver) (over 2500hours)

It is seen that pure resin sample has the biggest D and C_{sat} in moisture absorption. Samples with silica and silver have different D and C_{sat}, and samples with higher amount fillers have a smaller D and C_{sat}. Time for reaching 90% equilibrium [Wong, 2001] varies between the pure resin and resin with fillers. For samples with the same thickness, those made of pure resin reached 90% equilibrium first before samples with higher silica

content. This indicates that moisture diffusion in samples with this type of resin matrix is dependent on the resin itself, and fillers act as barriers which blocked the diffusion path for moisture, hence, prolonging the time to reach saturation. The greater the percentage of fillers in the polymeric materials, the smaller D, the smaller C_{sat}, and the longer the time for reaching saturation. Besides, different fillers will influence the moisture diffusion differently.

Material	D (10^{-9}cm/s)	Msat (mg)	C_{sat} (mg/cc)	Thickness (mm)	t_{sat} =0.45l^2/D (hrs)	t_{sat} =0.45l^2/D for 1mm thickness (hrs)	Standard Deviation (mg)	Relative Error= = δ /M_{sat} ×100%
Resin /Hardener	447.220	156.361	0.032	2.460	16.880	2.790	3.982	2.547
Resin /Highsilica	272.220	90.311	0.020	2.260	23.410	4.580	2.447	2.710
Resin /Lowsilica	283.330	99.940	0.028	1.820	14.660	4.420	4.190	4.192
Resin /Highsiliver	327.780	89.361	0.020	2.250	19.310	3.820	2.622	2.934
Resin /Lowsilver	386.110	128.966	0.029	2.260	16.550	3.240	3.952	3.064

Table 6.3 Moisture absorption coefficients D and C_{sat} in resins with different amounts (high/low) of different fillers (silica/silver)

6.3.4 Aging of Polymeric Materials After Long-term Exposure at 85°C/ 85%RH

In all of the absorption experiments, after long-term exposure to 85°C/ 85%RH, a tendency of weight loss was found. In figure 6.1, 6.5, 6.6, it can be seen that weight gain of the samples starts to drop after long duration of experiments. However, it is polymer matrix dependent, and obviously the samples with lower T_g such as Die Attach and resins with different fillers have more severe aging tendency. Therefore, to get better performance of these polymeric materials, in the premise of meeting the requirements of

use in the packaging, having higher T_g and better microstructure will stand more severe situations.

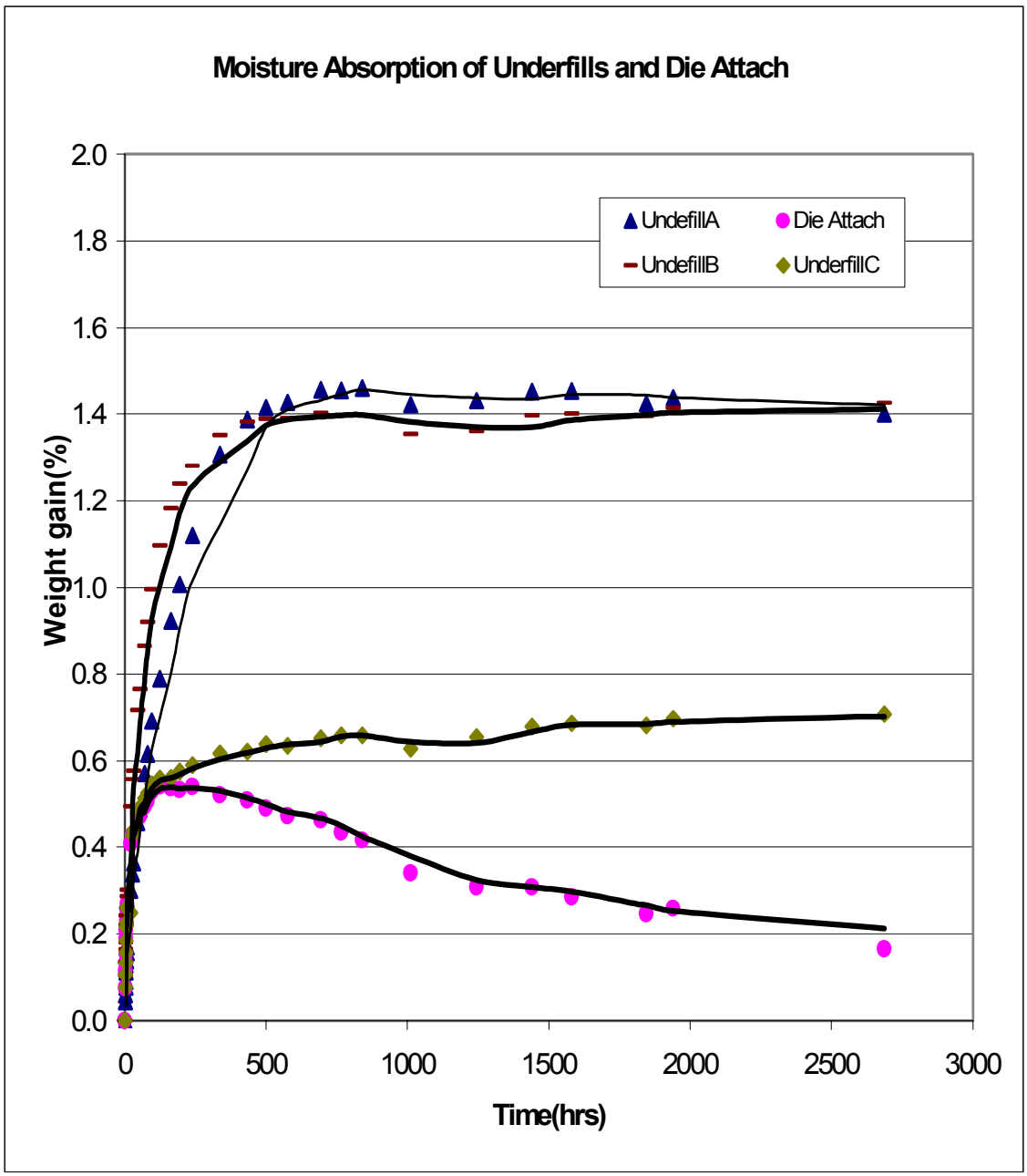

Figure 6.6 Moisture absorption of Underfills and Die Attach (over 2500 hours)

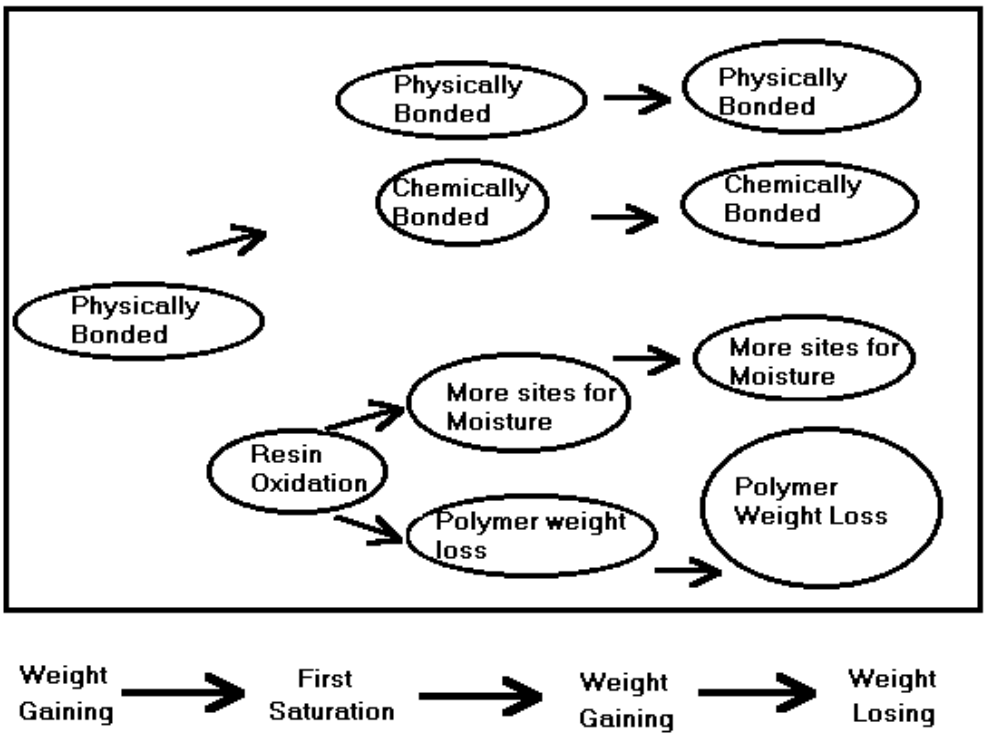

Figure 6.7 Moisture absorption and the states of water and polymer in different stages during the long-term exposure to 85 ^{o}C/ 85%RH

A tentative mechanism is proposed based on this study on the water states in the polymer as well as the state of polymer itself during the long-term exposure at 85^{o}C / 85%RH. As shown in figure 6.7, moisture diffuses into polymer in free volume as in physically bonded state initially, it soon reaches equilibrium, " first saturation'. Then, the physically bonded moisture starts to bond to polymer chain chemically (e.g Hydrogen bonds) and leave space in free volume for more moisture diffusing in. Due to the long-term exposure to this environment with high temperature and high humidity, polymer matrix oxidizes slowly, which probably creates some available polarizing site for moisture chemical bonding. However, it causes the chemical degradation of polymer and this breaks some of the polymer chains and produces some volatiles. This will result in a weight loss and this

part of weight loss becomes severe in the latter stage of experiment. When the balance is broken, the result of weight gain of the sample becomes to drop.

6.4 Repeatability and Accuracy of the Experiments

Similar to section 5.3, diffusivity D computed is a function of time, temperature and weight, the systematic error will be as the sum of all of the errors in percentages form. If we ignore the errors from time and temperature based on the assumption that these two factors are handled properly during the tests, we will focus on the error of the weight.

As described in the section 4.4, the standard deviation and relative error are calculated. The values are listed in table 6.1, 6.2 and 6.3. As can be seen, the relative errors are less than 5%. This indicates that the experimental results are acceptable.

Due to the limitation of sample sources, only one sample for each material was prepared for the testing.

6.5 Conclusions

Moisture absorption experiments were carried out using different polymeric packaging materials. Results have shown that moisture absorption behaviors are Fickian-like and moisture absorption coefficients D are polymer matrix dependent.

The comparison of moisture absorption coefficients and moisture desorption coefficients has shown the similarities in D at absorption and at desorption, which also further

confirmed the desorption technique TGA was good at temperatures below T_g and KF Titration was good at temperatures above T_g.

The effects of fillers on moisture diffusion in polymeric packaging materials were discussed. Fillers acted as barriers for moisture diffusion. Different fillers influenced the same resin differently. For same fillers in same resins, the higher amount of fillers resulted in smaller moisture absorption coefficients.

Aging in polymeric packaging materials were observed after long-term exposure to an environment of 85°C/ 85%RH. The level of aging was found polymer matrix dependent. Polymeric materials with lower T_g that were close to 85 °C, had severe aging phenomena. Therefore, in the premise to meet the functional needs of packaging, it is important to design polymeric materials with higher T_g to obtain the best performance of materials under severe environments with high temperatures and high relative humidity.

Chapter 7
Conclusions

Through comparing with standard and conventional testing technique such as TGA (Thermal Gravimetric Analysis) and with a furthermore confirmation test of GC/MS (Gas Chromatography/Mass Spectrometry), moisture desorption experiment with Karl Fischer Titration was performed in this research by using 3 types materials: Molding compound, Underfill and Die Attach materials.

The possible causes for the decreased D and the larger C_{sat} by TGA tests were discussed. It has been shown that TGA is incapable of characterizing the moisture diffusion at high temperatures because volatiles might get involved in the weight loss. This also challenged other gravimetric testing methods for high temperature desorptions of polymeric materials.

Both Fickian and non-Fickian behaviors were observed for all of polymeric packaging materials used in this research. Molding compound displayed non-Fickian behaviors and different levels of moisture concentration were obtained at different temperatures for its samples, especially at high temperatures. This indicates that non-Fickian diffusion depends on the polymer matrix and happens apparently at elevated

temperatures. The longer exposure to high humidity-temperature environment probably caused more non-Fickian behaviors in adsorption, therefore, more non-Fickian behaviors in desorption.

T_g effects on moisture desorption are found to be polymer matrix dependent. KF titration is good at desorbing moisture at high temperatures far above T_g. However, it is not suitable for moisture desorption at temperatures below T_g due to some absorbed moisture being immobilized, which may not be desorbed below T_g. Arrenhius relationships show a smooth change in D_o and E_d during the T_g traversing, because the traverse of T_g is a period instead of a point. E_d has different values for temperature above and below T_g and it is smaller at the temperatures above T_g.

KF titration is a reliable and efficient testing method for high temperatures desorption of polymeric packaging materials with careful sample preparation, handling and testing in a stable testing environment and TGA, for the temperatures below T_g.

Moisture absorption experiments were carried out using different polymeric packaging materials. Results have shown that moisture absorption behaviors are Fickian-like and moisture absorption coefficients D are polymer matrix dependent.

The comparison of moisture absorption coefficients and moisture desorption coefficients has shown the similarities in D at absorption and at desorption, which also further confirmed the desorption technique TGA was good at temperatures below T_g and KF Titration was good at temperatures above T_g.

The effects of fillers on moisture diffusion in polymeric packaging materials were discussed. Fillers acted as barriers for moisture diffusion. Different fillers influenced the same resin differently. For same fillers in same resins, the higher amount of fillers resulted in smaller moisture absorption coefficients.

Aging in polymeric packaging materials were observed after long-term exposure to 85^{o}C/ 85%RH. The level of aging was found polymer matrix dependent. Polymeric materials with lower T_g that were close to 85 ^{o}C, had severe aging phenomena. Therefore, in order to meet the functional needs of packaging, it is important to design polymeric materials with higher T_g to obtain the best performance of materials under severe environments with high temperatures and high relative humidity.

References

Adamson, Michael J., "Thermal Expansion and Swelling of Cured Epoxy Resin Used in Graphite/Epoxy Composite Materials", Journal of Materials Science 15 (1980), pp.1736-1745

Amagai, Masazumi "Investigation of Stress Singularity Fields and Stress Intensity Factors for Cracks" 1996 IEEE, pp.246-257

Bao, Li-Rong, Yee, Albert F. Charles and Lee, Y.C., "Moisture Absorption and Hygrothermal Aging in a Bismaleimide Resin", Polymer 42(2001) 7273-7333, Elsevier

Blikstad, Sjoblom and Johannesson, "Long-term moisture absorption in graphite/epoxy angle-ply laminates", Journal of Composite Materials, Vol. 18, Jan 1984, pp32-46

Bonniau, P. and Bunsell, A.R., "A comparative Study of Water Sorption Theories Applied to Glass Epoxy Composites", Environmental Effects on Composites Materials, George S. Springer, pp209-229

Buchhold, R., Nakladal, A., Gerlach, G., Sahre, K., Muller, M., Eichhorn, K.J., Herold, M. and Gougliz, G., "A Study on the Microphysical Mechanisms of Adsorption in Polyimide Layers for Microelectronic Applications" Journal of Electrochem. Soc, Vol.145, No.11, November 1998

Cai, L. W. and Weitsman, Y., "Non-Fickian Moisture Diffusion in Polymeric Composites" Journal of Composite Materials, Vol.28, No.2, 1994, pp.130-154
Crank, J and Park, G.S.., "Diffusion in Polymers", Academic Press, London and New York, 1968

Crank, J, "The mathematics of diffusion," by. Imprint Oxford, [Eng]: Clarendon Press, 1975. 2d ed. P2-4, P202, P238, P255

Deiasi, R. J. and Schulte, R.L., "Moisture Detection in Composites Using Nuclear Reaction Analysis", Environmental Effects on Composites Materials, George S. Springer, pp144-150

De Neve, B. and Shanahan, M. E. R. "Physical and Chemical Effects in An Epoxy Resin Exposed to Water Vapor", J. Adhesion, 1995,Vol49, pp.165-176

Designation: D5229/F5229M-92 (Reapproved 1998) "Standard Test Method for Moisture Absorption Properties and Equilibrium Conditioning of Polymer Matrix Composite Materials", Published June 1992

Diamant, Y., Marom, G. and Broutman, L.J., "The effects of Network Structures on Moisture Absorption of Epoxy Resins", Journal of Applied Polymer Science, Vol.26, 3015-3025(1981)

EL-SA'AD, Leila, Darry, M.I. and YATES, B., "Moisture Absorption by Epoxy Resins: the Reverse Thermal Effect", Journal of Materials Sceince, Vol.25, No.8, pp.3577-3582, 1990

Fremont, H., Deletage, J.Y. and Danto, A.Pintus.Y. "Evaluation of the Moisture Sensitivity of Molding Compounds of IC's Packages" Transactions of the ASME, March2001, Vol.123, pp16-18

Galloway, J.E., and Miles,B.M, "Moisture Absorption and Desorption Predictions for Ball Grid Array Packages", IEEE Transaction on Components, Packaging, and Manufacturing Technology-Part A, Vol.20, No.3, pp. 274-279, Spet.1997

Isengard, H-D. "Rapid Water Determination in Foodstuffs" Trends in Food Science & Technoledgy May 1995, Vol.6.pp155-162

IPC/JEDEC J-STD-020A, "Moisture/Reflow Sensitivity Classification for Plastic Integrated Circuit Surface Mount Devices", April, 1999

JEDEC Standard No. 22-A120, "Test Method for the Moisture Diffusivity and Water Solubility in Organic Materials Used in Integrated Circuits", JUNE 2001, JEDEC SOLID STATE TECHNOLOGY ASSOCIATION

Kim, Samuel, "The role of Plastic Package Adhesion in Performance", IEEE Transactions on Components, Hybrids, and Manufacturing Technology, 1991,Vol 14, No.4, pp.809-817

Kim, Samuel, "The role of plastic package adhesion in IC performance", 1991IEEE, pp.750-758

Kitano, Makoto "Analysis of package cracking during reflow soldering process", 1988 IEEE, pp.90-95

Kongarshi, Mark. M., "Effects of Tg and CTE on Semiconductor Encapsulants", Loctite Corporation, http://www.loctite.com

Kreyszig, E. Advanced Engineering mathematics, sixth edition, New York : Wiley, 1988. pp1029-1031

Lau, John H. and Chang, Chris "Characterization of Underfill Materials for Functional Solder Bumped Flip Chips on Board Applications", IEEE, 1999

Li, Yanmei, Miranda, John and Sue, Hung-Jue "Hygrothermal Diffusion Behavior in Bismaleimide Resin", Polymer 42(2001) 7791-7799, Elsevier

Li, Yanmei, Miranda, John, and Sue, Hung-Jue, "Hygrothermal Diffusion Behavior in Bismaleimide Resin", Polymer 42(2001) 7791-7799, Elsevier

Lim, J. H. "Vapor Pressure Analysis of Popcorn Cracking In Plastic IC Packages By Fracture Mechanics", 1998 IEEE/CPMT, pp.36-42

Lin, Jing, Teng, Annette and Yuen, Matthew M F "A Fast Low Cost Method to Check for Moisture in Epoxy Molding Compound", IEEE/CPMT Electronic Packaging Technology Conference, 1998, pp359-361

Liu, Sheng, "Behavior of Delaminated Plastic IC Packages Subjected to Encapsulation Cooling, Moisture Absportion, and Wave Soldering", 1995 IEEE, Part A, Vol. 18, No. 3, Sept., pp.634-645

Lowry, R.K., Hanley, K. and Berriche, R., "Effects of Temperatures above the Glass Transition on Properties of Plastic Encapsulant Materials", 2001 International Symposium on Advanced Packaging Materials, pp57-62

Luo, Shijian and Wong, C.P., "Fundamental Study on Moisture Adsorption in Epoxy for Electronic Application", 2001 International Symposium on Advanced Packaging Materials, pp293-298

March, L.L. and Lasky, R. "Moisture Solubility and Diffusion in Epoxy and Epoxy-glass Composite", Environmental effects on composite materials, George S. Springer**,** 1981, pp. 51-61,ISBN0877623007

March,L.L., Van Hart, D.C. and Kotkiewicz, S.M. "A Dielectric Loss Investigation of Mositure in Epoxy-Glass Composites", IBM Journal of Research and Development, Vol.29, No.1, January 1985

Marjanski, Malgorzata, Srivasarao, Mohan and Mirau, Peter A., "Solid-state Multipulse Proton Nuclear Magnetic Resonance (NMR0 Charaterization of Self-assembling Polymer Films", Solid State Nuclear Resonance 12, (1998), pp.113-118, elsevier

Mcmaster, Michael G. and Soane, David S., "Water sorption in Epoxy Thin films", IEEE Transactions on Components, Hybrids, and Manufacturing Technology, 1989,Vol 12, No.3, pp.373-385

Miettinen, Varpu M., Narva, Katja K. and Vallittu, Pekka K., "Water Sorption, Solubility and Effect of Post-curing of Glass Fibre Reinforced Polymers", Biomaterials 20 (1999) pp1187-1194, Elsevier

Neogi, P., "Diffusion in Polymers", 1996, pp.185-193, ISBN 0-8247-9530-X

Ogata, Masatsugu, Kinjo, Noriyuki and Kawata, Tatsuo "Effects of Crosslinking on Physical Propertires of Phenol-Formaldehyde Novolac Cured Epoxy Resins", Journal of Applied Polymer Science, Vol.48, 583-601 (1993)

Osswald, Tim A. and Menges Georg, " Materials Science of Polymers for Engineers", 1995, pp431-439

Park Y. B. and Yu, Jin "A Fracture Mechanics Analysis of the Popcorn cracking in the Plastic IC packages", 1997 IEEE, pp.12-19

Plueddemann, Edvin P., Composite Materials, Vol.6, "Interfaces in Polymeric Matrix", pp.201, 1974, Academic Press

Predecki, P. and Barrett, C.S., "Detection of Moisture in Graphite/Epoxy Laminates by X-Ray Diffraction", Environmental Effects on Composites Materials, George S. Springer, 1988, pp137-142

Rao, R.M.V.G.K., Balasubramanian, N. and Chanda, M,. "Factors Affecting Moisture Absorption in Polymer Composites Part II: Influence of External Factors" Environmental effects on composite materials, George S. Springer**,** 1981, pp. 89-95,ISBN0877623007

Resin Oxidation,http://www.arlonmed.com/Everything/Materials/Resin%20oxidation.htm

RTC Group, "New Hope for Plastic Encapsulated CHIPS in Military Projects, March 2000" http://www.rtcgroup.com/cotsjournal/cots3400/cots3400p21.html

Schadt, R.J. and Vanderhart, D. L., "Solid-State Proton Nuclear Magnetic Resonance of Glassy Epoxy Exposed to Water", Macromolecules, 1995, 28, pp.3416-3424

Schen, Michael A., Wu, Wen-Li, Wallace, William E., Tan, Nora Beck, Vanderhart, David and Davis, G. T., "Molecular Insights on Interfacial Properties and Moisture Uptake of Plastic Packaging Materials" 1997 International Symposium on Advanced Packaging Materials, pp85-87

Schitsky, M. and Suhir, E., "Moisture Diffusion in Epoxy Molding Compounds Filled With Particles", Jounal of Electronic Packaging, March 2001, Vol.123, pp47-51

Shirrell, C.D. "Diffusion in Water Vapor in Graphite/Epoxy Composites", Advanced Composite Materials-Environmental Effects, pp21-42

Shook, R.L., Gerlach, D.L. and Vaccaro, B.T., "Moisture Blocking Planes and Their Effect on Reflow Performance in Achieving Reliable Pb-free Assembly Capability for PBGAs", 2001

Sivakesave, S and Irudayaraj, Joseph, "Analysis of Potato Chips Using FTIR Photoacoustic Spectroscopy" Journal of he Science of Food and Agriculture 80, 2000,pp.1805-1810

Smith, Gordon, Androff, Nancy and Kamla, Jeff "Moisture Absorption Properties of Laminates Used in Chip Packaging Applications", IPC Expo, March11-13, 1997

Suhl, David, "Thermally Induced IC Package Cracking", 1990 IEEE, Vol.13, No.4, December pp.940-945

Tae-je, Lee, Kyu-jin, Lee, Min-ho, et al., "An Improvement in Relow Performance of Plastic Packages", Samsung Electronics.Co., IEEE, 1996, pp931-934

Tay, A.O. and Lin, T.Y. "The Impact of Moisture Diffusion During Solder Reflow on Package Reliability", 1999 Electronic Components and Techology Conference, pp.830-836

Teo, Yong Chua, Wong, Ee Hua and Lim, Thiam Beng, "Enhancing Moisture Resistance of PBGA" IEEE 1998 Electronic Compinets and Technology Conference, pp.930-935

Van Der Wel, G. K.and G Adan, O.C. "Moisture in Organic Coatings—A Review", Progress in Organic Coatings, 1999(37), pp.1-14

Vanderhart, D.L, Davis, G.T. and Schen, M.A. " Partitioning of Water between Voids and the Polymer Matrix in a Moulding Compound by Proton NMR: The Role of Larger Voids in the Phenomena of Popcorning and Delamination" The international Journal of Microelectronics and Electronics Packaging, 1999, ol.22, No. 41000 pp.423-441, (ISSN 1063-1774)

Vanlandingham, M.R., Eduljee, R.F. and Gillespie, J.W. "Moisture diffusion in Epoxy Systems", Center for Composite Materials and Materials Science Program, University of Delavware, Newwark, DE19716, 1998, http://www.me.udel.edu/~vanlandi/C3-4paper.html

Wong, E.H., Chan, K.C., Lim, T.B. and Lam, T.F. "Non-Fickian Moisture Properties Characterisation and Diffusion Modeling for Electronics Packages" IEEE 1999 Electronic Compinets and Technology Conference, pp.302-306

Wong, E.H., Teo, Yong Chua and Lim, Thiam Beng "Moisture Diffusion and Vapour Pressure Modeling of IC packaging" IEEE 1998 Electronic Compinets and Technology Conference, pp.1372-1378

Wong, E.H., private communication.2001

Wong, T.C. and Broutman, L.J., "Moisture Diffusion in Epoxy Resins Part 1. Diffusion Mechanism", Polymer Engineering and Science, June, 1985, Vol.25, No.9, pp521-528

Wong, T.C. and Broutman, L.J., "Water in Epoxy Resins Part I1.Non-Fickian Sorption Processes", Polymer Engineering and Science, June, 1985, Vol.25, No.9, pp529-534

Woo, Monica and Piggott, Michael R. "Water Absorption of Resins and Composites: I. Epoxy Homopolymers and Copolymers", The American Society for Testing and Materials, 1987, pp101-107

Woo, Monica and Piggott, Michael R., "Water Absorption of Resins and Composites: II. Diffusion in Carbon and Glass Reinforced Epoxies", The American Society for Testing and Materials, 1987, pp162-166

Woo, Monica and Piggott, Michael R., "Water Absorption of Resins and Composites: III. Water Distribution as Indicated by Capacitance Measurement", The American Society for Testing and Materials, 1988, pp16-19

Woo, Monica and Piggott, Michael R., "Water Absorption of Resins and Composites: IV. Water Transport in Fiber Reinforced Plastics", The American Society for Testing and Materials, 1988, pp20-24

Wu, Chuanbin James and McGinity, W. "Influnece of Relative Humidity on the Mechanical and Drug Release Properties of Theophylline Pellets Coated with an Acrylic Polymer Containing Methylparaben as a Non-traditional Plasticizer", European Journal of Pharmaceutics and Biopharmaceutics 50 (2000) 277-284, 2000 Elsevier Science

Yi, Sung, "Finite Element Analysis of Hygrothermally induced stresses in plastic IC packages", 1995 IEEE, 5th IPFA '95: Singapore, pp. 32-39

Yoshioka, Osamu, Okabe, Norio, Nagayama, Sadao and Yamagishi, Ryozo, "Improvement of Moisture Resistance in Plastic Encapsulants MOS-IC by Surface Finishing Copper Leadframe" IEEE 0569-5503/89/0464

Appendix 1.Excel solver program

1. Excel solver program for TGA (3-dimensional samples)

```
Function mt3d(n0, z, x, y, d, t, msat)
Pi = 3.1416
Sum = 0

For L = 0 To n0
For m = 0 To n0
For n = 0 To n0
   aL = (2 * L + 1) ^ 2
   am = (2 * m + 1) ^ 2
   an = (2 * n + 1) ^ 2
   Leqv = aL * (Pi / x) ^ 2 + am * (Pi / y) ^ 2 + an * (Pi / z) ^ 2
   b = Exp(-d * t * Leqv) / (aL * am * an)
   Sum = Sum + b
Next
Next
Next

mt3d = msat * (1 - 512 * Sum / Pi ^ 6)

End Function

Rem Three dimensional solution for mass fraction of moisture
Rem mt3d/msat=1-(512/Pi^6)*sum,L sum,m sum,n exp{(-
D*t*Leqv)/(aL^2*am^2*an^2)}
Rem where x, y, z are the dimensions of the rectangular block
Rem where aL, am, an =[(2*L+1)*Pi]^2,[(2*m+1)*Pi]^2,[(2*n+1)*Pi]^2
Rem where Leqv=aL/x^2+am/y^2+an/z^2
Rem mt3d = mass of moisture at any time
Rem Msat = saturated mass of moisture
Rem D = diffusivity
Rem t = time
Rem x,y,z = dimension of rectangular specimen
Rem n0 = number of summation terms
```

2. Excel solver program for Titration (1-demensional program)

```
Function mt1d(n0, z, d, t, msat)
Pi = 3.1416
Sum = 0
```

```
For n = 0 To n0

   a = ((2 * n + 1) * Pi) ^ 2
   b = Exp(-d * t * a / z ^ 2) / a
   Sum = Sum + b
Next

mt1d = msat * (1 - 8 * Sum)


End Function

Rem One dimensional solution for mass fraction of moisture
Rem mt1d/msat=1-sum{8/[(2n+1)*Pi]^2*exp{-D*t*[(2n+1)*Pi/z]^2}
Rem mt1d = mass of moisture at any time
Rem Msat = saturated mass of moisture
Rem D = diffusivity
Rem t = time
Rem z = total thickness of the disc
Rem n0 = numb terms
```

Appendix 2. Method of least squares [Kreyszig, 1988]

N points (pairs of numbers) are given in curve fitting, and we want to determine a function f(x) such that $f(x_j) \approx y$, j=1, …, n . According to the nature of the problem (the underlying physical law, for instance), the type of function (for polynomials, exponential functions, sine and cosine functions) may be suggested, and in many cases a polynomial of a certain degree will be appropriate.

However, in certain situations this would not be the appropriate solution of the actual problem. For instance, to the four points

(1) (-1.0, 1.000), (-0.1, 1.099), (0.2, 0.808), (1.0, 1000)

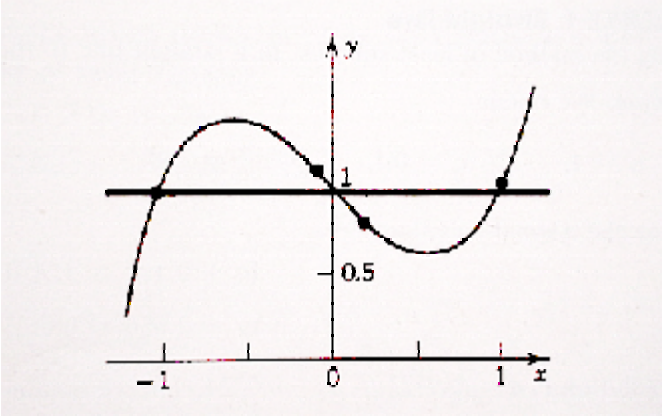

Figure 1. The approximate fitting of a straight line

there corresponds the Lagrange polynomial $f(x)=x^3-x+1$ (Fig. 1), but if we graph the points, we see that they lie nearly on a straight line. Hence if these values are obtained in an experiment, thus this involves an experimental error, and if the nature of the experiment suggests a linear relation, we better fit a straight line through the points (Fig. 1). Such a line may be useful for predicting values to be expected for other values of x. In simple cases a straight line may be fitted by eye, but if the points are scattered, this becomes unreliable and we better use a mathematical principle. A widely used procedure of this type is the method of least squares by Gauss. In the present situation it may be formulated as follows.

Method of least squares

The straight line y =a +bx

should be fitted through the given points(x1, y1), …(xn, yn) so that the sum of the squares of the distances of those points from the straight line is minimum, where the distance is measured in the vertical direction(the y-direction).

The point on the line with abscissa x_j has the ordinate $a + bx_j$. Hence its distance from (xj, yj) is [yj-a-bxj] (cf. Fig. 433) and that sum of squares

$$q = \sum_{j=1}^{n} (y_j - a - bx_j)^2$$

q depends on a and b. A necessary condition for q to be minimum is

$$\frac{\partial q}{\partial a} = -2\sum (y_j - a - bx_j) = 0$$

$$\frac{\partial q}{\partial b} = -2\sum x_j (y_j - a - bx_j) = 0$$

(where we sum over j from 1 to n). Writing each sum as three sums and taking one of them to the right, we obtain the result

$$an + b\sum x_j = \sum y_j$$

$$a\sum x_j + b\sum x_j^2 = \sum x_j y_j$$

These equations are called the normal equations of our problem.

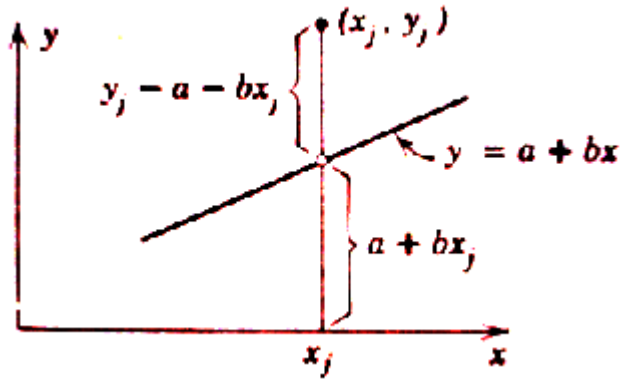

Figure 2. Vertical distance of a point (x_j, y_j) from a straight line y=a+bx

Appendix 3. Data sheet for trial testing of repeatability

Raw Data for Karl Fisher Titration (KFT) Trial Tests (Samples: Molding compound, approximately 1.91g)

	140°C			170°C			220°C		
	Set 1	Set 2	Set 3	Set 1	Set 2	Set 3	Set 1	Set 2	Set 3
Time (mins)									
0	0	0	0	0	0	0	0	0	0
0.5	0.02872	0.03622	0.0364	0.01742	0.03642	0.01712	0.0932	0.0260	0.0770
1	0.05512	0.05862	0.0602	0.04292	0.07142	0.04302	0.1640	0.0780	0.1553
1.5	0.08212	0.08022	0.0826	0.08062	0.11812	0.08362	0.2445	0.1552	0.2491
2	0.10952	0.10232	0.1052	0.12752	0.17142	0.13472	0.3221	0.2433	0.3403
2.5	0.13502	0.12272	0.1261	0.18192	0.22362	0.19142	0.3902	0.3326	0.4216
3	0.15672	0.14042	0.1454	0.23182	0.27262	0.24592	0.4464	0.4098	0.4852
3.5	0.17572	0.15572	0.1629	0.27712	0.31412	0.29302	0.4915	0.4755	0.5355
4	0.19112	0.16872	0.1772	0.31582	0.34932	0.33432	0.5268	0.5216	0.5735
4.5	0.20472	0.18002	0.1897	0.34932	0.37842	0.36922	0.5537	0.5601	0.6017
5	0.21592	0.18972	0.2004	0.37702	0.40242	0.39772	0.5754	0.5898	0.6225
5.5	0.22542	0.19892	0.2095	0.39982	0.42262	0.42202	0.5919	0.6129	0.6384
6	0.23362	0.20682	0.2175	0.41922	0.43972	0.44162	0.6056	0.6295	0.6506
6.5	0.24122	0.21452	0.225	0.43502	0.45402	0.45822	0.6166	0.6426	0.6597
7	0.24792	0.22202	0.2319	0.44802	0.46562	0.47212	0.6262	0.6529	0.6673
7.5	0.25502	0.22902	0.2387	0.45942	0.47552	0.48362	0.6348	0.6613	0.6738
8	0.26132	0.23592	0.2452	0.46892	0.48392	0.49302	0.6429	0.6688	0.6798
8.5	0.26742	0.24212	0.2512	0.47702	0.49152	0.50162	0.6495	0.6753	0.6852
9	0.27342	0.24802	0.2569	0.48402	0.49822	0.50862	0.6558	0.6812	0.6901
9.5	0.27882	0.25392	0.2625	0.49072	0.50472	0.51522	0.6616	0.6865	0.6945
10	0.28422	0.25972	0.2681	0.49702	0.51082	0.52142	0.6676	0.6915	0.6985
10.5	0.28952	0.26512	0.2734	0.50312	0.51652	0.52772	0.672	0.696	0.7022
11	0.29472	0.27042	0.2784	0.50872	0.52212	0.53372	0.6767	0.699	0.7058
11.5	0.30002	0.27552	0.2832	0.51412	0.52742	0.53932	0.6812	0.7036	0.7088
12	0.30442	0.28042	0.2881	0.51962	0.53242	0.54462	0.6851	0.7072	0.7119
12.5	0.30912	0.28532	0.2927	0.52452	0.53752	0.54952	0.6889	0.7103	0.7148
13	0.31392	0.29032	0.2972	0.52932	0.54232	0.55462	0.6925	0.7136	0.7174
13.5	0.31812	0.29502	0.3015	0.53392	0.54692	0.55922	0.6959	0.7163	0.7199
14	0.32272	0.29952	0.3057	0.53842	0.55132	0.56352	0.6991	0.719	0.7221
14.5	0.32692	0.30422	0.3099	0.54262	0.55562	0.56782	0.702	0.7215	0.7243
15	0.33102	0.30862	0.3141	0.54672	0.55972	0.57202	0.7048	0.7241	0.7263
15.5	0.33512	0.31292	0.318	0.55082	0.56382	0.57612	0.7076	0.7264	0.7283
16	0.33912	0.31702	0.3219	0.55452	0.56752	0.57982	0.7101	0.7287	0.7305
16.5	0.34322	0.32112	0.3257	0.55832	0.57142	0.58312	0.7127		0.7324
17	0.34712	0.32542	0.3296	0.56222	0.57502	0.58672	0.7149		0.7342
17.5	0.35092	0.32942	0.3333	0.56562	0.57822	0.59012	0.7172		
18	0.35432	0.33322	0.337	0.56902	0.58162	0.59332	0.7193		
18.5	0.35802	0.33722	0.3404	0.57232	0.58492	0.59622			

19	0.36172	0.34102	0.3439	0.57542	0.58812	0.59932
19.5	0.36492	0.34472	0.3474	0.57862	0.59112	0.60212
20	0.36832	0.34852	0.3508	0.58142	0.59422	0.60502
20.5	0.37172	0.35232	0.3541	0.58422	0.59712	0.60752
21	0.37522	0.35572	0.3574	0.58692	0.60002	0.61002
21.5	0.37812	0.35942	0.3608	0.58952	0.60272	0.61272
22	0.38112	0.36312	0.3639	0.59202	0.60532	0.61532
22.5	0.38422	0.36642	0.367	0.59462	0.60782	0.61772
23	0.38762	0.36972	0.3702	0.59712	0.61022	0.62002
23.5	0.39052	0.37312	0.3733	0.59932	0.61262	0.62202
24	0.39342	0.37642	0.3765	0.60152	0.61492	0.62432
24.5	0.39632	0.37982	0.3796	0.60372	0.61732	0.62652
25	0.39922	0.38312	0.3827	0.60582	0.61952	0.62872
25.5	0.40202	0.38602	0.3857	0.60802	0.62172	0.63092
26	0.40472	0.38932	0.3887	0.61022	0.62382	0.63282
26.5	0.40742	0.39252	0.3916	0.61202	0.62572	0.63472
27	0.41002	0.39552	0.3944	0.61402	0.62772	0.63642
27.5	0.41292	0.39862	0.3973	0.61592	0.62982	0.63842
28	0.41542	0.40152	0.4001	0.61772	0.63172	0.64002
28.5	0.41792	0.40482	0.4028	0.61962	0.63362	0.64182
29	0.42022	0.40772	0.4055	0.62132	0.63542	0.64362
29.5	0.42282	0.41082	0.4082	0.62322	0.63722	0.64532
30	0.42522	0.41362	0.4108	0.62472	0.63882	0.64712
30.5	0.42762	0.41652	0.4134	0.62612	0.64042	0.64872
31	0.43022	0.41932	0.4159	0.62782	0.64212	0.65022
31.5	0.43242	0.42222	0.4185	0.62942	0.64382	0.65152
32	0.43482	0.42512	0.421	0.63112	0.64542	0.65312
32.5	0.43702	0.42782	0.4235	0.63262	0.64702	0.65482
33	0.43912	0.43052	0.4259	0.63402	0.64852	0.65622
33.5	0.44142	0.43332	0.4282	0.63532	0.65002	0.65762
34	0.44362	0.43602	0.4306	0.63662	0.65152	0.65872
34.5	0.44572	0.43872	0.4328	0.63802	0.65302	0.66012
35	0.44802	0.44122	0.4354	0.63932	0.65442	0.66152
35.5	0.44992	0.44392	0.4376	0.64062	0.65562	0.66282
36	0.45192	0.44632	0.4397	0.64192	0.65712	0.66412
36.5	0.45402	0.44902	0.442	0.64332	0.65842	0.66532
37	0.45592	0.45142	0.444	0.64442	0.65972	0.66652
37.5	0.45812	0.45402	0.4464	0.64542	0.66102	0.66772
38	0.46012	0.45652	0.4487	0.64682	0.66232	0.66902
38.5	0.46192	0.45902	0.4508	0.64782	0.66352	0.67022
39	0.46372	0.46142	0.4527	0.64892	0.66472	0.67142
39.5	0.46562	0.46382	0.4548	0.65002	0.66592	0.67252
40	0.46742	0.46622	0.4569	0.65112	0.66732	0.67362
40.5	0.46932	0.46862	0.459	0.65212	0.66852	0.67462
41	0.47112	0.47092	0.4611	0.65312	0.66952	0.67582
41.5	0.47292	0.47322	0.463	0.65402	0.67062	0.67692
42	0.47472	0.47552	0.4648	0.65492	0.67162	0.67792
42.5	0.47662	0.47792	0.4669	0.65592	0.67262	0.67892
43	0.47832	0.48012	0.4689	0.65692	0.67362	0.67982
43.5	0.47992	0.48252	0.4707	0.65772	0.67472	0.68082

44	0.48142	0.48482	0.4727	0.65872	0.67582	0.68172
44.5	0.48302	0.48692	0.4744	0.65962	0.67672	0.68262
45	0.48462	0.48912	0.4764	0.66052	0.67802	0.68372
45.5	0.48642	0.49142	0.4782	0.66132	0.67892	0.68462
46	0.48782	0.49352	0.4802	0.66222	0.67992	0.68552
46.5	0.48952	0.49582	0.4818			
47	0.49102	0.49782	0.4837			
47.5	0.49252	0.50002	0.4857			
48	0.49402	0.50212	0.4872			
48.5	0.49552	0.50432	0.4888			
49	0.49702	0.50642	0.4904			
49.5	0.49852	0.50842	0.4922			
50	0.49982	0.51042	0.494			
50.5	0.50112	0.51252	0.4956			
51	0.50252	0.51462	0.4973			
51.5	0.50412	0.51662	0.499			
52	0.50532	0.51862	0.5006			
52.5	0.50662	0.52052	0.5023			
53	0.50792	0.52252	0.5039			
53.5	0.50922	0.52452	0.5056			
54	0.51052	0.52652	0.507			
54.5	0.51172	0.52852	0.5085			
55	0.51282	0.53032	0.5099			
55.5	0.51412	0.53212	0.5117			
56	0.51542	0.53402	0.5133			
56.5	0.51662	0.53592	0.5147			
57	0.51782	0.53782	0.5161			
57.5	0.51902	0.53962	0.5178			
58	0.52032	0.54132	0.5192			
58.5	0.52142	0.54312	0.5206			
59	0.52252	0.54502	0.5219			
59.5	0.52362	0.54672	0.5235			
60	0.52462	0.54832	0.5249			
60.5	0.52542	0.55012	0.5263			
61	0.52662	0.55162	0.5274			
61.5	0.52762	0.55342	0.5287			
62	0.52882					
62.5	0.52992					
63	0.53082					

	85°C		120 °C	
Time (mins)				
0	0	0	0	0
1	0.00922	0.01122	0.08532	0.03102
2	0.02222	0.02722	0.12682	0.06752
3	0.03812	0.04592	0.15862	0.11072
4	0.05422	0.06272	0.18672	0.15062
5	0.06832	0.07842	0.21302	0.18312
6	0.08072	0.09082	0.23782	0.20842
7	0.09132	0.10182	0.26062	0.22842

8	0.09962	0.11072	0.28102	0.24392
9	0.10602	0.11772	0.29912	0.25672
10	0.11202	0.12272	0.31462	0.26732
11	0.11702	0.12722	0.32872	0.27572
12	0.12112	0.13172	0.34062	0.28282
13	0.12462	0.13542	0.35082	0.28962
14	0.12782	0.13812	0.36012	0.29632
15	0.13072	0.14102	0.36802	0.30202
16	0.13332	0.14332	0.37512	0.30782
17	0.13582	0.14602	0.38162	0.31332
18	0.13842	0.14802	0.38702	0.31882
19	0.14092	0.15082	0.39192	0.32432
20	0.14322	0.15312	0.39632	0.32952
21	0.14572	0.15562	0.40012	0.33432
22	0.14802	0.15782	0.40412	0.33902
23	0.15022	0.16012	0.40742	0.34352
24	0.15242	0.16232	0.41032	0.34842
25	0.15462	0.16442	0.41342	0.35282
26	0.15672	0.16692	0.41612	0.35722
27	0.15882	0.16882	0.41872	0.36162
28	0.16082	0.17072	0.42112	0.36572
29	0.16292	0.17302	0.42362	0.36972
30	0.16492	0.17482	0.42582	0.37382
31	0.16682	0.17692	0.42822	0.37772
32	0.16872	0.17902	0.42992	0.38202
33	0.17092	0.18082	0.43182	0.38612
34	0.17272	0.18262	0.43392	0.39002
35	0.17452	0.18452	0.43572	0.39402
36	0.17642	0.18642	0.43732	0.39782
37	0.17832		0.43892	0.40142
38	0.18002		0.44052	0.40452
39	0.18182		0.44192	0.40782
40	0.18352		0.44322	0.41092
41	0.18572		0.44432	0.41402
42	0.18722		0.44522	0.41702
43	0.18942		0.44662	0.42002
44			0.44782	0.42312
45			0.44872	0.42632
46			0.44962	0.42922
47			0.45062	0.43202
48			0.45142	0.43502
49			0.45212	0.43792
50			0.45292	0.44112
51				0.44382
52				0.44662